Small chicken, big story:
Detection of the genetic background of dwarfism in chicken using genomic analyses

Zhou Wu

Propositions

1. In genetic mapping, it is essential to account for the potential heterogeneity of a phenotype.
(this thesis)

2. To avoid inbreeding, genome editing should be used to introduce a dwarf phenotype into a population.
(this thesis)

3.The popularity of high-performance computing clusters (hpc) in academia is not matched by the awareness of the needs for hpc administrators.

4. Understanding unpredictable outcomes is as important as understanding the intended outcomes in scientific research.

5. The covid-19 pandemic demonstrates that weakness and ignorance are not barriers to survival, but arrogance is.

6. Biased reports in the media lead to narrow thinking about human rights.

Propositions belonging to the thesis, entitled
Small chicken, big story: Detection of the Genetic Background of Dwarfism in Chicken Using Genomic Analyses

Zhou Wu
Wageningen, 23 February 2021

Small chicken, big story:
Detection of the genetic background of dwarfism in chicken using genomic analyses

Zhou Wu

Thesis committee

Promotor

Prof. Dr M.A.M. Groenen

Professor of Animal Breeding and Genomics

Wageningen University & Research

Co-promotor

Dr R.P.M.A. Crooijmans

Assistant professor, Animal Breeding and Genomics

Wageningen University & Research

Other members

Prof. Dr D.K. Aanen, Wageningen University & Research

Prof. Dr M. Tixier-Boichard, National Institute of Agricultural Research (INRA), France

Dr F.R. Leenstra, Wageningen University & Research

Prof. Dr N. Buys, KU Leuven, Belgium

This research was conducted under the auspices of the Graduate School of Wageningen Institute of Animal Sciences (WIAS).

Small chicken, big story:
Detection of the genetic background of dwarfism in chicken using genomic analyses

Zhou Wu

Thesis

submitted in fulfillment of the requirements for the degree of doctor
at Wageningen University
by the authority of the Rector Magnificus
Prof. Dr A.P.J. Mol,
in the presence of the
Thesis Committee appointed by the Academic Board
to be defended in public
on Tuesday 23 February 2021
at 4 p.m. in the Aula

Wu, Z.
Small chicken, big story:
Detection of the genetic background of dwarfism in chicken using genomic analyses

PhD thesis, Wageningen University, Wageningen, the Netherlands (2021)
With references, with summary in English

ISBN: 978-94-6395-680-2
DOI: https://doi.org/10.18174/538829

Abstract

Wu. Z. (2020). Small chicken, big story: Detection of the genetic background of dwarfism in chicken using genomic analyses. PhD thesis, Wageningen University and Research, the Netherlands.

Body size of animals is a trait that has received a lot of interest and emphasis during domestication and breeding. The wide variation in size of domesticated animals is reflected in their genomes. An extreme size variation is dwarfism, a condition of unusually reduced growth caused by a variety of genetic components. In chicken, dwarfism is a complex trait studied and utilized for a long time. Because of the reduced body size, incorporating the dwarf trait into the breeding scheme can provide potential advantages and benefits. In this thesis, I focus on two types of dwarfism and analyze the genetic background of these dwarf phenotypes with respect to underlying genetic variants, gene expression, and population genomics. More specifically, I perform fine-mapping to detect the causative genetic variant underlying the autosomal dwarfism (adw) in chickens. Results demonstrate that a novel nonsense mutation in the *TMEM263* gene is associated with the adw phenotype resulting in the premature termination of the open reading frame, and a truncation of the transmembrane protein. Moreover, I study the genetic basis of the bantam phenotype in Dutch traditional chicken breeds by using a variety of genomic analyses. Genome mapping and differential gene expression analysis identify novel candidate genes responsible for the bantam phenotype. The results further demonstrate the heterogeneity of this trait and the signaling pathways involved in growth. Furthermore, I focus on the admixed population structure of Dutch chicken breeds and show how human-mediated crossbreeding may influence the genomic landscape of a population in a complex manner. Collectively, I provide a comprehensive understanding of the genetic background of dwarf phenotypes in chicken, which not only can be utilized in poultry breeding but also provides a case study of utilizing multi-omics data to study the phenotype-genotype relation.

Contents

1
General Introduction

1.1 Introduction

Unlike Alice experienced the shifting of size variation during the adventures in wonderland (Carroll, 1865), to shrink smaller or to grow taller in the real world is not as easy as a “drink me” potion. In nature, differences in body size and growth between and within species were driven by the adaptation to divergent environments (Roy, 2008). Over the last millions of years, the evolutionary rate of change in body size exhibits the bias in which favors towards small size (Roy, 2008; Polly, 2012). As one of the extreme consequences, dwarfism is a condition characterized by restricted growth. The definition of dwarfism is as general as reduced height (Boegheim et al., 2017). However, measurements of the dwarf phenotype involve multiple factors including height, adult body weight, and the length of certain bones (Boegheim et al., 2017). Dwarfism is caused by various genetic and molecular mechanisms, including hormonal levels, bone/cartilage and muscle development, and signaling pathways that influence growth development. In human, dwarfism is an unusually short stature and considered as a growth deficiency (Shirley and Ain, 2013). There are 189 entries in the OMIM (Online Mendelian Inheritance in Man) database describing dwarf phenotypes with known molecular basis (https://www.omim.org/). While according to the OMIA catalog (Online Mendelian Inheritance in Animals), 37 dwarf-related phenotypes were recorded for diverse organisms, including cattle, chicken, dog, and pig (https://www.omia.org/). The efforts made to optimize the diagnosis and treatment regarding the genetic causes of dwarfism in animals is important in terms of the wellbeing of the affected individual and the merit of animal breeding.

Glossary

Heterogeneity: The state of being diverse and nonuniform in feature.

Genome-wide association study (GWAS): An approach used to identify genetic variants across the genome that are statistically associated with a phenotype.

Meta-analysis: A statistical method that combines the results of multiple studies.

Haplotype: A set of alleles at several loci that are inherited together from a parent.

Linkage Disequilibrium (LD): The non-random association of alleles at two or more different loci.

Population stratification: The population substructure that has a systematic difference in allele frequencies between several subgroups.

Introgression: The transfer of genetic material (i.e., gene flow) from one population to another by hybridization.

1.2 Dwarfism in animals

1.2.1 Definition of dwarfism

Dwarfism is actually one of the most important traits in agriculture applied in both plant and animal breeding (Figure 1.1). For instance, for wheat (*Triticum aestivum*) and rice (*Oryza sativa*) breeding, introducing the dwarf or semi-dwarf character into the germplasms has increased the yield and improved the resistant to lodging (Liu et al., 2018; Wu et al., 2018b). As for the breeding program in domesticated animals, such as dogs (*Canis lupus familiaris*) whose morphological variation is surprisingly diverse, the diversity exhibited in body size across breeds is especially abundant (Rimbault et al., 2013). This body size variation has been undergoing artificial selection and has become part of the phenotypic definition of breed standards, e.g., for Dachshund and Chihuahua. More classic examples of reduced body size, intentionally selected within domesticated livestock species and defined as breed standard, include pigs (e.g., Banna miniature pig (Deng et al., 2011) and Gottingen miniture pig (Simianer and Köhn, 2010; Reimer et al., 2018)), horses (e.g., Shetland pony (Rafati et al., 2016)), and cattle (e.g., Dexter cattle (Cavanagh et al., 2007)). In poultry, usually chickens and ducks, dwarf organisms are sometimes called bantam. Human has been developing bantam fowl for the use of exhibition, decoration, pets, and extended to assist hunting. For example the bantam duck breed Call, which likely originated from the Netherlands, was developed to attract wild ducks for hunters (Holderread, 2011).

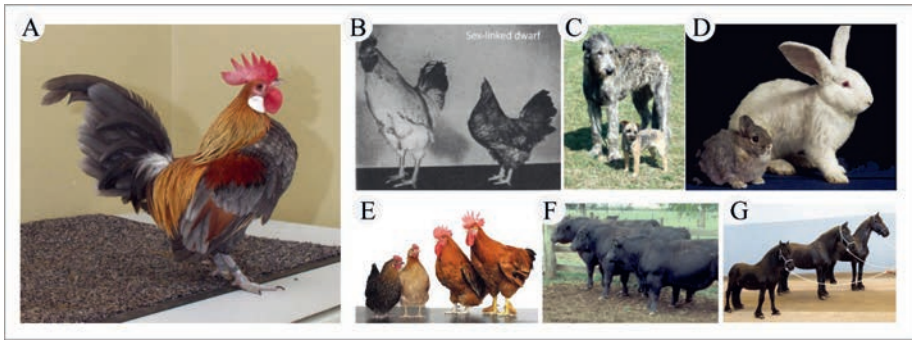

Figure 1.1 Dwarfism in domesticated animals (Photo adopted from published literatures). (A) Dutch bantam chicken (Bortoluzzi et al., 2020). (B) Sex-linked recessive dwarfism (Hutt, 1949) (C) Dog body size variation (Plassais et al., 2019) (D) The dwarf rabbit (Carneiro et al., 2017). (E) Xingyi creeper chickens (Jin et al., 2016). (F) Standard and miniature Angus cattle (Bouwman et al., 2018). (G) Dwarfism in the Friesian horse (Boegheim et al., 2017).

1.2.2 Phenotypic heterogeneity: (dis)proportionate short stature

The phenotype of dwarfisms can be characterized as either disproportionate or proportionate dwarfism. The main differences between the two types are determined by the coordinated reduction among body parts, e.g., between the limbs (arms and

legs) and torso (trunk of the body). In typical proportionate dwarfism, the individuals with short height tend to maintain normal body proportions, e.g., Laron syndrome in human (Godowski et al., 1989). As for disproportionate dwarfism, individuals have either (one pair or more) short limbs or a short torso, e.g., the short-leg but normal torso trait in corgi (Parker et al., 2009). However, there is sometimes a discrepancy between the definition and the measure among body parts, where the overall body proportions are maintained in a short stature, but the head is reported to be enlarged and/or with altered craniofacial development. An example can be found for chicken autosomal dwarfism (adw), which is a "proportionate" dwarfism, as determined by the measurements of skeletal elements of the hind limb (Cole, 2000). However, some researchers indicated that an abnormally enlarged head was observed (Ruyter-Spira et al., 1998a)(Leenstra et al., 1984, as cited in Cole, 2000). In human clinical diagnosis, the examination of (dis)proportionate dwarfism is usually adequate to determine certain types of dwarfism and the corresponding treatments thereafter. While in animal studies, the difference between these two categories is not always so prominent in practice.

A review in dwarfisms in livestock suggested that proportionate or disproportionate dwarfism may be determined by a different genetic basis (Boegheim et al., 2017). In general, proportionate dwarfism is mostly caused by signaling disruptions, in particular, hormonal disruptions or signaling pathway deficiencies. Whereas disproportionate dwarfism can be cause by signaling abnormalities or structural disruptions, which are usually loss-of-function variants affecting bone and cartilage development and extracellular matrix components.

1.3 Dwarf chicken as study species

1.3.1 Dwarfism in chicken

Regardless of its important role in providing proteins for humans (in forms of meat and egg), chicken (*Gallus gallus*) has also been an important animal in the religious and cultural life. Since the 18th century, chicken has been presented as fighting cocks or fancy birds in poultry shows (Potts, 2012). This resulted in extensive human-mediated breeding for chicken, leading to the expansion of the popularity of poultry keeping and the creation of early breed standard guidelines. The development of (local) chicken breeds has been further boosted by selective breeding. Although, the emphasis of livestock breeding has always been on production, the selection for superlative fowl with diverse phenotypes (especially morphological traits) has contributed greatly to the conservation of traditional chickens. Particularly, attention was paid towards dwarf/bantam chickens, which is shown by the increased breeding activities introducing bantam traits and exploring revived indigenous breeds. The selective breeding substantially reshaped the genetic characteristics of animals, rapidly leaving footprints across their genomes.

Chicken was the first livestock species to have its genome sequenced (Hillier et al., 2004). Hence, chicken genomics comprises a rich history and diversity of genetic resources to untangle the genotype-to-phenotype mechanisms. The genome of current chicken has been shaped by a fascinating course of domestication (Wang et al., 2020), but also subjected to the more recent adaptation and selection. Adaptation to a variety of climates and environments coincided with the world-wide dispersal of chicken populations. The long-term selection for (inbred) lines of chicken populations has further made it an excellent model to study phenotypic differentiation. A compelling selection experiment can be found in the Virginia lines which is a chicken population that has undergone consecutively bi-directional selection for body weight since 1957 (Johansson et al., 2010; Sheng et al., 2015). The experimental lines showed the phenotypic response and the genetic dynamics of long-term selection for a single trait, which highlights the important bridge between the genetic variation and body size diversification. Thanks to the human-mediated selection and the conservation of chickens that exhibit contrasting size variation, we are now able to obtain a comprehensive understanding of the genetic nature of dwarfism using chicken as a model organism. This enables the identification of the genomic regions underlying dwarfism on a fundamental and molecular basis.

1.3.2 Different types of chicken dwarfism

Up to now, several forms of dwarfism in chicken have been described, resulting in distinct types of body size reduction. The performance, heredity and physiology of these dwarf phenotypes have been studied for almost a century from the perspective of variation in body size. Different possible genetic mechanisms of dwarfism are shown in Box 1.1. In Table 1.1, I have listed seven classical and rather well understood types of dwarfism in chickens. Note that there are likely more dwarf phenotypes for which the genetic causes are studied. However, the description of the phenotype and the mode of inheritance of those dwarf/bantam chickens are not always clearly acknowledged. For instance, many bantam phenotypes are not identical with regards to the body weight, and the underlying genetics may differ. I will discuss this in more detail in the following paragraphs. In several instances of dwarfism, the body size reduction is accompanied either by semi-lethality or poor viability (Guillaume, 1976; Cole, 2000) . An example is the Creeper which is a short-legged semi-lethal dwarf (Landauer, 1932). Three non-fatal types of body reduction explained in detail below are sex-linked dwarfism, autosomal dwarfism, and bantam. Although in this thesis my focus is on autosomal dwarfism and bantam, I will describe all three types in more detail.

Box 1.1 Inheritance mode of dwarfism

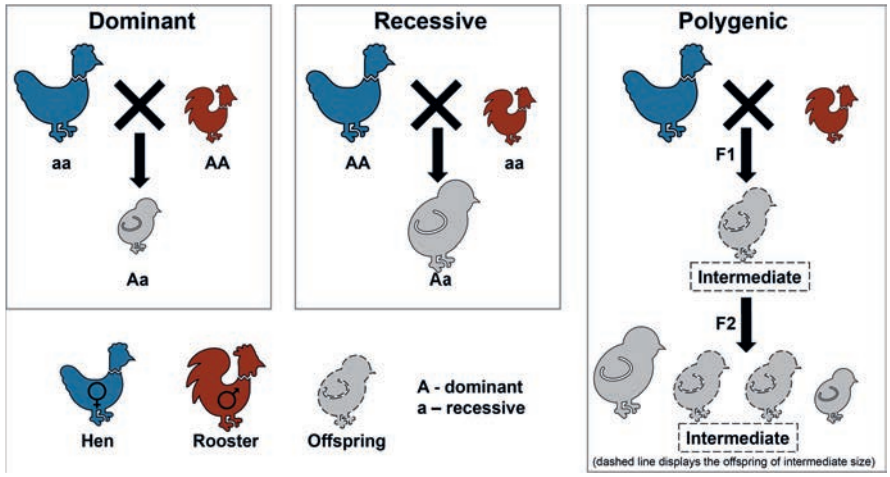

According to the basic mode of inheritance, dwarfism can be classified as Mendelian trait or quantitative trait. Mendelian inheritance has two basic modes of inheritance for a monogenic phenotype: dominant and recessive, both can be either autosomal or sex-linked (sex-linked is not shown here). Mendelian traits segregate with alleles at the locus of a single gene that in itself is sufficient to cause the dwarf phenotype. In contrast, a quantitative trait has a polygenic inheritance mode, the mating between dwarf and normal-sized chickens produce F1 offspring of intermediate size and F2 offspring segregating for a range of size variation. The polygenic pattern refers to the mode of inheritance where coexistence of variants at multiple loci and variance in environmental factors are considered to manifest the phenotype.

Sex-linked dwarfism

Recessive sex-linked dwarfism (dw) is well studied in chickens. This trait was described by F. B. Hutt (Hutt, 1949, 1959), where the dysfunctional growth hormone receptor (*GHR*) gene on the Z chromosome is responsible for the dwarfism. A number of different molecular variants in the *GHR* gene (i.e., the deletion and the missense mutation, as described in Table 1.1) result in protein alterations affecting the signaling of the circulating growth hormone, which subsequently affects the level of serum IGF-I through the GH-IGF-I axis (Guillaume, 1976; Burnside et al., 1991; Luo et al., 2016). As a consequence, the muscle cell and myofiber hyperplasia and hypertrophy is reduced, leading to a proportionate growth reduction (Coleman et al., 1995; Haddad and Adams, 2004; Hu et al., 2012; Luo et al., 2016). The dw chicks show no sign of dwarfing at hatch but become recognizable small at later age (8 to 10 weeks) (Hutt, 1949).

Autosomal dwarfism (adw)

The discovery of the autosomal dwarfism (adw) was recorded in a Cornell K-strain of White Leghorns (Cole and Hutt, 1973). These adw chickens were described as "proportionally reduced in size and in good fleshing", the effect of *adw* gene causes 30–40% reduced adult body weight with short shank length (Cole and Hutt, 1973; Cole, 2000). In terms of production performance, the adw chicken performs similarly to the sex-linked dwarf when compared with normal-sized controls. Unlike sex-linked dwarfism, the adw trait results in an observed reduction in body size during embryonic development (Cole, 2000). The autosomal dwarf chicken was discarded for over twenty years, but a comprehensive understanding of its genetic basis is still of interest.

Bantam

Another fascinating type of dwarfism is bantam. The word "bantam" originally derives from the name of a city located close to the islands Java and Sumatra and is now used to describe miniature varieties of fowl, usually chickens and ducks. There has been broad interest in the exhibition and production of bantam chickens as well as utilizing the effect of bantams for modifying current populations and breeding for small size. Currently, there are numerous (distinct) bantam breeds known across the world (Danforth, 1929; Custodio and Jaap, 1973; Malomane et al., 2018). These bantams can be classified into two categories, true (or traditional) bantams and bantamized (neo-bantam) breeds. The American Bantam Association (https://www.bantamclub.com/) reported over 400 recognized bantam breeds of different color varieties, of which close to 30 are true bantams. True bantams are small-sized breeds without a large equivalent. Some true bantam breeds are believed to be at least 2,000 years old, as reported by Columella (60 AD) in "de Re Rustica". On the other hand, the neo-bantams are the corresponding dwarf counterpart of normal-sized fowl which were recently developed by breeders due to the passion for downsizing over the last decades, particularly at the end of the 19th century (Esther Verhoef and Rijs, 2014; Bortoluzzi et al., 2018).

Studies suggested that the genetic factors for reduced size are not all identical in bantams (Danforth, 1929; Custodio and Jaap, 1973). This probably is because of the less rigorous definition of the bantam phenotype, which is generally considered as exquisite and a remarkably small body size (usually with weights around 500-900 gram). For instance, the Japanese bantam breed "Chabo" actually exhibits the creeper trait (Kinoshita et al., 2020); the dwarf traits in Serama, Chinese yuanbao, and Daweishan bantams, harboring unique genetic makeups, appear to involve separate molecular pathways (Wang et al., 2017). The hidden pattern of different bantam phenotypes and the distinct histories of these breeds make that bantams are a valuable model to study the genetic mechanism underlying this phenotypic variation.

Table 1.1 Overview of Different Chicken Dwarfisms

Traits	Gene*	Associated mutation	Phenotype	Inheritance	Source breed(s)	Ref#
Recessive sex-linked dwarfism(dw)	GHR	1) 1.8 Kb deletion (exon 10 and 3' UTR) 2) A single mutation (T>C) at boundary of exon 5	Growth hormone deficiency	Recessive	1) Connecticut (CT) strain; White Plymouth Rock; 2) White Leghorn; Cornell	a
Thyroid dwarfism(td)	N.A.	N.A.	Hypothyroidism	Recessive	Rhode Island Reds	b
Creeper(cp)	IHH	Deletion 1)12 Kb; 2)25 kb	Chondrodystrophy	Dominant	1) Chinese Xingyi bantam;2) Japanese bantam	c
Dominant sex-linked dwarfism (some also called it bantam)	N.A.	N.A.	N.A.	Dominant (may be incomplete)	Golden Sebright bantam**	d
Crooked neck dwarfism(cn)	Suspected RYR1	N.A.	Muscular dysgenesis	Recessive	UCD-Crooked-neck dwarf.003	e
Autosomal dwarfism(adw)	TMEM263	Nonsense mutation Trp59*	Truncation of the transmembrane protein	Recessive	K-strain of White Leghorns	f
Bantam	HMGA2	Variants in intron or upstream region	N.A.	Polygenic	Dutch local population (e.g. Dutch bantam)	g

*Candidate gene name abbreviation

GHR: growth hormone receptor; *IHH*: Indian hedgehog; T*MEM263*: transmembrane protein 263; *HMGA2*: high mobility group AT-hook 2; *RYR1*: ryanodine receptor 1

**Studies suggested the factors for size are not all identical in bantams (Danforth, 1929; Custodio and Jaap, 1973).

#Reference

a: (Hutt, 1959; Burnside et al., 1991; Huang et al., 1993; Agarwal et al., 1994; Tanaka et al., 1995; Tahara et al., 2009; Ouyang et al., 2012); **b**: (Landauer, 1929); **c**:(Landauer, 1932; Jin et al., 2016; Kinoshita et al., 2020); **d**:(Maw, 1935); **e**:(Asmundson, 1945; Airey et al., 1993; Robb et al., 2011); **f**: (Cole and Hutt, 1973; Ruyter-Spira et al., 1998a, 1998b; Wu et al., 2018a (this thesis)); **g**: (Wandelt and Wolters, 1998; Esther Verhoef and Rijs, 2014; this thesis)

1.3.3 A short history of Dutch chicken breeds regarding bantam

In the Netherlands, historic chicken resources have received attention and admiration since at least the 16th century, and continued to be maintained in diverse forms (Woelders et al., 2006; Dana et al., 2011). The geographic locations and phenotypic characteristics were used to classify and name the Dutch chicken breeds, resulting in many subdivided groups or populations under different managements (Figure 1.2). The long tradition and diversification of Dutch chicken breeds have been profiled in many previous studies (Hillel et al., 2003; Dana et al., 2011; Elferink et al., 2012; Bortoluzzi et al., 2018). This in turn enhanced the utilization and preservation of the breeds as well as the different genetic variants by various organizations (private and governmental) (Woelders et al., 2006).

Throughout history, the traditional breeds in the Netherlands experienced bottlenecks due to, e.g., World War II and diseases (Bortoluzzi et al., 2018). Some breeds were lost in time but have been re-introduced and revived in the past decades (Dana et al., 2011; Bortoluzzi et al., 2018). Currently, populations exhibit a new ongoing bottleneck due to a reduction in the number of breeders (mostly hobby breeders), resulting in most breeds being vulnerable or in danger of becoming extinct (Bortoluzzi et al., 2018). This suggests the molecular characterization will offer detailed insights on the Dutch chicken breeds that can help in establishment of a conservation plan.

Up to now, almost half of the Dutch traditional breeds are neo-bantam breeds that with integrated genetics from bantams into normal-sized local breeds. This bantam-oriented integration between local breeds and existing bantams (true or neo) is conveyed through crossbreeding, also known as bantamization. Followed by backcrossing, the bantamization process finally resulted in numerous crossbred neo-bantam breeds. Neo-bantams are selected to exhibit the same/similar appearance as corresponding local breeds while having a smaller size. Usually a 50-60% reduction in body weight is desired. Apart from the neo-bantams in the Netherlands, some true bantam breeds including Dutch bantam, Dutch booted bantam and the Eikenburger bantam also exhibit precious genetic resources and cultural values in the context of body size variation (Dana et al., 2011; Bortoluzzi et al., 2018). Often these true bantams represent very old histories, e.g., a booted bantam features in a painting dating back to the16th century (van Wulfften Palthe, 1992). Bantam breeds of both Dutch and international origins have been extensively used in the last century to downsize the Dutch traditional breeds. Nowadays, for almost every Dutch traditional breed there is a corresponding bantam counterpart (Esther Verhoef and Rijs, 2014) (Figure 1.2). Despite the widened interest, the bantam phenotype in the Netherlands is yet to be characterized in terms of its genetic basis. The neo-bantams along with the corresponding normal-sized breeds make them a valuable proxy to study the molecular mechanisms underlying growth reduction in a case-control study.

Therefore, in this thesis, I aim to characterize, at the molecular level, the genetic causes and genomic mechanisms underlying dwarfisms in chicken, including the autosomal dwarfism and bantam traits.

Bantam breed in English (or in Dutch)	Abbrev.
Assendelft Fowl Bantam	AssFwB
Barnevelder Bantam	BarnevB
Brabanter Bantam	BrabB
Breda Fowl Bantam (Kraienkoppe)	BreFwB
Chaam Fowl	ChaFw
Drenthe Fowl Bantam	DrFwB
Drenthe Fowl Rumpless	DrFwBls
Dutch Bantam	DB
Dutch Booted Bantam	DBdB
Dutch Fowl Bantam	DFwB
Dutch Owl Bearded Bantam	DOwBdB
Dutch Polish Bearded Bantam	DPBdB
Dutch Polish non Bearded Bantam	DPnBdB
Eikenburger Bantam	Eikenb
Frisian Fowl Bantam	FriFwB
Groninger Mew Bantam	GrMwB
Kraienkoppe Fowl Bantam (Twentse)	KraiKFwB
Lakenvelder Bantam	LakVeB
North Holland Blue Bantam	NHBlB
Schijndelaar Bantam	SchijdB
Welsummer Bantam	WelsumB

Breeds exist in both bantam and normal-sized forms are highlighted.

Figure 1.2 The table at the left shows the Dutch chicken breeds. The figure at the right displays the map of the Netherlands with a representation of traditional indigenous breeds (adopted from https://www.kleindierliefhebbers.nl/).

1.4 Advantages of keeping dwarf chicken

In current poultry industry, introducing the dwarf/bantam trait and incorporating it into the breeding scheme can be of potential advantage and benefit (Merat, 1984; Mincheva et al., 2015). First of all, an obvious advantage of keeping dwarf chickens over the normal-sized fowl is reduced feed consumption and improved feed conversion rate (Mincheva et al., 2015). The saving on the feed of sex-linked dwarf (dw) hens is more than 20% during both rearing and egg production stages (Merat, 1984). In addition, thanks to their small size, keeping dwarf chickens can greatly save the space in animal houses, which is economically efficient and may be advantageous for animal welfare. Further interest is held for backyard breeders since less house spacing is required. For example, there is about a 40% reduction on stocking density in the breeding house for dw chickens (Merat, 1984). Additionally, because of the reduced feed intake, dwarf chickens are expected to dispense with restricted feeding which is usually adopted in the broiler industry to avoid dramatic weight gain causing poor performance, e.g., affected reproductive fertility and leg abnormality (Haye and Simons, 1978; Wilson et al., 1983; Bruggeman et al., 1999). Therefore, the use of

dwarf chicken potentially improves the management regarding animal welfare and reduces maintenance requirements. Moreover, there are hints about better heat tolerance of dwarf chickens due to reduced metabolic heat output in dwarf animals. Because dwarfs showed less severe heat stress and a better performance under torrid climates (Khan et al., 1987; Islam, 2005; Mincheva et al., 2015). However, other studies reported uncertain advantages in terms of performance under overheating conditions (Lin et al., 2006; Gowe and Fairfull, 2008). Furthermore, the immune response of dwarf chickens has been presumed to be better compared to that of normal-sized birds. In particular, sex-linked dwarf fowl showed higher resistance to Marek's disease (Merat, 1984; Islam, 2005), which is related to the association between growth hormone levels and Marek's disease resistance (Liu et al., 2001). Specifically, it suggested that dwarf birds generally demonstrate a stronger cell-mediated immune response, and may have more competent T-cell subpopulations and weaker B-cell reactivity (Klingensmith et al., 1983).

With the above-mentioned advantages, hypothetically, introducing a recessive dwarf/bantam trait can be of high value in a breeding program. This can be beneficial for both industrial animal production (e.g., a four-way crossing strategy) and smallholder farmers (e.g., hobby breeders). However, the question remains whether the dwarf or bantam genes are unaffected on performance (e.g., with side-effect) and are desirable for popularization and commercial applications. This knowledge will highlight the feasibility of utilizing dwarf and introducing the phenotype into current poultry industry.

1.5 Challenges and open questions

1.5.1 Determination of the phenotypic heterogeneity of dwarfism

To utilize dwarf phenotypes requires better insight into the phenotype of dwarfism. Dwarf phenotype determination is mostly based on morphological and anatomical features of the dwarf fowl. Measuring the reduction of the trunk size and the length of the long bones, especially the tibia and tarsometatarsus, can be particularly helpful to determine whether the phenotype represents proportionate or disproportionate dwarfism (Guillaume, 1976). Additional determination is based on physiological and biochemical indexes. Examining the abundance and composition of hormones regulating body growth (e.g., GH, IGF-I and thyroid) can usually further help to characterize the phenotype. One of the challenges in determining dwarf phenotypes is that the levels of circulating hormones in the blood are highly variable during the growth of chickens, which could lead to uncertainty and misinterpretation of the phenotype. Moreover, distinguishing dwarf phenotypes can be difficult because the chicks may not show any difference in size during the first few weeks after hatch (e.g., dw).

1.5.2 Genetic basis of dwarfism

Another important question to answer, following the determination of phenotype, is the genetic basis of different dwarfism phenotypes, i.e., what the mode of inheritance is and what the causative genetic variants are. Many strategies exist for mapping causative genetic loci for respective phenotypes in farm animals (Andersson, 2001). Before genomic approaches became available, experimental crosses (e.g., test cross) between contrasting sized chickens had already been applied as a solution to genetic mapping, inspired and introduced by Gregor Mendel (Danforth, 1929; Hutt, 1949). Since the early 90s, many experimental lines and mutant stocks have been developed acting as a model for studying size variations (Danforth, 1929; Landauer, 1932; Hutt, 1949). Nowadays, advances in genomics have allowed genome-wide association studies (GWAS) as a powerful approach to detect the genetic variants that may underlie the phenotype (Hardy and Singleton, 2009; Schaid et al., 2018). Mapping the causative genetic variant is relatively straightforward for a simple monogenic Mendelian trait, inherited by a single locus or limited number of loci (Visscher et al., 2017). However, whether dwarfism(s) is a monogenic or polygenic trait varies among different types of dwarfism. So far, the reported genetic loci are mostly monogenic, however, the growth of an animal is a generally highly polygenic trait. In human for example, more than 700 variants have been reported to be associated with height (Weedon et al., 2008; Allen et al., 2010; Marouli et al., 2017). Previous studies have shown that dwarfisms in chickens can evolve from variants in separate biological pathways, facilitated by different underlying breed histories (Wang et al., 2017; Yuan et al., 2018). Bantams in the Netherlands appear to be caused by polygenic inheritance (Wandelt and Wolters, 1998) indicating that the accumulation of short stature alleles at several distinct quantitative trait loci (QTL) is an alternative scenario for growth reduction.

The extended challenge with dwarf traits lies in untangling its genetic heterogeneity. The genetic heterogeneity is the state of that different genetic causes determine the similar/same phenotype. Two scenarios of genetic heterogeneity are known, allelic heterogeneity (multiple causative variants at the same locus) and locus heterogeneity (multiple causative genes) (Korte and Farlow, 2013). Therefore, there is no reason to believe that different dwarf phenotypes are necessarily inherited in the same way. Even for subclasses of sex-linked dwarfism, there are different underlying genetic determinants (causative mutations) including a deletion and a point mutation (Table 1.1).

1.5.3 Dissection of population structure mediated by selective breeding

The ability of genomic strategies to identify genes and variants associated with dwarfism depends largely on the study population. Segregating alleles in a phenotypically variable population are important for identifying the candidate

genomic regions, which usually exist as haplotype blocks composed of the causative mutation and its surrounding variants in Linkage Disequilibrium (LD). Because populations differ in allele frequencies and sample size, the local haplotype structure is often difficult to disentangle (Schaid et al., 2018). Allele frequency differences can subdivide the population based on the genetic composition (i.e., population stratification), which leads to possible confounding effects in GWAS analyses (Price et al., 2010). The power of a study can be increased by improving the sample size e.g., by pooling data from different studies or by applying meta-analyses. However, this in turn increases the potential of phenotypic and genetic heterogeneity (Evangelou and Ioannidis, 2013; Schaid et al., 2018). In particular, the population structure of local traditional breeds can be more complex relative to that of selective inbred lines, resulted from diverse and unsupervised human-mediated hybridizations. In particular, this human-mediated selective breeding is a challenge in defining the genetic basis and assigning the ancestral group of the population (Evangelou and Ioannidis, 2013).

1.6 Aims and outline of this thesis

In this thesis, I aimed to study the genetic and genomic basis of dwarfism(s) in chickens. First, I investigate different phenotypes of chicken dwarfism, and perform genomic analyses to detect the causative genes and variants underlying the phenotypes using whole genome sequence data. With this objective, I performed a series of analyses to map two types of dwarfism in chickens: autosomal dwarfism (adw) and bantam. Second, I utilize the genetic resources of Dutch dwarf chickens (i.e., bantam breeds) to study the influence of human-mediated crossbreeding. A Schematic overview of the outline of the thesis is presented in Figure 1.3.

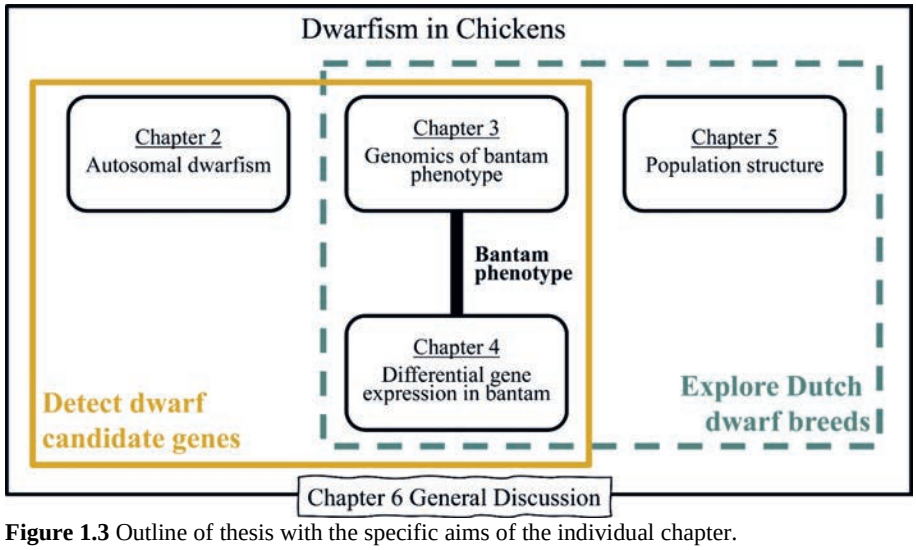

Figure 1.3 Outline of thesis with the specific aims of the individual chapter.

In **Chapter 2**, I performed genetic mapping to identify the causative variants underlying autosomal dwarfism (adw). Applying functional and comparative analyses provides insight how a novel loss-of-function mutation alters the body growth and development of adw chicken. In **Chapter 3** and **Chapter 4**, I addressed the phenotype of bantam in different breeds, using the (neo-)bantam breeds from the Netherlands as a proxy. In **Chapter 3**, I characterize the associated genetic variants underlying the bantam phenotype. To do so, I studied the matching pairs of Dutch native breeds that exhibit normal-sized and (neo-)bantam phenotypes. Using a series of genomic analyses, including Genome-Wide Association Studies (GWAS) and a meta-analysis based on whole-genome sequence data, I reveal the heterogeneity of the bantam breeds. The genetic heterogeneity among divergent bantam groups is illustrated by the associated patterns and haplotype diversity. I further examined how the introgression of bantam haplotypes during the crossbreeding can contribute to and reshape the genomic characteristics of bantam chickens. To further our insight in the mechanisms of the bantam phenotype, I studied the bantam embryos and identified differentially expressed genes between bantam and normal-sized samples using RNA-Seq data (**Chapter 4**). In **Chapter 5**, I further addressed the genomic influence of bantam crossbreeding on the complex population structure of Dutch chicken breeds and studied the impact of phenotypic selection and geography. Finally, in **Chapter 6**, I present the overall findings of this thesis contributing to the knowledge of chicken dwarfisms, especially in the population genetics and functional genomics aspects. I further discuss the attempt to validate the causal effect of an adw candidate mutation in *TMEM263* gene by using the genome-editing tool in a model organism (zebrafish). Moreover, I discuss the potential utilization of dwarf phenotypes and how to apply into poultry breeding.

1.7 Reference

Agarwal, S. K., Cogburn, L. A., and Burnside, J. (1994). Dysfunctional growth hormone receptor in a strain of sex-linked dwarf chicken: Evidence for a mutation in the intracellular domain. *J. Endocrinol.* 142, 427–434. doi:10.1677/joe.0.1420427.

Airey, J. A., Baring, M. D., Beck, C. F., Chelliah, Y., Deerinck, T. J., Ellisman, M. H., et al. (1993). Failure to make normal α ryanodine receptor is an early event associated with the Crooked Neck Dwarf (cn) mutation in chicken. *Dev. Dyn.* 197, 169–188. doi:10.1002/aja.1001970303.

Allen, H. L., Estrada, K., Lettre, G., Berndt, S. I., Weedon, M. N., Rivadeneira, F., et al. (2010). Hundreds of variants clustered in genomic loci and biological pathways affect human height. *Nature* 467, 832–838. doi:10.1038/nature09410.

Andersson, L. (2001). Genetic dissection of phenotypic diversity in farm animals. *Nat. Rev. Genet.* 2, 130–138. doi:10.1038/35052563.

Asmundson, V. S. (1945). Crooked neck dwarf in the domestic fowl. *J. Hered.* 36, 173–176. doi:10.1093/oxfordjournals.jhered.a105491.

Boegheim, I. J. M., Leegwater, P. A. J., van Lith, H. A., and Back, W. (2017). Current insights into the molecular genetic basis of dwarfism in livestock. *Vet. J.* 224, 64–75. doi:10.1016/j.tvjl.2017.05.014.

Bortoluzzi, C., Bosse, M., Derks, M. F. L., Crooijmans, R. P. M. A., Groenen, M. A. M., and Megens, H. J. (2020). The type of bottleneck matters: Insights into the deleterious variation landscape of small managed populations. *Evol. Appl.* 13, 330–341. doi:10.1111/eva.12872.

Bortoluzzi, C., Crooijmans, R. P. M. A., Bosse, M., Hiemstra, S. J., Groenen, M. A. M., and Megens, H. J. (2018). The effects of recent changes in breeding preferences on maintaining traditional Dutch chicken genomic diversity. *Heredity (Edinb).* 121, 564–578. doi:10.1038/s41437-018-0072-3.

Bouwman, A. C., Daetwyler, H. D., Chamberlain, A. J., Ponce, C. H., Sargolzaei, M., Schenkel, F. S., et al. (2018). Meta-analysis of genome-wide association studies for cattle stature identifies common genes that regulate body size in mammals. *Nat. Genet.* 50, 362–367. doi:10.1038/s41588-018-0056-5.

Bruggeman, V., Onagbesan, O., D'Hondt, E., Buys, N., Safi, M., Vanmontfort, D., et al. (1999). Effects of timing and duration of feed restriction during rearing on reproductive characteristics in broiler breeder females. *Poult. Sci.* 78, 1424–1434. doi:10.1093/ps/78.10.1424.

Burnside, J., Liou, S. S., Cogburn, L. A., and Burnside, J. (1991). Molecular cloning of the chicken growth hormone receptor complementary deoxyribonucleic acid: Mutation of the gene in sex-linked dwarf chickens. *Endocrinology* 128, 3183–3192. doi:10.1210/endo-128-6-3183.

Carneiro, M., Hu, D., Archer, J., Feng, C., Afonso, S., Chen, C., et al. (2017). Dwarfism and altered craniofacial development in rabbits is caused by a 12.1 kb deletion at the HMGA2 locus. *Genetics* 205, 955–965. doi:10.1534/genetics.116.196667.

Carroll, L. (1865). *Alice's Adventures in Wonderland*.

Cavanagh, J. A. L., Tammen, I., Windsor, P. A., Bateman, J. F., Savarirayan, R., Nicholas, F. W., et al. (2007). Bulldog dwarfism in Dexter cattle is caused by mutations in ACAN. *Mamm. Genome* 18, 808–814. doi:10.1007/s00335-007-9066-9.

Cole, R. F., and Hutt, F. B. (1973). Selection of heterosis in Cornell White Leghorns: a review, with special consideration of interstrain hybrids. *Anim. Breed. Abstr.* 41, 103–118.

Cole, R. K. (2000). An autosomal dwarfism in the domestic fowl. *Poult. Sci.* 79, 1507–1516. doi:10.1093/ps/79.11.1507.

Coleman, M. E., Demayo, F., Kuo Chang Yin, Heung Man Lee, Geske, R., Montgomery, C., et al. (1995). Myogenic vector expression of insulin-like growth factor I stimulates muscle cell differentiation and myofiber hypertrophy in transgenic mice. *J. Biol. Chem.* 270, 12109–12116. doi:10.1074/jbc.270.20.12109.

Custodio, R. W., and Jaap, R. G. (1973). Sex-linked reduction of body size in Golden Sebright Bantams. *Poult. Sci.* 52, 204–210. doi:10.3382/ps.0520204.

Dana, N., Megens, H. J., Crooijmans, R. P. M. A., Hanotte, O., Mwacharo, J., Groenen, M. A. M., et al. (2011). East asian contributions to dutch traditional and western commercial chickens inferred from mtDNA analysis. *Anim. Genet.* 42, 125–133. doi:10.1111/j.1365-2052.2010.02134.x.

Danforth, C. H. (1929). Bantam Genetics. *J. Hered.* 20, 573–582. doi:10.1093/oxfordjournals.jhered.a103139.

Deng, J. Z., Hao, L. L., Li, M. T., Lang, S., Zeng, Y. Z., Liu, S. C., et al. (2011). Growth hormone and receptor gene mutations in Chinese Banna miniature pig. *Animal Cells Syst. (Seoul).* 15, 310–314. doi:10.1080/19768354.2011.616644.

Elferink, M. G., Megens, H. J., Vereijken, A., Hu, X., Crooijmans, R. P. M. A., and Groenen, M. A. M. (2012). Signatures of selection in the genomes of commercial and non-commercial chicken breeds. *PLoS One* 7, e32720. doi:10.1371/journal.pone.0032720.

Esther Verhoef, and Rijs, A. (2014). *De kippen encyclopedie*. Rebo Productions.

Evangelou, E., and Ioannidis, J. P. A. (2013). Meta-analysis methods for genome-wide association studies and beyond. *Nat. Rev. Genet.* 14, 379–389. doi:10.1038/nrg3472.

Godfrey, E. F. (1953). The Genetic Control of Growth and Adult Body Weight in the Domestic Fowl. *Poult. Sci.* 32, 248–259.

Godowski, P. J., Leung, D. W., Meacham, L. R., Galgani, J. P., Hellmiss, R., Keret, R., et al. (1989). Characterization of the human growth hormone receptor gene and demonstration of a partial gene deletion in two patients with Laron-type dwarfism. *Proc. Natl. Acad. Sci. U. S. A.* 86, 8083–7. doi:10.1073/pnas.86.20.8083.

Gowe, R. S., and Fairfull, R. W. (2008). "Breeding for resistance to heat stress," in *Poultry Production in Hot Climates: Second Edition*, 13–29. doi:10.1079/9781845932589.0000.

Guillaume, J. (1976). The Dwarfing Gene dw: Its Effects on Anatomy, Physiology, Nutrition, Management. Its Application in Poultry Industry. *Worlds. Poult. Sci. J.* 32, 285–305. doi:10.1079/wps19760009.

Haddad, F., and Adams, G. R. (2004). Inhibition of MAP/ERK kinase prevents IGF-I-induced hypertrophy in rat muscles. *J. Appl. Physiol.* 96, 203–210. doi:10.1152/japplphysiol.00856.2003.

Hardy, J., and Singleton, A. (2009). Genomewide association studies and human disease. *N. Engl. J. Med.* 360, 1759–1768. doi:10.1056/NEJMra0808700.

Haye, U., and Simons, P. C. M. (1978). Twisted Legs in Broilers. *Br. Poult. Sci.* 19, 549–557. doi:10.1080/00071667808416512.

Hillel, J., Groenen, M. A. M., Tixier-Boichard, M., Korol, A. B., David, L., Kirzhner, V. M., et al. (2003). Biodiversity of 52 chicken populations assessed by microsatellite typing of DNA pools. 35. Available at: http://www.gsejournal.org/content/35/6/533 [Accessed April 30, 2018].

Hillier, L. W., Miller, W., Birney, E., Warren, W., Hardison, R. C., Ponting, C. P., et al. (2004). Sequence and comparative analysis of the chicken genome provide unique perspectives on vertebrate evolution. *Nature* 432, 695–716. doi:10.1038/nature03154.

Holderread, D. (2011). *Storey's Guide to Raising Ducks: Breeds, Care, Health*. , ed. 2 Storey Publishing Available at: https://books.google.nl/books?hl=en&lr=&id=sB6g95tyzg4C&oi=fnd&pg=PR5&dq=bantam+ducks+&ots=LvCQ7Z78Nz&sig=Jx-Wfo7qt_tCfZcdzwV4bR9v7pk&redir_esc=y#v=onepage&q=bantam ducks&f=false [Accessed September 22, 2020].

Hu, S. Y., Tai, C. C., Li, Y. H., and Wu, J. L. (2012). Progranulin compensates for blocked IGF-1 signaling to promote myotube hypertrophy in C2C12 myoblasts via the PI3K/Akt/mTOR pathway. *FEBS Lett.* 586, 3485–3492. doi:10.1016/j.febslet.2012.07.077.

Huang, N., Cogburn, L. A., Agarwal, S. K., Marks, H. L., and Burnside, J. (1993). Overexpression of a truncated growth hormone receptor in the sex-linked dwarf chicken: evidence for a splice mutation. *Mol Endocrinol.* 7, 1391–1398. doi:10.1210/mend.7.11.8114754.

Hutt, F. B. (1949). *Genetics of the fowl*. 1st ed. New York, NY: McGraw-Hill.

Hutt, F. B. (1959). Sex-linked dwarfism in the fowl. *J. Hered.* 50, 209–221. doi:10.1093/oxfordjournals.jhered.a106909.

Islam, M. A. (2005). Sex-linked dwarf gene for broiler production in hot-humid climates. *Asian-Australasian J. Anim. Sci.* 18, 1662–1668. doi:10.5713/ajas.2005.1662.

Jin, S., Zhu, F., Wang, Y., Yi, G., Li, J., Lian, L., et al. (2016). Deletion of Indian hedgehog gene causes dominant semi-lethal Creeper trait in chicken. *Sci. Rep.* 6, 30172. doi:10.1038/srep30172.

Johansson, A. M., Pettersson, M. E., Siegel, P. B., and Carlborg, Ö. (2010). Genome-Wide Effects of Long-Term Divergent Selection. *PLoS Genet.* 6, e1001188. doi:10.1371/journal.pgen.1001188.

Khan, A. G., Tiwari, R. N. S., Baghel, K. K. S., and Gupta, R. D. (1987). Influence of the dwarfing gene dw on egg production and viability under summer heat stress. *Br. Poult. Sci.* 28, 541–546. doi:10.1080/00071668708416988.

Kinoshita, K., Suzuki, T., Koike, M., Nishida, C., Koike, A., Nunome, M., et al. (2020). Combined deletions of IHH and NHEJ1 cause chondrodystrophy and embryonic lethality in the Creeper chicken. *Commun. Biol.* 3, 1–11. doi:10.1038/s42003-020-0870-z.

Klingensmith, P. M., Donahoe, J. P., and Stephens, J. F. (1983). The effect of the sex-linked dwarfing gene, dw, on the immune responses of broiler breeder chickens. *Poult. Sci.* 62, 733–740. doi:10.3382/ps.0620733.

Korte, A., and Farlow, A. (2013). The advantages and limitations of trait analysis with GWAS: A review. *Plant Methods* 9. doi:10.1186/1746-4811-9-29.

Landauer, W. (1929). Thyrogenous dwarfism (myxoedema infantilis) in the domestic fowl. *Am. J. Anat.* 43, 1–42. doi:10.1002/aja.1000430102.

Landauer, W. (1932). Studies on the Creeper fowl. *J. Genet.* 26, 285–290. doi:10.1007/BF02984694.

Leenstra, F., Congress, R. P.-17th W. P., Helsinki, U., August, 8-12, and 1984, U. (1984). The autosomal dwarf as broiler sire mated to normal and sexlinked dwarf broiler dams: performance of progeny. in *17th World's Poultry congress* (Helsinki).

Lin, H., Jiao, H. C., Buyse, J., and Decuypere, E. (2006). Strategies for preventing heat stress in poultry. *Worlds. Poult. Sci. J.* 62. doi:10.1079/WPS200585.

Liu, C., Zheng, S., Gui, J., Fu, C., Yu, H., Song, D., et al. (2018). Shortened Basal Internodes Encodes a Gibberellin 2-Oxidase and Contributes to Lodging Resistance in Rice. *Mol. Plant* 11, 288–299. doi:10.1016/j.molp.2017.12.004.

Liu, H. C., Kung, H. J., Fulton, J. E., Morgan, R. W., and Cheng, H. H. (2001). Growth hormone interacts with the Marek's disease virus SORF2 protein and is associated with disease resistance in chicken. *Proc. Natl. Acad. Sci. U. S. A.* 98, 9203–9208. doi:10.1073/pnas.161466898.

Luo, W., Lin, S., Li, G., Nie, Q., and Zhang, X. (2016). Integrative analyses of miRNA-mRNA interactions reveal let-7b, miR-128 and MAPK pathway involvement in muscle mass loss in sex-linked dwarf chickens. *Int. J. Mol. Sci.* 17, 276. doi:10.3390/ijms17030276.

Malomane, D. K., Reimer, C., Weigend, S., Weigend, A., Sharifi, A. R., and Simianer, H. (2018). Efficiency of different strategies to mitigate ascertainment bias when using SNP panels in diversity studies. *BMC Genomics* 19, 22. doi:10.1186/s12864-017-4416-9.

Marouli, E., Graff, M., Medina-Gomez, C., Lo, K. S., Wood, A. R., Kjaer, T. R., et al. (2017). Rare and low-frequency coding variants alter human adult height. *Nature* 542, 186–190. doi:10.1038/nature21039.

Maw, A. J. G. (1935). The Inheritance of Skeletal Dimensions in the Domestic Fowl. *Sci. Agric.* 16, 85–112.

Merat, P. (1984). The sex-linked dwarf gene in the broiler chicken industry. *Worlds. Poult. Sci. J.* 40, 10–18. doi:10.1079/wps19840002.

Mincheva, N., Oblakova, M., Hristakieva, P., Ivanova, I., and Lalev, M. (2015). Effect of sex-linked dwarf gene on exterior appearance, productive performance and egg characteristics in a colored broiler dam line. *Biotechnol. Anim. Husb.* 31, 163–174.

Ouyang, J. H., Xie, L., Nie, Q. H., Zeng, H., Peng, Z. J., Zhang, D. X., et al. (2012). The Effects of Different Sex-Linked Dwarf Variations on Chinese Native Chickens. *J. Integr. Agric.* 11, 1500–1508. doi:10.1016/S2095-3119(12)60150-6.

Parker, H. G., VonHoldt, B. M., Quignon, P., Margulies, E. H., Shao, S., Mosher, D. S., et al. (2009). An expressed fgf4 retrogene is associated with breed-defining chondrodysplasia in domestic dogs. *Science (80-.).* 325, 995–998. doi:10.1126/science.1173275.

Plassais, J., Kim, J., Davis, B. W., Karyadi, D. M., Hogan, A. N., Harris, A. C., et al. (2019). Whole genome sequencing of canids reveals genomic regions under selection and variants influencing morphology. *Nat. Commun.* 10, 1489. doi:10.1038/s41467-019-09373-w.

Polly, P. D. (2012). Measuring the evolution of body size in mammals. *Proc. Natl. Acad. Sci. U. S. A.* 109, 4027–4028. doi:10.1073/pnas.1201030109.

Potts, A. (2012). *Chicken*. Reaktion books.

Price, A. L., Zaitlen, N. A., Reich, D., and Patterson, N. (2010). New approaches to population stratification in genome-wide association studies. *Nat. Rev. Genet.* 11, 459–463. doi:10.1038/nrg2813.

Rafati, N., Andersson, L. S., Mikko, S., Feng, C., Raudsepp, T., Pettersson, J., et al. (2016). Large deletions at the SHOX locus in the pseudoautosomal region are associated with skeletal atavism in shetland ponies. *G3 Genes, Genomes, Genet.* 6, 2213–2223. doi:10.1534/g3.116.029645.

Reimer, C., Rubin, C.-J., Sharifi, A. R., Ha, N.-T., Weigend, S., Waldmann, K.-H., et al. (2018). Analysis of porcine body size variation using re-sequencing data of miniature and large pigs. *BMC Genomics* 19, 687. doi:10.1186/s12864-018-5009-y.

Rimbault, M., Beale, H. C., Schoenebeck, J. J., Hoopes, B. C., Allen, J. J., Kilroy-Glynn, P., et al. (2013). Derived variants at six genes explain nearly half of size reduction in dog breeds. *Genome Res.* 23, 1985–1995. doi:10.1101/gr.157339.113.

Robb, E. A., Gitter, C. L., Cheng, H. H., and Delany, M. E. (2011). Chromosomal mapping and candidate gene discovery of chicken developmental mutants and genome-wide variation analysis of MHC congenics. *J. Hered.* 102, 141–156. doi:10.1093/jhered/esq122.

Roy, K. (2008). Evolution: Dynamics of body size evolution. *Science (80-.).* 321, 1451–1452. doi:10.1126/science.1163097.

Ruyter-Spira, C. P., De Groof, A. J. C., Van Der Poel, J. J., Herbergs, J., Masabanda, J., Fries, R., et al. (1998a). The HMGI-C gene is a likely candidate for the autosomal dwarf locus in the chicken. *J. Hered.* 89, 295–300. doi:10.1093/jhered/89.4.295.

Ruyter-Spira, C. P., Herbergs, J., Limpens, E., Marsh, J. A., Van Der Poel, J. J., Ayoubi, T. A. Y., et al. (1998b). Nucleotide sequence of the chicken HMGI-C cDNA and expression of the HMGI-C and IGF1 genes in autosomal dwarf chicken embryos. *Biochim. Biophys. Acta - Gene Struct. Expr.* 1399, 83–87. doi:10.1016/S0167-4781(98)00101-8.

Schaid, D. J., Chen, W., and Larson, N. B. (2018). From genome-wide associations to candidate causal variants by statistical fine-mapping. *Nat. Rev. Genet.* 19, 491–504. doi:10.1038/s41576-018-0016-z.

Sheng, Z., Pettersson, M. E., Honaker, C. F., Siegel, P. B., and Carlborg, Ö. (2015). Standing genetic variation as a major contributor to adaptation in the Virginia chicken lines selection experiment. *Genome Biol.* 16, 219. doi:10.1186/s13059-015-0785-z.

Shirley, E. D., and Ain, M. C. (2013). "Achondroplasia," in *Brenner's Encyclopedia of Genetics: Second Edition* (Elsevier Inc.), 4–6. doi:10.1016/B978-0-12-374984-0.00005-X.

Simianer, H., and Köhn, F. (2010). Genetic management of the Göttingen Minipig population. *J. Pharmacol. Toxicol. Methods* 62, 221–226. doi:10.1016/j.vascn.2010.05.004.

Tahara, K., Tsukada, A., Hanai, T., Okumura, K., Yamada, K., Murai, A., et al. (2009). Identification of Two Types of Growth Hormone Receptor Mutations in Two Strains of Sex-linked Dwarf Chickens. *J. Poult. Sci.* 46, 249–256. doi:10.2141/jpsa.46.249.

Tanaka, M., Hayashida, Y., Wakita, M., Hoshino, S., and Nakashima, K. (1995). Expression of aberrantly spliced growth hormone receptor mRNA in the sex-linked dwarf chicken, Gifu 20.(abstrct). *Growth Regul.* 5, 218–23. Available at: http://www.ncbi.nlm.nih.gov/pubmed/8745148 [Accessed January 10, 2017].

van Wulfften Palthe, A. W. (1992). *C.S.Th.Van Gink's poultry paintings (1890-1968)*. Dutch branch of the world's poultry science association.

Visscher, P. M., Wray, N. R., Zhang, Q., Sklar, P., McCarthy, M. I., Brown, M. A., et al. (2017). 10 Years of GWAS Discovery: Biology, Function, and Translation. *Am. J. Hum. Genet.* 101, 5–22. doi:10.1016/j.ajhg.2017.06.005.

Wandelt, R., and Wolters, J. (1998). "Handbuch der Zwerghuhnrassen: die Zwerghuhnrassen der Welt," in (Bottrop: Verlag Wolters), 14–15.

Wang, M.-S., O. Otecko, N., Wang, S., Wu, D.-D., Yang, M.-M., Xu, Y.-L., et al. (2017). An Evolutionary Genomic Perspective on the Breeding of Dwarf Chickens. *Mol. Biol. Evol.* doi:10.1093/molbev/msx227.

Wang, M.-S., Thakur, M., Peng, M.-S., Jiang, Y., Frantz, L. A. F., Li, M., et al. (2020). 863 genomes reveal the origin and domestication of chicken. *Cell Res.*, 1–9. doi:10.1038/s41422-020-0349-y.

Weedon, M. N., Lango, H., Lindgren, C. M., Wallace, C., Evans, D. M., Mangino, M., et al. (2008). Genome-wide association analysis identifies 20 loci that influence adult height. *Nat. Genet.* 40, 575–583. doi:10.1038/ng.121.

Wilson, H. R., Ingram, D. R., and Harms, R. H. (1983). Restricted feeding of broiler breeders. *Poult. Sci.* 62, 1133–1141. doi:10.3382/ps.0621133.

Woelders, H., Zuidberg, C. A., and Hiemstra, S. J. (2006). Animal genetic resources conservation in The Netherlands and Europe: Poultry perspective. *Poult. Sci.* 85, 216–222. doi:10.1093/ps/85.2.216.

Wu, Z., Derks, M. F. L., Dibbits, B., Megens, H. J., Groenen, M. A. M., and Crooijmans, R. P. M. A. (2018a). A novel loss-of-function variant in transmembrane protein 263 (TMEM263) of autosomal dwarfism in chicken. *Front. Genet.* 9, 193. doi:10.3389/fgene.2018.00193.

Wu, Z., Tang, D., Liu, K., Miao, C., Zhuo, X., Li, Y., et al. (2018b). Characterization of a new semi-dominant dwarf allele of SLR1 and its potential application in hybrid rice breeding. *J. Exp. Bot.* 69, 4703–4713. doi:10.1093/jxb/ery243.

Yuan, Y., Peng, D., Gu, X., Gong, Y., Sheng, Z., and Hu, X. (2018). Polygenic basis and variable genetic architectures contribute to the complex nature of body weight -A genome-wide study in four Chinese indigenous chicken breeds. *Front. Genet.* 9, 229. doi:10.3389/fgene.2018.00229.

2

A novel loss-of-function variant in transmembrane protein 263 (TMEM263) of autosomal dwarfism in chicken

Zhou Wu[1], Martijn F.L. Derks[1], Bert Dibbits[1], Hendrik-Jan Megens[1], Martien A.M. Groenen[1], Richard P.M.A. Crooijmans[1]

[1] Wageningen University & Research, Animal Breeding and Genomics, P.O. Box 338, 6700 AH, Wageningen, the Netherlands

Based on *Frontiers in Genetics* (2018) 9:193

Abstract

Autosomal dwarfism (adw) in chickens is a growth deficiency caused by a recessive mutation. Characteristic for autosomal dwarfism is an approximately 30% growth reduction with short shank. The adw variant was first recognized in the Cornell K-strain of White Leghorns, but the genetic causal variant remained unknown.

To identify the causal variant underlying the adw phenotype, fine mapping was conducted on chromosome 1, within 52 to 56 Mb. This region was known to harbor the causal variant from previous linkage studies. We compared whole-genome sequence data of this region from normal-sized and adw chickens in order to find the unique causal variant. We identified a novel nonsense mutation NP_001006244.1:p.(Trp59*), in the transmembrane protein 263 gene (*TMEM263*), completely associated with autosomal dwarfism. The nonsense mutation truncates the transmembrane protein within the membrane-spanning domain, expected to cause a dysfunctional protein. *TMEM263* is reported to be associated with bone mineral deposition in humans, and the protein shows interaction with growth hormone 1 (GH1). Our study presents molecular genetic evidence for a novel loss-of-function variant, which likely alters body growth and development in autosomal dwarf chicken.

Keywords: Autosomal dwarfism, body size, recessive trait, chicken, loss-of-function mutation

2.1 Introduction

Unusually short body stature, known as dwarfism, is a condition of growth deficiency and reduced body weight caused by a variety of hereditary and hormonal disruptions. In humans, different dwarf syndromes have been characterized by genetic mutations affecting a wide range of genes (Godowski et al., 1989; Mortier et al., 2000; Richette et al., 2008). Various short body statures have also been investigated in animal species including dogs, cattle, pigs, and chickens (Boegheim et al., 2017). Dwarf animals in native or commercial breeds, have held the interest of humans over the past century, and have been bred for either ornamental or economic reasons. For example, plenty of distinct dwarf phenotypes have been described and studied in the chicken literature (Hutt, 1949). One of the best-studied hereditary variations in growth deficiency is sex-linked dwarfism, which is a proportional dwarfism, caused by the mutation in the *GHR* (Agarwal et al., 1994; Burnside et al., 1991).

Autosomal dwarfism (adw) in chicken is a recessive trait resulting in reduced body weight with short stature, despite the normal hormonal concentration of GH and insulin-like growth factor 1 (IGF1). The locus responsible for chicken autosomal dwarfism (*adw*) was first, and uniquely, found in a Cornell K-strain of White Leghorns, and shown to be caused by a recessive single locus (Cole and Hutt, 1973). The overall appearance of autosomal dwarf chicken was recognized as a small body stature by short shank length, with 30-40% reduced adult body weight (Cole, 1973, 2000). Investigations into known hormonal factors related to body growth showed no significant decrease in the plasma concentrations of GH and IGF1 compared with normal animals, which is distinct from other types of dwarfisms (Scanes et al., 1983; Huybrechts et al., 1985). Only a slight decrease in plasma thyroid hormones T3 and T4 was observed (Lam et al., 1989). Therefore, autosomal dwarfism is not considered to be determined by a direct genetic aberration in the GH-IGF1 molecular pathway, which is known to determine body size in other vertebrates (Yakar et al., 2002). While the metabolic and genetic factors underlying adw have been studied (Huybrechts et al., 1985; Ruyter-Spira et al., 1998a; Scanes et al., 1983), the causative variation determining the autosomal dwarf locus have remained elusive. The *adw* locus was mapped to chromosome 1, by using bulked segregant analysis with microsatellite markers (Ruyter-Spira et al., 1998a). In that study, genotype frequencies of markers were evaluated respectively from affected and unaffected individuals in the autosomal dwarf segregating population. The *adw* locus is closely linked to microsatellite marker LEI0146 on chromosome 1, with a recombination fraction of 0.03 and LOD score of 31.98 (Ruyter-Spira et al., 1998a). Two potential candidate genes were harbored in the region associated; the gene coding for the high-mobility group protein I-C (*HMGI-C*), an alias for *HMGA2*, and *IGF1* (Ruyter-Spira et al., 1998a). A continuation of this research showed no mutations in the coding sequence of these two genes, and no difference in expression of *HMGA2* (Ruyter-Spira et al., 1998b). With the whole-

genome sequence techniques, we are now able to explore the *adw* genome. In the present study, we aimed to identify the *adw* associated region and the potential causal variant underlying the autosomal dwarf phenotype.

2.2 Method and materials

2.2.1 Animals used for sequencing and genotyping

To identify the variant underlying autosomal dwarfism, we performed the whole-genome sequencing on a 6-day homozygous embryo (*adw/adw*), collected from the mating dwarf parents. For candidate validation; we genotyped two 6-day and one 8-day old dwarf embryos (*adw/adw*), as well as two pooled sperm samples from 20 Cornish and 20 White Leghorn adw cocks respectively. In addition, two normal-sized embryos; 6 and 8 days of age respectively, were used as controls for genotype and expression analyses. The dwarf samples we used for this study have no genetic relationship.

2.2.2 Whole-genome sequencing and variant calling

Whole-genome sequence data were generated for the embryos of autosomal dwarf and normal-sized chickens. We sequenced the genomic DNA by Illumina HiSeq 2000 paired-end sequencing (2x100 bp read length). The sequence reads were then trimmed for quality using Sickle (Joshi and Fass, 2011). The software BWA-MEM (version 0.7.15) (Li and Durbin, 2009) was used to map the clean reads to the Red Jungle fowl genome assembly, with the build Gallus_gallus-5.0 (International Chicken Genome Consortium, 2015). Duplicate reads were removed by using Samtools dedup function (Li et al., 2009). Local realignment of the reads around small indel was done using GATK IndelRealigner (McKenna et al., 2010). We performed variant calling by using Freebayes with sound settings (-min-base-quality 10, -min-alternate-fraction 0.2, -haplotype-length 0, -pooled-continuous, -min-alternate-count 2) (Garrison and Marth, 2012). Variant filtering was conducted towards the SNPs and indels using VCFtools (Danecek et al., 2011), with a mean depth between 3 to 25, and genotype call rate >0.7. In addition, we used LUMPY to identify the structural variants, with the default settings for split-read detection (Layer et al., 2014). Functional annotation for all types of detected variants was generated by Variant Effect Predictor (VEP) (McLaren et al., 2016).

2.2.3 Mapping of adw candidate variant by sequence comparison

We used the previous linkage data to construct the candidate region. In the adw linkage study published by Ruyter-Spira et al. (1998a), the *adw* locus was mapped 3 cM downstream of marker LEI0146 (NC_006088.4:g.53,274,224_53,274,474). The average linkage resolution on chromosome 1 is around 0.3 to 0.4 Mb/cM (Groenen et al., 2009), which suggests the most likely location of *adw* is at around 54.1-54.4 Mb. Because of the mapping uncertainty, we used a margin of 2 Mb around this location

and therefore extended the candidate region from 52 to 56 Mb, which harbors *IGF1* for subsequent investigation. We used sequence data within the candidate interval from 261 White Leghorns as controls. We compared the genetic variants, including SNPs and indels, of the *adw/adw* chicken against the normal-sized controls by using VCFtools. We compared the allele at each position, and focused on the unique allele carried by adw for subsequent fine mapping. Schematic representations of the candidate region were visualized using Gviz (v1.22.2) (Hahne and Ivanek, 2016) with ideogram track and the gene of interest. For homozygosity analysis, we calculated the Runs of Homozygosity (ROH) to estimate autozygosity for the sequenced adw individual. ROHs for an individual were calculated based on the following criteria specified in Bosse et al., (2012). This included the number of SNPs, in a window size of 10 Kb, counted below 0.25 times the average whole-genome SNP count; and the homozygous stretches contained at least 10 consecutive windows which showed a total SNP average lower than the genomic average. Sufficiently covered windows with 0.5 to 2 times the average depths were taken into account. The relaxed threshold for individual windows were used within a homozygous stretch to avoid local assembly or alignment errors, which was done by allowing for maximum twice the genomic average SNP count, and the average SNP count within the candidate ROH to not exceed 1/4 the genomic average.

Fine mapping inside the candidate region was conducted by a four-step filtering procedure. In step 1, at each position, we compared unique variants that are only present in the adw dataset, and absent in the normal-sized White Leghorns. Autosomal dwarfism, inherited as a recessive trait, is expected to be homozygous for the *adw* locus. Therefore, in step 2, heterozygous sites were filtered out, and only the *adw* homozygous sites were kept for further analyses. In step 3, we filtered variants based on the consequence annotation. We predicted the variant consequence with the uniform terms defined by Sequence Ontology (Eilbeck and Lewis, 2004), using VEP (McLaren et al., 2016). The consequence terms evaluate the effect that each substitution may have, based on their properties on different transcripts, with more than one variant consequence. To help categorize the impact of the variants, we assessed the consequence terms with four impact categories; high, moderate, low, and modifier, by using SnpEff (Cingolani et al., 2012). We split the variant list into two groups: one containing variants with high and moderate impact, which likely alter protein structure and function; another list with variants of low to modifier impact, which are mostly non-coding variants. We investigated the expression among tissues of long intergenic non-coding RNAs (lincRNAs) in the list, the quantification of each lincRNAs was calculated and retrieved from two baseline transcriptome studies on Expression Atlas (Barbosa-Morais et al., 2012; Merkin et al., 2012; Petryszak et al., 2016, 2017). The missense variants were predicted with SIFT score (Sim et al., 2012), to estimate the alteration of the amino acid and the degree of conservatism among

species. The SIFT score defines a missense variant as “deleterious” (0 to 0.05) or “tolerated” (0.05 to 1). In step 4, we screened the public sequence and SNP repositories for novel variants. The *adw* mutation is not segregating within other population, hence variants identified in these other populations were excluded to ensure that potential causative mutations are not harbored by normal-sized population.

2.2.4 Validation of the adw mutation

Based on the fine mapping steps outlined above, three adw chicken embryos and two mixed sperms were genotyped to validate the candidate mutation. We performed genotyping for the mutation NM_001006244.1:c.433G>A on chromosome 1 in transmembrane protein 263 (*TMEM263*) by Polymerase Chain Reaction-Restriction Fragment Length Polymorphism (PCR-RFLP) analysis. We genotyped both dwarf (*adw/adw*) and normal-sized (*ADW/ADW*) chickens. The mutation in *TMEM263* was amplified with the following primers; TMEM263_1F: 5'-AGGTTCAATCAAAGACCACCCG-3'; TMEM263_1R: 5'-CCCGTTAAAGGCACTTTGCT-3'. The PCR products were then digested with the enzyme *Ddel* (New England Biolabs, UK) and analyzed by 3% agarose gel electrophoresis, the adw samples are expected to include fragments of 109 and 184 bp, while the normal-sized ones are expected with fragments of 294 bp.

2.2.5 Candidate gene expression analyses

We estimated the gene expression difference between the dwarf and normal-sized chicken for *TMEM263* and *IGF1*, using Reverse Transcription quantitative PCR (RT-qPCR). RNA was extracted from the same two 6-day and one 8-day old embryos used in genotyping, from which cDNA was synthesized. Three normal-sized embryos (*ADW/ADW*) of 6 and 8 days old respectively, were used as controls. We conducted three technical replicates for each sample. The expression differences were determined by the ΔΔCt method using 28s rRNA as a housekeeping gene for normalization. Target sequences were amplified from cDNA with the following primers, TMEM263_2F: 5'-GCCACCAGAAGGTTCAATCAAAG-3'; TMEM263_2R: 5'-CTGAAGATGCCACCAGTCACA-3'; IGF1_F: 5'-CTTGAAGGTGAAGATGCACACTG-3'; IGF1_R:5'-GGCAGCAGCAGAACTGGTTA-3'. The RT-qPCR was performed on an Applied Biosystems® 7500 Real-Time PCR Systems, using MESA Blue qPCR Mix Plus for SYBR Assay (Eurogentec, Belgium).

2.2.6 Functional comparative analyses of orthologous genes

As the function of TMEM263 protein in chicken is poorly characterized, we used the orthologous gene to investigate the potential function. A multi-species alignment of TMEM263 was generated by Clustal Omega (v1.2) (Sievers et al., 2014). The orthologous proteins of TMEM263 aligned were obtained from 10 representative

vertebrates (*D.rerio, H.sapiens, P.troglodytes, M.mulatta, B.taurus, C.lupus, M.musculus, R.norvegicus, X.tropicalis,* and *G.gallus*) at NCBI HomoloGene. We reconstructed a Neighbor-Joining Tree of the TMEM263 proteins with zebra fish as the outgroup, and visualized the result using Jalview (v2.10.3) (Waterhouse et al., 2009). The secondary topology of the transmembrane domain of TMEM263 was predicted by TMHMM Server (v. 2.0) based on a Hidden Markov Model (Krogh et al., 2001). The predicted protein feature was displayed using Protter 1.0 (Omasits et al., 2014). We could not predict the three-dimensional structure in the study, due to low coverage (< 50%) and low confidence (<20%) of the prediction. With the human orthologous gene, a gene network analysis was generated by using the association network predicting server GeneMANIA (Zuberi et al., 2013). Based on the function and properties of human *TMEME263*, the program explored the functional associated gene networks in genomic and proteomic data sources. Each network is weighted by the corresponding data source based on Gene Ontology biological process co-annotation, and with label propagation algorithm, which represents how well the genes are connected and interacted with each other.

2.3 Results

2.3.1 Identification of the candidate causal mutation for autosomal dwarfism

To study the causal variants that underlie autosomal dwarfism, we investigate the whole-genome sequence data of an adw chicken. The adw sequence data was aligned to the reference genome (Gallus_gallus 5.0), which resulted in an average coverage of 9.1x. Linkage analyses previously located the *adw* locus downstream microsatellite marker LEI0146 at around 54 Mb. Therefore, the gene *HMGA2* studied by Ruyter-Spira et al, (1998a, b) was mapped on the current reference genome at position 34 Mb, and was not considered as a candidate in the present study. ROH analysis for chromosome 1 showed an ROH of 14.8 Mb, spanning the region from 51.2 Mb to 65.9 Mb, which is expected to be identical by descent. Although larger, the ROH overlaps with the location of the candidate region (Figure S2.1) most likely as a consequence of the strong selection for the *adw* haplotype in the chicken lines used. The candidate region we defined spanned position 52-56 Mb on chromosome 1 (Figure 2.1). Within the candidate region, we found 146,070 variants, including genic variants in 72 genes and intergenic variants; we did not observe any specific structural variants that could contribute to growth reduction, as they were not located in the coding region. Supplementary Table S2.1 showed the structural variation identified in the candidate region.

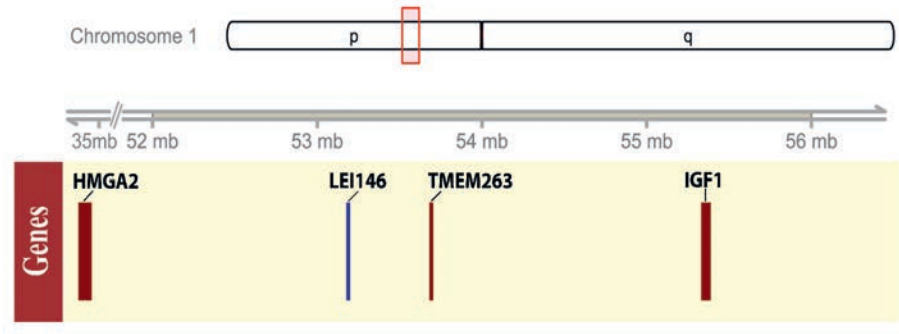

Figure 2.1 Schematic representation of the candidate region for *adw* locus on chromosome 1. The upper panel showed the ideogram of the chicken chromosome 1, the candidate region, 52-56Mb, was shown by a red box on the ideogram tracks. The lower panel showed the gene model by the solid box, indicating the size of the coding region of the representative candidate genes or the microsatellite marker. The associated microsatellite marker LEI146 was plotted in blue, while the genes with interest, *HMGA2, TMEM263, IGF1,* presented in red boxes.

We performed a four-step filtering procedure for all the variants identified by variant calling (Figure 2.2). After comparing the variants in the dwarf and normal-sized chickens in step 1, we generated a set of 5,713 variants in the candidate region that are unique for adw. Because adw is a recessive trait, we removed all heterozygous sites seen in the dwarf chicken; after step 2, 4,558 homozygous variants remained. In step 3, homozygous variants were predicted for substitution impact by VEP and SIFT, resulting in a list of 11 variants with moderate to high impact (Table 2.1), and a list of 4,558 variants within non-coding regions, all with low and modifier impact. At step 4, of the variants list with moderate to high impact, we further excluded 10 SNPs by screening the NCBI database, as they were not unique or exclusive for the adw chicken. The final candidate causal mutation is a nonsense variant in *TMEM263* gene (NM_001006244.1:c.433G>A). It is the only mutation with a high consequence impact that results in a loss-of-function alteration in the transmembrane protein 263. Among the non-coding variants, 709 variants in the dataset were shown to be absent from the dbSNP database (Table S2.2). Of these variants, 38 SNPs are located in six known lincRNAs. Two baseline transcriptome studies show the expression of the six lincRNAs in chicken tissues, which are ubiquitously expressed (Figure S2.2).

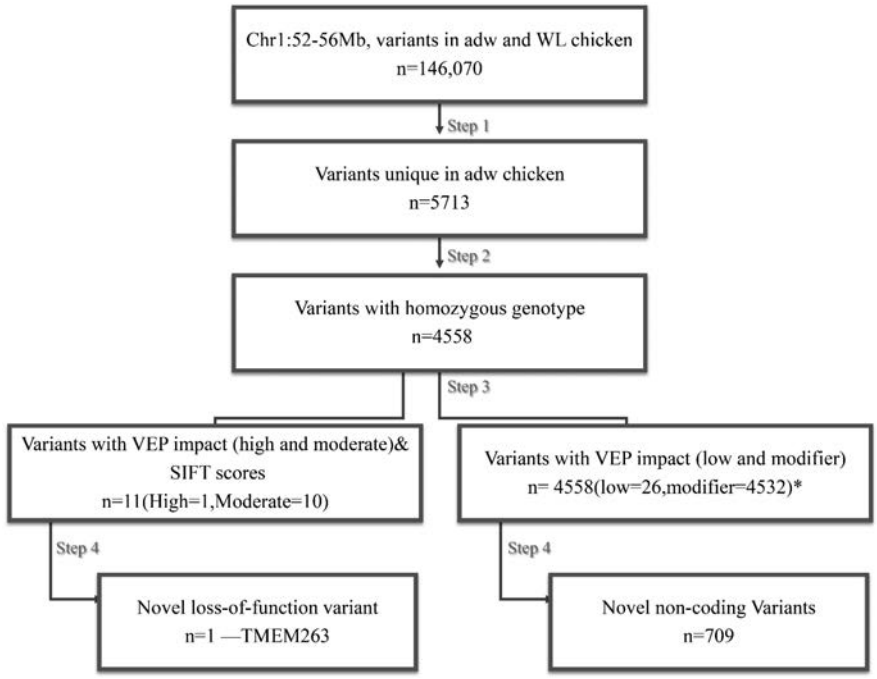

Figure 2.2 Schematic representation of the four steps filtering to identify the candidate variant for the chicken adw locus. n=number of variants after each filtering step. Autosomal dwarfism is represented by adw, while WL is the White Leghorn chickens. After the filtering, there is one candidate SNP exclusively found in adw and with a high impact on the consequence, shown at the left path. While there is a list of variants also uniquely fond in the adw chicken, they are mainly located on the non-coding region, shown at the right path. During variant impact prediction, each variant could have more than one impact assigned, as the impact estimation was based on different transcript. *Note that among these variants, eleven of them contain more than one impact. The sum of variant numbers therefore is not consistent with the result from the last step.

The nonsense mutation in *TMEM263* causes premature termination of the protein, leading to a truncation of the transmembrane protein. The mutation alters the 59th amino acid residue from tryptophan (Trp) to a stop codon (*) at the first membrane-spanning helix. The alteration truncates the protein to 50% and was expected to essentially affect the protein function. We validated the loss-of-function mutation in *TMEM263* using PCR-RFLP in all autosomal dwarf samples. The five autosomal dwarf samples indeed showed homozygous for the variant allele, whereas all normal-sized controls do not carry the mutation (Figure 2.3). The NP_001006244.1:p.(Trp59*) variant in *TMEM263* was identified to be the most interesting candidate causal mutation. The RT-qPCR revealed that the expression level of *TMEM263* and *IGF1* mRNA showed no significant difference between normal and dwarf individuals (Figure S2.3).

Table 2.1 Variants uniquely found in autosomal dwarf chicken and completely associated with dwarfism.

Position	Reference dbsnp	Ref/Alt	Gene	Variants	Impact	Database
52195787	rs736218372	TC/CT	HMGXB4	missense variant	Moderate	NCBI
53369104	rs14825651 and rs14825651	AA/TT	ASCL4	missense variant and splice region variant	Moderate	NCBI
53369406	rs741302250	G/A	ASCL4	missense variant (deleterious)	Moderate	NCBI
53376828	rs733697531	C/T	PRDM4	intron variant	Moderate	NCBI
53380585	rs313232660	G/A	PRDM4	missense variant	Moderate	NCBI
53683208	rs15270486	A/G	MTERF2	missense variant	Moderate	NCBI
53688583	N.A.	C/T	TMEM263	stop gained	High	N.A.
54232753	rs732172030	G/A	C12orf75	missense variant	Moderate	NCBI
54834890	rs733216275	AT/GA	STAB2	downstream gene variant and missense variant (deleterious)	Moderate	NCBI
54838941	rs14827457and rs14827458	TG/CC	STAB2	missense variant and upstream gene variant	Moderate	NCBI
55461367	rs13869828	A/G	PARPBP	missense variant	Moderate	NCBI

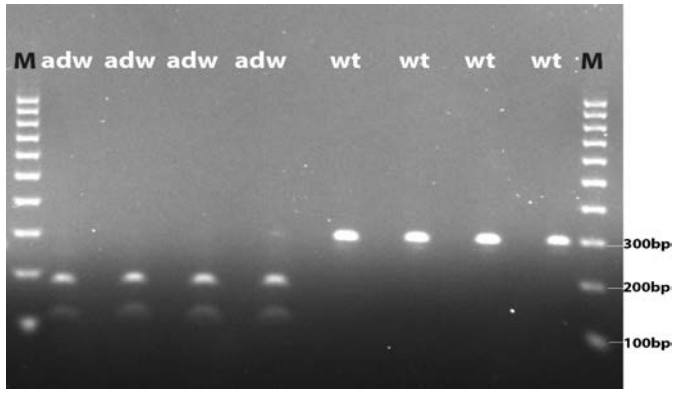

Figure 2.3 The photo of agarose gel of amplified fragments for genotyping candidate mutation in *TMEM263*. Autosomal dwarf (adw) and normal-sized (wt) samples were analyzed by PCR-RFLP method. Amplified DNA was digested with *Ddel* and separated by electrophoresis. Markers were used in both end lanes (M).The autosomal dwarf samples (adw/adw) were shown with two sequence fragments, around 109 and 184 bp respectively, while the wild-type samples shown with one band on the right four lanes, the size is around 294 bp.

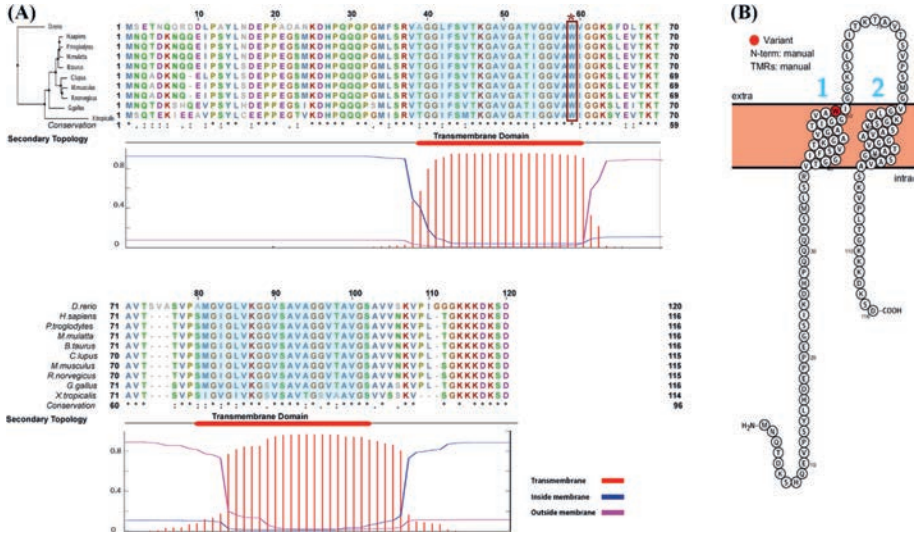

Figure 2.4 Comparative analyses and the predicted topology of TMEM263. (A). Multi-species alignment of orthologous TMEM263 protein sequence. The Neighbor-Joining tree of TMEM263 is at the top left side of the alignment, sequence of zebra fish (*D. rerio*) was used as outgroup. The upper panel shows the alignment of TMEM263 protein, the bottom sequence represents the conservation of the each amino acid. The asterisk (*) indicates position which has a single, fully conserved residue. The period (.) indicates conservation between groups of weakly similar properties, and the colon (:) indicates strongly similar conservative properties. The lower panel is the prediction of the transmembrane domains, shows the location and the orientation of transmembrane domains in the TMEM263 sequence. The x-axis refers to the location of amino acid residue sites; y-axis represents the probability of topology for each region. The predicted transmembrane region is shown in red (amino acid residue sites: 38-60; 80-102), blue lines stand for intracellular region, and the magenta line is the amino acid predicted outside the membrane. The consensus line is placed at the top of the plot. The transmembrane domains are highlighted in sequence alignment with light blue background. The nonsense mutation (Trp59*) is demonstrated by dark red rectangle. (B). The predicted topology of TMEM263 protein. The topology was illustrated with the position of the variation shown in red. The N-terminal location and the transmembrane regions (TMRs) were generated based on the topology prediction, and input manually. The number 1 and 2 in blue refer to the two transmembrane regions, the cell membrane is in light orange, and N-term is predicted on the cytoplasmic side of the membrane.

2.3.2 Functional and comparative analyses of the candidate gene

The *TMEM263* gene is highly conserved across various species, from primates to craniata (Figure 2.4A). The protein sequence identity of orthologous *TMEM263* genes between chicken and other vertebrates ranges around 73-89%. The comparison with human homologous protein presented the conservation around 89%. The tryptophan amino acid site at position 59, which harbors the nonsense mutation, is present fully conserved across all species analyzed. The predicted topology of the vertebrate TMEM263 protein is a multi-pass membrane structure, which consists of two transmembrane domains (from amino-acid positions 38 to 60, and from 80 to 102),

with the nonsense mutation located at the first transmembrane region (Figure 2.4B). Based on human orthologous genes, we generated a gene network analysis to investigate the potential function of *TMEM263*. Interestingly, TMEM263 was shown to have physical interactions with growth hormone (*GH1*), and to be co-expressed with Bone Morphogenetic Protein (*BMP2*) in human cells (Figure 2.5).

2.4 Discussion

In this study, we fine-map and report the likely causal variant of the chicken autosomal dwarfism locus, located on chromosome 1, by comparing whole-genome sequence data of an autosomal dwarf with normal-sized chickens. Given the origin of adw in chickens, emerging from the Cornell White Leghorn strain, we used normal-sized White Leghorn chickens as the control in this study. Moreover, the causal variant for autosomal dwarfism is unlikely to be segregating in other non-dwarf populations. The linkage results show the strong association between *adw* locus and microsatellite marker LEI0146, which defined a 4 Mb surrounding interval on chromosome 1 as the candidate region. The ROHs analyses show low SNP abundance in the candidate region, and overlaps with the location of the candidate region. The candidate region was chosen to include *IGF1*, known to be functionally associated with growth traits in humans (Yakar et al., 2002). As endocrinological study revealed unaffected IGF1 concentration in adw chickens (Ruyter-Spira et al., 1998b), as well as the unaffected differential expression we identified, the IGF1 was not considered the best candidate of the study. After screening the variants, only one novel nonsense mutation in *TMEM263* remained as a strong candidate and proven associated with the autosomal dwarf phenotype.

In an autosomal dwarf dataset, we found, in total, 710 variants in the candidate region are associated with the adw phenotype, including a nonsense mutation in gene *TMEM263* likely underlying the autosomal dwarfism phenotype. The gene *TMEM263* encodes for a transmembrane protein, but its function in chicken is not well known. Meanwhile, the 709 variants of lower impact fall within 58 genes and six known lincRNAs. The genic variants with lower impact in the list are mostly located within the non-protein coding region, containing intron and UTR, and are assumed not to disrupt the function of these genes. The six lincRNAs in the candidate region are barely studied, their ubiquitous expression in chicken tissues makes it hard to predict the contribution of these lincRNAs (Barbosa-Morais et al., 2012; Merkin et al., 2012; Petryszak et al., 2017). Due to the limited annotation for non-coding variants in the reference chicken genome, detailed studies on those variants as causal mutation is less favorable in this study. In summary, it is unlikely, although still possible, that the 709 variants harbor the causal mutation; therefore we consider these variants as less potential candidates for *adw* mutation.

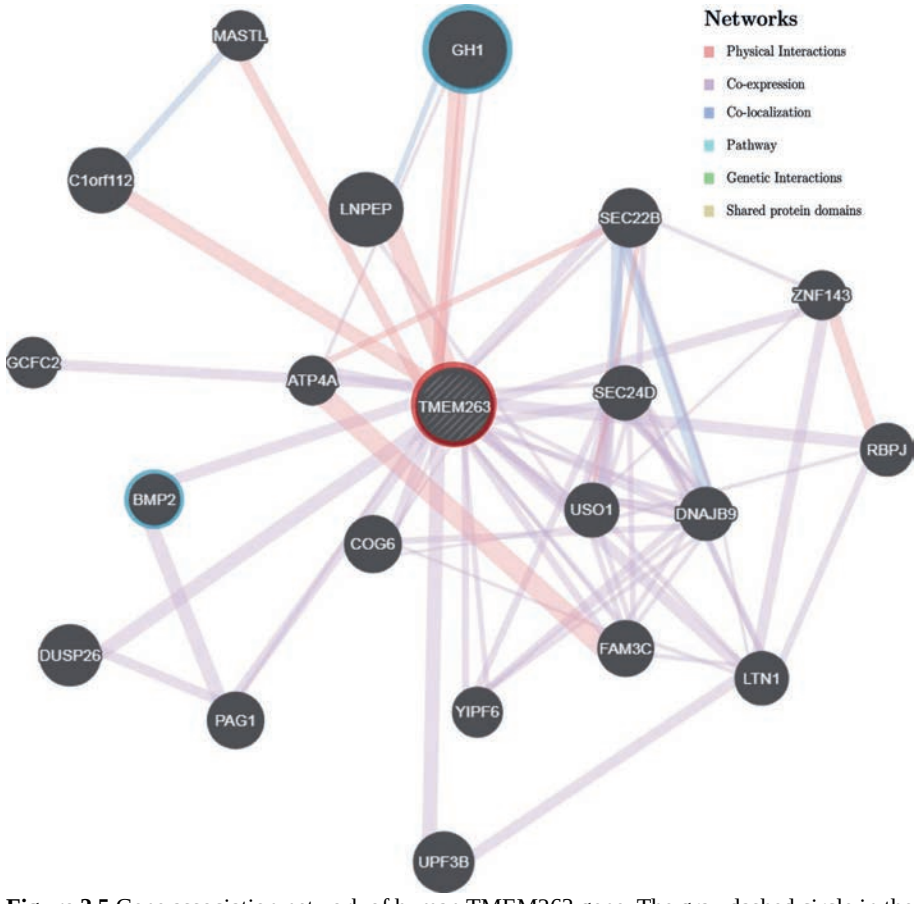

Figure 2.5 Gene association network of human TMEM263 gene. The gray dashed circle in the center with red ring represents TMEM263. The size of the solid circles representing other genes is proportional to the number of interactions they have. Gene GH1 and BMP2 are highlighted with blue rings to emphasize the two network branches. Red branch stands for physical interaction, purple branch displays co-expression, and blue branch means co-localization.

The *TMEM263* protein is conserved across species, and the transmembrane protein sequence belongs to a conserved protein domain (model UPF0444, pfam15475). This domain is a conserved unit from a superfamily of proteins representing multi-pass membrane structure, including two helical membrane-spanning domains. The membrane-spanning domains are located between amino acid positions 38 to 60, and 80 to 102. The protein consists of an intracellular N- and C-terminus, along with an extracellular loop. The nonsense mutation is uniquely found in adw chicken in the first transmembrane-spanning domain, and is completely associated with the autosomal dwarf phenotype. The expression level of *TMEM263* in 6-8 day embryos does not differ between dwarf and non-dwarf chickens. In two baseline transcriptome experiments, *TMEM263* expressed ubiquitously in chicken tissue, including skeletal

muscle tissue (Barbosa-Morais et al., 2012; Merkin et al., 2012). As a consequence of the nonsense mutation, the transmembrane protein is truncated and only contains the N-terminal amino acids 1 to 58. Accordingly, the altered transmembrane protein loses part of the conserved domain UPF0444, as well as one of the membrane-spanning domains, almost certainly resulting in protein function loss.

Although little is known about the role of the *TMEM263*, evidence from studies in humans implied that *TMEM263* (former alias: *C12orf23*) is associated with growth and bone development (Ewing et al., 2007; Estrada et al., 2012; Calabrese et al., 2017). In a human Genome-Wide Association Study, *TMEM263* was shown to be significantly associated with femoral neck bone mineral density (FN-BMD) (Estrada et al., 2012). The expression level of *TMEM263* was also correlated with BMD and osteoporotic fracture risk. A cortical bone co-expression network study showed the expression of *TMEM263* to be significantly correlated with the osteoblast functional modules (OFM), which impacts bone mineral density by altering the activity of bone-forming osteoblasts (Calabrese et al., 2017). Considering the strong positive correlation between bone mass and bone size, the co-expression between *TMEM263* and OFM indicates that *TMEM263* is likely functionally involved in cartilage and bone formation. In addition, a large-scale human disease study reported that *TMEM263* physically interacts with growth hormone 1 (Ewing et al., 2007), an important regulation somatotropin in growth development. In the protein-protein interaction study, TMEM263 was identified by co-immunoprecipitation with GH1 followed by mass spectrometry. Therefore, TMEM263 may be involved in the growth pathway by potentially acting as a regulator in transport or signal transduction. *TMEM263* was also identified as an interaction partner of potassium channel genes *Slick* and *Slack*, which is a sodium-activated channel widely expressed in the central nervous system (Rizzi et al., 2015). Taken together, these studies in humans suggest a potential role of *TMEM263* in skeletal development, like cartilage and bone formation. This supports our hypothesis that the loss-of-function mutations in gene *TMEM263* will likely influence the deposition of bone mineral, thereby affecting skeletal development and body growth, which were observed in autosomal dwarf chickens.

2.5 Conclusion

We describe a novel nonsense mutation on chromosome 1, located in the highly conserved gene *TMEM263*, which is associated with chicken autosomal dwarfism (*adw*). The adw associated NP_001006244.1:p.(Trp59*) mutation in the TMEM263 protein was expected to functionally affect the protein and exclusively found in adw chicken. The novel premature termination is the most likely variant that underlying the chicken autosomal dwarfism. Functional information in humans supports its potential role in bone development and growth. Our results suggest a potentially vital

role of *TMEM263* in growth reduction and provide the basis for future systematically verifying the function of the transmembrane protein 263.

2.6 Data Accessibility

The sequence data of autosomal dwarf chicken was deposited in ENA, under the primary accession: PRJEB25937, sample ERS2374285. The sequence data within the 4 Mb candidate region used in the study is available upon the request.

2.7 Funding

Zhou Wu has received financial support from the China Scholarship Council (No.201606350175). Part of the work is supported by the IMAGE project from the European Union's Horizon 2020 Research and Innovation Programme (Grant Agreement No. 677353).

2.8 Acknowledgments

We would like to thank Center for Genetic resources, the Netherlands and Stichting Zeldzaam Huisdier for providing the sperm and samples. We thank Chiara Bortoluzzi for helping with ROH analysis; Kimberley Laport for the experimental support; Langqing Liu for the data analyses; Michael Aldridge for editing the paper, and Fei Wu for the earlier candidate gene screening.

2.9 Reference

Agarwal, S. K., Cogburn, L. A., and Burnside, J. (1994). Dysfunctional growth hormone receptor in a strain of sex-linked dwarf chicken: Evidence for a mutation in the intracellular domain. *J. Endocrinol.* 142, 427–434. doi:10.1677/joe.0.1420427.

Barbosa-Morais, N. L., Irimia, M., Pan, Q., Xiong, H. Y., Gueroussov, S., Lee, L. J., et al. (2012). The evolutionary landscape of alternative splicing in vertebrate species. *Science* 338, 1587–93. doi:10.1126/science.1230612.

Boegheim, I. J. M., Leegwater, P. A. J., van Lith, H. A., and Back, W. (2017). Current insights into the molecular genetic basis of dwarfism in livestock. *Vet. J.* 224, 64–75. doi:10.1016/j.tvjl.2017.05.014.

Bosse, M., Megens, H. J., Madsen, O., Paudel, Y., Frantz, L. A. F. F., Schook, L. B., et al. (2012). Regions of Homozygosity in the Porcine Genome: Consequence of Demography and the Recombination Landscape. *PLoS Genet.* 8, e1003100. doi:10.1371/journal.pgen.1003100.

Burnside, J., Liou, S. S., Cogburn, L. A., and Burnside, J. (1991). Molecular cloning of the chicken growth hormone receptor complementary deoxyribonucleic acid: Mutation of the gene in sex-linked dwarf chickens. *Endocrinology* 128, 3183–3192. doi:10.1210/endo-128-6-3183.

Calabrese, G. M., Mesner, L. D., Stains, J. P., Tommasini, S. M., Horowitz, M. C., Rosen, C. J., et al. (2017). Integrating GWAS and Co-expression Network Data Identifies Bone Mineral Density Genes SPTBN1 and MARK3 and an Osteoblast Functional Module. *Cell Syst.* 4, 46-59.e4. doi:10.1016/j.cels.2016.10.014.

Cingolani, P., Platts, A., Wang, L. L., Coon, M., Nguyen, T., Wang, L., et al. (2012). A program for annotating and predicting the effects of single nucleotide polymorphisms, SnpEff: SNPs in the genome of Drosophila melanogaster strain w1118; iso-2; iso-3. *Fly (Austin).* 6, 80–92. doi:10.4161/fly.19695.

Cole, R. F., and Hutt, F. B. (1973). Selection of heterosis in Cornell White Leghorns: a review, with

special consideration of interstrain hybrids. *Anim. Breed. Abstr.* 41, 103–118.

Cole, R. K. (1973). An Autosomal Dwarfism in the Fowl. *Poult. Sci.* 52, 2012–2013.

Cole, R. K. (2000). An autosomal dwarfism in the domestic fowl. *Poult. Sci.* 79, 1507–1516. doi:10.1093/ps/79.11.1507.

Danecek, P., Auton, A., Abecasis, G., Albers, C. A., Banks, E., DePristo, M. A., et al. (2011). The variant call format and VCFtools. *Bioinformatics* 27, 2156–2158. doi:10.1093/bioinformatics/btr330.

Eilbeck, K., and Lewis, S. E. (2004). Sequence Ontology annotation guide. *Comp. Funct. Genomics* 5, 642–647. doi:10.1002/cfg.446.

Estrada, K., Styrkarsdottir, U., Evangelou, E., Hsu, Y. H., Duncan, E. L., Ntzani, E. E., et al. (2012). Genome-wide meta-analysis identifies 56 bone mineral density loci and reveals 14 loci associated with risk of fracture. *Nat. Genet.* 44, 491–501. doi:10.1038/ng.2249.

Ewing, R. M., Chu, P., Elisma, F., Li, H., Taylor, P., Climie, S., et al. (2007). Large-scale mapping of human protein–protein interactions by mass spectrometry. *Mol. Syst. Biol.* 3, 89. doi:10.1038/msb4100134.

Garrison, E., and Marth, G. (2012). Haplotype-based variant detection from short-read sequencing. *arXiv Prepr.* Available at: http://arxiv.org/abs/1207.3907 [Accessed February 14, 2018].

Godowski, P. J., Leung, D. W., Meacham, L. R., Galgani, J. P., Hellmiss, R., Keret, R., et al. (1989). Characterization of the human growth hormone receptor gene and demonstration of a partial gene deletion in two patients with Laron-type dwarfism. *Proc. Natl. Acad. Sci. U. S. A.* 86, 8083–7. doi:10.1073/pnas.86.20.8083.

Groenen, M. A. M., Wahlberg, P., Foglio, M., Cheng, H. H., Megens, H. J., Crooijmans, R. P. M. A., et al. (2009). A high-density SNP-based linkage map of the chicken genome reveals sequence features correlated with recombination rate. *Genome Res.* 19, 510–519. doi:10.1101/gr.086538.108.

Hahne, F., and Ivanek, R. (2016). "Visualizing genomic data using Gviz and bioconductor," in *Methods in Molecular Biology*, 335–351. doi:10.1007/978-1-4939-3578-9_16.

Hutt, F. B. (1949). *Genetics of the fowl*. 1st ed. New York, NY: McGraw-Hill.

Huybrechts, L. M., King, D. B., Lauterio, T. J., Marsh, J., and Scanes, C. G. (1985). Plasma concentrations of somatomedin-C in hypophysectomized, dwarf and intact growing domestic fowl as determined by heterologous radioimmunoassay. *J. Endocrinol.* 104, 233–239. doi:10.1677/joe.0.1040233.

Joshi, N., and Fass, J. (2011). Sickle: A sliding-window, adaptive, quality-based trimming tool for FastQ files (Version 1.33) [Software]. *Available at https://github.com/najoshi/sickle.*, 2011.

Krogh, A., Larsson, B., Von Heijne, G., and Sonnhammer, E. L. L. (2001). Predicting transmembrane protein topology with a hidden Markov model: Application to complete genomes. *J. Mol. Biol.* 305, 567–580. doi:10.1006/jmbi.2000.4315.

Lam, S. K., Harvey, S., and Scanes, C. G. (1989). Thyroid function in sex-linked and autosomal dwarf chickens. *Gen. Comp. Endocrinol.* 76, 200–204. doi:10.1016/0016-6480(89)90150-0.

Layer, R. M., Chiang, C., Quinlan, A. R., and Hall, I. M. (2014). LUMPY: A probabilistic framework for structural variant discovery. *Genome Biol.* 15, R84. doi:10.1186/gb-2014-15-6-r84.

Li, H., and Durbin, R. (2009). Fast and accurate short read alignment with Burrows-Wheeler transform. *Bioinformatics* 25, 1754–1760. doi:10.1093/bioinformatics/btp324.

Li, H., Handsaker, B., Wysoker, A., Fennell, T., Ruan, J., Homer, N., et al. (2009). The Sequence Alignment/Map format and SAMtools. *Bioinformatics* 25, 2078–2079. doi:10.1093/bioinformatics/btp352.

McKenna, A., Hanna, M., Banks, E., Sivachenko, A., Cibulskis, K., Kernytsky, A., et al. (2010). The genome analysis toolkit: A MapReduce framework for analyzing next-generation DNA sequencing

data. *Genome Res.* 20, 1297–1303. doi:10.1101/gr.107524.110.

McLaren, W., Gil, L., Hunt, S. E., Riat, H. S., Ritchie, G. R. S., Thormann, A., et al. (2016). The Ensembl Variant Effect Predictor. *Genome Biol.* 17, 122. doi:10.1186/s13059-016-0974-4.

Merkin, J., Russell, C., Chen, P., and Burge, C. B. (2012). Evolutionary dynamics of gene and isoform regulation in Mammalian tissues. *Science* 338, 1593–9. doi:10.1126/science.1228186.

Mortier, G. R., Weis, M., Nuytinck, L., King, L. M., Wilkin, D. J., De Paepe, A., et al. (2000). Report of five novel and one recurrent COL2A1 mutations with analysis of genotype-phenotype correlation in patients with a lethal type II collagen disorder. *J Med Genet* 37, 263–271. Available at: http://jmg.bmj.com/content/jmedgenet/37/4/263.full.pdf [Accessed January 12, 2018].

Omasits, U., Ahrens, C. H., Muller, S., and Wollscheid, B. (2014). Protter: Interactive protein feature visualization and integration with experimental proteomic data. *Bioinformatics* 30, 884–886. doi:10.1093/bioinformatics/btt607.

Petryszak, R., Fonseca, N. A., Füllgrabe, A., Huerta, L., Keays, M., Tang, Y. A., et al. (2017). The RNASeq-er API-A gateway to systematically updated analysis of public RNA-seq data. *Bioinformatics* 33, 2218–2220. doi:10.1093/bioinformatics/btx143.

Petryszak, R., Keays, M., Tang, Y. A., Fonseca, N. A., Barrera, E., Burdett, T., et al. (2016). Expression Atlas update—an integrated database of gene and protein expression in humans, animals and plants. *Nucleic Acids Res.* 44, D746–D752. doi:10.1093/nar/gkv1045.

Richette, P., Bardin, T., and Stheneur, C. (2008). Achondroplasia: From genotype to phenotype. *Jt. Bone Spine* 75, 125–130. doi:10.1016/J.JBSPIN.2007.06.007.

Rizzi, S., Schwarzer, C., Kremser, L., Lindner, H. H., and Knaus, H. G. (2015). Identification of potential novel interaction partners of the sodium-activated potassium channels Slick and Slack in mouse brain. *Biochem. Biophys. Reports* 4, 291–298. doi:10.1016/j.bbrep.2015.09.024.

Ruyter-Spira, C. P., De Groof, A. J. C., Van Der Poel, J. J., Herbergs, J., Masabanda, J., Fries, R., et al. (1998a). The HMGI-C gene is a likely candidate for the autosomal dwarf locus in the chicken. *J. Hered.* 89, 295–300. doi:10.1093/jhered/89.4.295.

Ruyter-Spira, C. P., Herbergs, J., Limpens, E., Marsh, J. A., Van Der Poel, J. J., Ayoubi, T. A. Y., et al. (1998b). Nucleotide sequence of the chicken HMGI-C cDNA and expression of the HMGI-C and IGF1 genes in autosomal dwarf chicken embryos. *Biochim. Biophys. Acta - Gene Struct. Expr.* 1399, 83–87. doi:10.1016/S0167-4781(98)00101-8.

Scanes, C. G., Marsh, J., Decuypere, E., and Rudas, P. (1983). Abnormalities in the plasma concentrations of thyroxine, tri-iodothyronine and growth hormone in sex-linked dwarf and autosomal dwarf White Leghorn domestic fowl (Gallus domesticus). *J. Endocrinol.* 97, 127–135.

Sievers, F., Wilm, A., Dineen, D., Gibson, T. J., Karplus, K., Li, W., et al. (2014). Fast, scalable generation of high-quality protein multiple sequence alignments using Clustal Omega. *Mol. Syst. Biol.* 7, 539–539. doi:10.1038/msb.2011.75.

Sim, N. L., Kumar, P., Hu, J., Henikoff, S., Schneider, G., and Ng, P. C. (2012). SIFT web server: Predicting effects of amino acid substitutions on proteins. *Nucleic Acids Res.* 40, W452–W457. doi:10.1093/nar/gks539.

Waterhouse, A. M., Procter, J. B., Martin, D. M. A., Clamp, M., and Barton, G. J. (2009). Jalview Version 2-A multiple sequence alignment editor and analysis workbench. *Bioinformatics* 25, 1189–1191. doi:10.1093/bioinformatics/btp033.

Yakar, S., Rosen, C. J., Beamer, W. G., Ackert-Bicknell, C. L., Wu, Y., Liu, J. L., et al. (2002). Circulating levels of IGF-1 directly regulate bone growth and density. *J. Clin. Invest.* 110, 771–781. doi:10.1172/JCI200215463.

Zuberi, K., Franz, M., Rodriguez, H., Montojo, J., Lopes, C. T., Bader, G. D., et al. (2013). GeneMANIA Prediction Server 2013 Update. *Nucleic Acids Res.* 41, W115–W122. doi:10.1093/nar/gkt533.

2.10 Supplementary materials

The Supplementary Material for this article can be found online at: https://www.frontiersin.org/articles/10.3389/fgene.2018.00193/full#supplementary-material

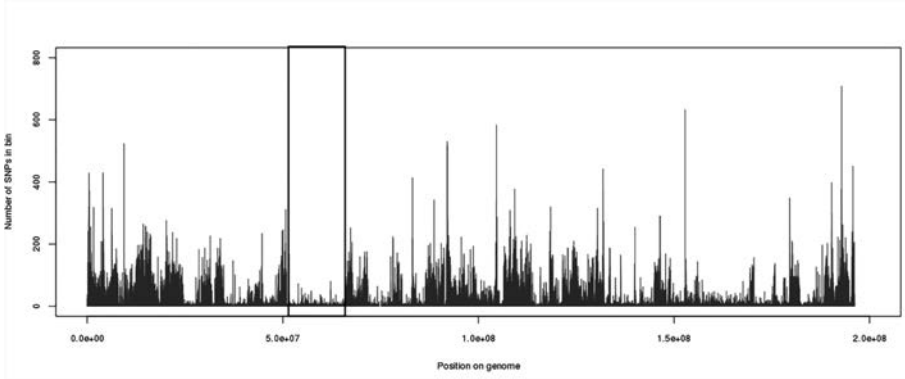

Figure S2.1 ROHs analyses and the distribution of nucleotide diversity over chromosome 1. The x-axis displays the physical position on the chromosome and the y-axis shows the corrected number of SNPs that was called in bins of 10 kb. The black rectangle illustrates the homozygous stretch, located around 51.0 Mb to 65.9 Mb, supporting to the candidate region of autosomal dwarfism.

Figure S2.2 Baseline Expression of the lincRNA and TMEM263 gene (online).

Figure S2.3 Expression of *IGF1* and *TMEM263* among normal-sized and autosomal dwarf chickens (online).

Table S2.1 Structrual Variations detected in the autosomal dwarf chicken (online).

Table S2.2 Uniqe variants of low to moderate impact in autosomal dwarf chicken (online).

3

Heterogeneity of a dwarf phenotype in Dutch traditional chicken breeds revealed by genomic analyses

Zhou Wu[1], Chiara Bortoluzzi[1], Martijn F.L. Derks[1], Langqing Liu[1], Mirte Bosse[1], Sipke Joost Hiemstra[2], Martien A.M. Groenen[1], and Richard P.M.A. Crooijmans [1]

[1]Wageningen University & Research Animal Breeding and Genomics, Wageningen, the Netherlands

[2]Centre for Genetic Resources, the Netherlands (CGN) of Wageningen University & Research, The Netherlands

Based on *Evolutionary Applications* (2021), DOI: 10.1111/eva.13183

Abstract

The growth of animals is a complex trait, in chicken resulting in a diverse variety of forms, caused by a heterogeneous genetic basis. Bantam chicken, known as an exquisite form of dwarfism, has been used for crossbreeding to create corresponding dwarf counterparts for native fowls in the Dutch populations. Here we demonstrate the heterogeneity of the bantam trait in Dutch chickens and reveal the underlying genetic causes, using whole-genome sequence data from matching pairs of bantam and normal-sized breeds. During the bantam oriented crossbreeding, various bantam origins were used to introduce the bantam phenotype, three major bantam sources were identified and clustered. The genome-wide association studies revealed multiple genetic variants and genes associated with bantam phenotype, including *HMGA2* and *PRDM16*, genes involved in body growth and stature. The comparison of associated variants among studies illustrated differences related to divergent bantam origins, suggesting a clear heterogeneity among bantam breeds. We show that in neo-bantam breeds, the bantam-related regions underwent a strong haplotype introgression from the bantam source, outcompeting haplotypes from the normal-sized counterpart. The bantam heterogeneity is further confirmed by the presence of multiple haplotypes comprising associated alleles, which suggests the selection of the bantam phenotype is likely subject to a convergent direction across populations. Our study demonstrates that the diverse history of human-mediated crossbreeding has contributed to the complexity and heterogeneity of the bantam phenotype.

Keywords: chicken, dwarfism, bantam, heterogeneity, whole-genome sequencing, genome-wide association study, convergent selection

3.1 Introduction

Human activities influence the demographic history and phenotypic diversity of animals through artificial selection and crossbreeding (Andersson, 2001; Bruford et al., 2003). In the course of domestication, the human-mediated selection was a major force that drove the phenotypic differentiation, which has been further enhanced by the breed formation during recent centuries (Andersson and Georges, 2004). The selection of body size in animals has been a major focus during domestication (Andersson and Georges, 2004; Mignon-Grasteau et al., 2005; Zeder, 2012). Albeit the rapid growth and the large body size are of great interest to commercial breeders, attention for small-sized animals has been raised as well.

Dwarf animals are characterized by a short body stature (Boegheim et al., 2017). Despite the general description of varying growth reduction, comprehensive phenotypic heterogeneity has been shown for dwarfism. A clear example is the extreme stature variations across dog breeds (Sutter et al., 2007; Parker et al., 2009; Hulsegge et al., 2013). The dwarf phenotype in chickens is observed and measured by different narratives, including but not limited to body weight, height, and shank length (Cole, 2000; Boegheim et al., 2017). Three distinct types of dwarfism have been described in chickens based on the physiological and genetic properties: sex-linked dwarfism, which is well studied and caused by mutations in the growth hormone receptor gene (*GHR*) (Burnside et al., 1992; Agarwal et al., 1994); autosomal dwarfism (adw) that is associated with a nonsense mutation in the transmembrane protein 263 gene (*TMEM263*) (Wu et al., 2018); and third the bantam phenotype, for which the genetic cause is unknown. The origin of the word 'bantam' refers to a region in south-east Asia (Java island) and came to be known as a form of small fowl of exquisite appearance that became prevalent in Europe.

Compared to other typical dwarfisms, bantam is unique in the way it shows the reduction in body weight, yet no clear other malformations and no evidence of affected viability. Bantams in the Netherlands usually have around 50-60% reduced body weight compared to their corresponding counterparts (Figure S3.1A-B, Supplementary file 3.1). Traditional bantam breeds or true bantams are known for their existence without a large form counterpart. Examples of true bantams from the Netherlands are the Dutch bantam, the Dutch booted bantam, and the Eikenburger bantam (Esther Verhoef and Rijs, 2014). Nowadays, the bantam chicken has become an important component of the Dutch chicken breeds, which encompasses a recent history of human-mediated crossbreeding of the bantam phenotype. Neo-bantam chickens are the hybrid bantam counterparts produced by this crossbreeding procedure with the goal of miniaturizing, which is called bantamization (Bortoluzzi et al., 2018). The creation of the neo-bantams is based on crossing the normal-sized indigenous breeds with existing bantam breeds, followed by repeated backcrossing

with the normal-sized indigenous breeds and selecting for the bantam phenotype. In other words, the normal-sized Dutch breeds have been artificially crossed with existing bantams, which resulted in neo-bantams that represent the dwarf stature, but meanwhile keep similar breed appearances as their normal-sized counterparts (Esther Verhoef and Rijs, 2014). The F1 offspring produced by a crossing between bantam and normal-sized chickens are expected intermediate in size, and offspring of F2 generation contain a range of segregating phenotypes (Wandelt and Wolters, 1998). Many neo-bantam breeds were developed in the past decades mediated mainly by hobby breeders for different cultural reasons (Dana et al., 2011; Bortoluzzi et al., 2018), resulting in diverse historical and genetic backgrounds. Currently, almost every Dutch native breed has a corresponding neo-bantam counterpart (Esther Verhoef and Rijs, 2014).

However, our knowledge about bantam is very limited when it comes to the historical background and genetic mechanism. Understanding the bantam phenotype and the underlying genetic basis requires a wide variety of bantam chicken resources, as the genome landscape is influenced by various factors. The genetic background differs in Dutch chicken breeds (Bortoluzzi et al., 2020a), and the backcrossing performed by breeders complicates the genetic tracing of bantam origin (Bortoluzzi et al., 2018), as well as the selective breeding for other phenotypes besides bantam, such as plumage color and comb morphology. The various bantams in the Dutch populations contain a unique and documented history of crossbreeding, which enables us to disentangle the genetic nature of the bantam phenotype. In this study, we used whole-genome sequence data for comprehensive genomic analyses to investigate the genetic architecture of the bantam phenotype. Understanding the genomic basis of bantam phenotype will help to understand how the practice of bantam-orientated crossbreeding has contributed to and reshaped the phenotypic and genetic heterogeneity of bantam chickens. The utility of the evolutionary analytical approaches in this study provides a phylogenetic perspective of how the genetic variations were subjected to the convergent or divergent human-mediated selection.

Given the complex history and limited knowledge of the bantam phenotype, the objectives of this research are: 1) identify the bantam associated genes in Dutch chicken breeds; 2) investigate the characteristics of associated genes in historical heterogeneous groups of bantam; 3) understand the molecular mechanisms underlying the bantam phenotype.

3.2 Materials and Methods

3.2.1 Sample collection and heterogeneous bantam backgrounds

Genomic DNA was isolated from 135 samples of 37 breeds (Table S1). We collected samples representing: 1) true bantams, which include the Dutch true bantam breeds and true bantams of Asian origin; 2) normal-sized Dutch traditional native breeds and

3) neo-bantam counterparts of the Dutch native breeds. We collected information from breed associations on the specific bantam breeds that have been used to create the neo-bantams. From the crossbreeding record, the Dutch breeds show various and divergent bantam origins among breeds (Table S2). The potentially non-uniform and heterogeneous genetic background in the population is suggested by the observation that some of the neo-bantam breeds share the same ancestral bantam breeds. Based on the neo-bantam crossbreeding record, we identify three clusters derived from the three major bantam sources reported, which are the Dutch bantam (cluster 1), Sebright and Java bantam (cluster 2), and other miscellaneous bantams including South East Asian and productive breeds (cluster 3). In the three cluster-based genome-wide association studies, we correspondingly analyzed the pairs of neo-bantam breeds and normal-sized native counterparts.

3.2.2 Whole-genome sequencing and variant calling

Samples collected were sequenced on the Illumina HiSeq 3,000 platform, including samples described in previous studies by Bortoluzzi et al. (Bortoluzzi et al., 2020a, 2020b), in total, we achieved 135 samples of 37 breeds. The number of animals for each breed varies from 1 to 9. Whole genome sequence data was processed by using an in-house analysis pipeline. In short, raw reads were first trimmed by Sickle (Joshi and Fass, 2011) using paired-end mode. The cleaned reads were mapped to the latest Red Jungle fowl reference genome assembly, build GRCg6a (GenBank Accession: GCA_000002315.5) by using default options in BWA-MEM (version 0.7.17) (Li and Durbin, 2009). With the markdup option in sambamba v0.6.3 (Tarasov et al., 2015), duplicated reads were removed. Mapping quality and coverage of the aligned samples were assessed with Qualimap v2.2 (Okonechnikov et al., 2016). Variant calling for SNPs and InDels was performed using Freebayes (Garrison and Marth, 2012) with the following criteria: minimum base quality 10; minimum mapping quality 20; and alternative calls need to have alternate fraction > 0.2 and min-alternate-count > 2.

3.2.3 Quality control

Variant quality control was performed using information from the depth of coverage, call rate, and minor allele frequency. We used VCFtools (Danecek et al., 2011) to include variants with a quality score over 10, call-rate more than 0.8, a mean depth between 3 and 100, and genotypes with a depth between 3 to 100. When more than one alternative allele is present at one genomic position, in order to track all possible alternatives, multi-allelic loci were split into few bi-allelic sites by using BCFtools (Li et al., 2009) and PLINK (V1.9) (Chang et al., 2015). We assigned different names for the alleles to avoid ambiguities, which ensures the use of complete information for every locus. Rare variants were then filtered out by using a threshold of minor allele frequency < 0.05.

3.2.4 Population structure analyses

The population structure of Dutch chickens was estimated by the principal component analysis (PCA) and Neighbor-Joining (NJ) tree. We calculated the principal components using PLINK (V1.9) (Chang et al., 2015) with all genomic autosomal variants and visualized the first two principal components using ggplot2 (v3.1.0) (Wickham, 2016). The 1-ibs distance matrix was computed in PLINK and then converted to a NJ-tree using the R package "ape" (Paradis and Schliep, 2019). The phylogenetic tree was visualized by using FigTree v1.4.4 (http://tree.bio.ed.ac.uk/software/figtree/). Additionally, in order to estimate the relative genetic relationships within the grouped population, the phylogenetic tree analyses were conducted in a similar fashion within each cluster using only neo-bantams of each cluster and the bantam sources.

3.2.5 Association study

Genome-wide association studies (GWAS) were performed based on a clustering strategy. In this cluster strategy, we identified three clusters based on heterogeneous bantam backgrounds (Table S2), and each cluster contains matching pairs of normal-sized breeds and corresponding bantam counterparts as the individual case and control phenotype. The number of individuals is 34 in cluster 1 (15 cases and 19 controls), 66 in cluster 2 (25 cases and 41 controls), and 35 in cluster 3 (12 cases and 23 controls). In each cluster, we employed the complete set of SNPs and InDels, and fitted a univariate linear mixed model including a relatedness matrix as the random effect by using the program GEMMA (Zhou and Stephens, 2012). The identity-by-state (IBS) relatedness matrix was computed by using the subset of SNPs corresponding to the chicken 60K SNP array, which is a good representation of Dutch chicken diversity (Bortoluzzi et al. 2018) and is computationally less demanding. The relatedness matrix was computed using (--distance square ibs) in PLINK (V1.9) (Chang et al., 2015). The significant level P-values were derived from the Wald-test. The corresponding significance threshold followed the suggestive threshold of P-value $<=5x10^{-8}$. A genomic control inflation factor lambda was calculated in each study to evaluate the confounding due to population stratification. The GWAS results were visualized using the R package qq-man (Turner, 2018).

3.2.6 Structural variation analysis

In order to investigate whether structural variation (SV) affects the bantam phenotype, the association analyses with SVs were performed as described in the GWAS analyses. Considering the peak signals of the three clusters, we detected structural variation (SV) on chromosomes 1 and 4 by using Smoove (https://github.com/brentp/smoove). Smoove combines various SV tools and removes spurious alignment reads to reduce the noise. Smoove first extracts discordant and split-reads from the alignment BAM file per individual. Subsequently, Lumpy (Layer et al., 2014) is used to call SVs, and genotyping of SVs is performed using SVtyper

(Chiang et al., 2015) after merging all SVs to generate a consensus output across samples. Mosdepth (Pedersen and Quinlan, 2018) was used to further filter SV calls, to discard reads from regions where the sequencing depth of split or discordant reads was extreme (>1,000), to remove regions that contribute to spurious calls. Duphold (Pedersen and Quinlan, 2019) was used to annotate depth changes within and on the breakpoints of SVs.

3.2.7 Meta-analysis

A meta-analysis was conducted to combine the evidence from independent GWAS analyses of the three clusters by using a fixed-effects inverse-variance weighting approach. Because the three cluster-based analyses were conducted in a uniform way, we used the classical estimate approach in METAL (Willer et al., 2010), in which each study provides the effect size of variants (beta), and the standard error was used to weight the study according to the inverse of squared standard error. In addition, we applied a genomic control correction for the P-value. The between-study heterogeneity was tested and addressed using ANALYZE HETEROGENEITY in METAL, which additionally evaluates the (in-) consistency of the effect among studies. Additionally, to minimize the effect of population structure for comparison, we tested the overall association without using the clustering strategy. We performed the fifth association analysis directly pooling all 135 individuals together. The analysis of "pooled" GWAS was conducted in the same fashion as described in cluster-based GWAS. Finally, although the bantam is not considered as a sex-linked phenotype according to its mode of inheritance, a sex-linked analysis was performed in order to examine and confirm this. We first inferred the gender of individuals using sequence coverage on the Z and W chromosome. The ratio of sequence coverage (W/Z) was used to discriminate between ZZ (male) or ZW (female) individuals. The sex-linked association analysis was performed in three clusters respectively and the results were synthesized in the meta-analysis. The gene associated with sex-linked dwarfism (*GHR*) and the flanking region was investigated in more detail.

3.2.8 Annotation of the variants

The significant GWAS variants were further annotated for protein-coding genes or known non-coding elements. In order to have eligible associations and reasonable control for the false-positive, the significantly associated variants were selected using the conventional threshold of $P <= 5x10^{-8}$. This roughly corresponds to a Bonferroni correction for 1 million common variants to maintain a 5% genome-wide false positive rate (Panagiotou et al., 2012). We used Ensembl gene sets (version 95) for annotation including both coding and non-coding genes. We firstly annotated the variants based on their chromosomal position and distance to known genes. We reported significantly associated variants located within a gene range and the 1 Kb up- and down-stream regions to consider the promoter region. Secondly, we used Variant

Effect Predictor (McLaren et al., 2016) to further estimate the potential effect of variants (--biotype --buffer_size 5000 --check_existing --distance 5000 --sift b --species gallus_gallus --symbol). We investigated and annotated the variants with existing SNPs, the affected gene, and the effect of the variant on the transcripts. To compare the results of the three association studies and one meta-analysis, we visualized the shared and unique genes or variants among the four analyses using a Venn diagram (Heberle et al., 2015). Genes were listed when there is at least one variant annotated within the region. Functional annotation was performed using PANTHER v.11 (Mi et al., 2019) based on the chicken to human one-to-one orthologues. The Gene Ontology (GO) enrichment analysis was then conducted using package clusterProfiler (Yu et al., 2012).

3.2.9 Genetic differentiation (Fst) and haplotype sharing (IBD)

Haplotypes were phased for all individuals per chromosome using Beagle (version 5.0) (Browning and Browning, 2007) with a sliding window size of 0.02 cM and 0.01 cM overlap between adjacent windows. The analysis consisted of 12 iterations and the chromosomal genetic distances are based on (Elferink et al., 2010). Identity-by-descent (IBD) segments were detected by Refined-ibd (Browning and Browning, 2013). Note that our goal was not to detect segments that are derived from a single co-ancestor, but segments that come from the same population. Therefore, in order to detect these segments, we set relatively flexible criteria as follows: window=0.06 cM, length=0.03cM, trim=0.001 cM, finally LOD=3.

To infer the relative fraction of haplotype shared with the traditional bantam versus the normal-sized counterpart, we studied the relative IBD (rIBD) frequency in each cluster. We followed the rIBD calculation specified in Bosse et al. (2014). In short, the count of IBD segments (cIBD) that is shared between the traditional bantam and neo-bantam was computed in windows of 10 Kb and normalized for the total possible pair-wise comparison (tIBD). The normalized IBD (nIBD) was then compared with the nIBD computed between normal-sized counterpart and neo-bantam. The relative value of nIBD sharing was defined as rIBD.

Count of IBD segments that were shared between the traditional bantam and neo-bantam: $cIBD_{Bantam\_Neo\text{-}bantam}$

Total possible pair-wise comparison between the traditional bantam and neo-bantam: $tIBD_{Bantam\_Neo\text{-}bantam}$

Normalized IBD between neo-bantam and traditional bantam:

$nIBD_{Bantam\_Neo\text{-}bantam}=cIBD_{Bantam\_Neo\text{-}bantam}/tIBD_{Bantam\_Neo\text{-}bantam}$

Normalized IBD between normal-sized counterpart and neo-bantam was computed respectively: $nIBD_{Counterpart\_Neo\text{-}bantam}=cIBD_{Counterpart\_Neo\text{-}bantam}/tIBD_{Counterpart\_Neo\text{-}bantam}$

The relative value of nIBD sharing: $rIBD=nIBD_{Bantam\_Neo\text{-}bantam}-nIBD_{Counterpart\_Neo\text{-}bantam}$

If rIBD>0, the neo-bantam haplotypes within the region are considered more similar to the traditional bantam breeds compared to their normal-sized counterparts, and vice versa.

To measure the genetic differences between clusters, we estimated the fixation index (Fst) between the neo-bantam with either their inferred bantam source or with the normal-sized counterpart from the same cluster. The Fst was calculated in windows of 10 Kb using Vcftools with the method from Weir and Cockerham (Weir and Cockerham, 1984). We performed a similar comparison as for rIBD, the Fst between neo-bantam and traditional bantam was compared against the Fst between neo-bantam and normal-sized counterpart. The same approach was applied to the three bantam clusters separately.

3.2.10 Haplotype analysis: "PhyloGWAS" for topology comparison between groups

To identify genetic regions that might have been selected from a common source, we borrowed the concept of "PhyloGWAS" (Pease et al., 2016) that correlates phenotypes with a subset of standing genetic variation regardless of overall relatedness. The "PhyloGWAS" approach was originally designed to detect the sorting of common ancestral variation among populations that are subject to common environmental conditions or similar selection pressures (e.g., parallel evolution). We applied a similar comparative strategy studying the different pairs of bantam and normal-sized Dutch traditional breeds. In other words, the bantam variants selected from the common ancestry might group populations according to shared body size variation, despite the differences among breed pairs. To be more specific, such variants may be divergently fixed among the neo-bantam and normal-sized pairs, resulting in the expected topology that groups (neo-) bantams together according to the phenotype rather than following the overall relatedness.

We constructed the genetic relatedness using regional information of candidate regions, both variant and haplotype based. For the significant variants identified in the meta-GWAS, the genetic distance and phylogenetic tree were reconstructed similarly as described above including flanking regions. As for haplotype-based analyses, sequences were extracted around the lead variants including 1kb phased extending regions. As a next step, we computed 1-ibs distance matrix and constructed the phylogenetic tree using the two phased haplotypes of every individual. In order to compare the haplotype blocks of each cluster and the linkage disequilibrium (LD) around the *HMGA2* gene, we computed the r^2 between the markers of this region against the highest associated variant.

3.3 Results

3.3.1 Population structure of Dutch chickens

The Dutch chicken breeds show a diverse and admixed population structure. To perform a genomic analysis for the Dutch chicken population, whole-genome sequence data of 135 individuals representing 37 breeds was generated. After filtering, 13.5 million autosomal bi-allelic variants (including 11.6 million SNPs and 1.8 million InDels) were processed and used in the analyses to investigate the population structure. We classified the three clusters according to the bantam sources, which are the Dutch bantam in cluster 1, Sebright and Java bantam in cluster 2, and other miscellaneous bantams such as productive breeds in cluster 3. A clear structure of the population (Figure 3.1A) is shown by the Principal Component Analysis (PCA) and supported by the population tree (Figure 3.1B). Overall, neo-bantam breeds show the distribution of closely clustering with the corresponding normal-sized counterparts instead of a phenotype-specific substructure, showing the higher genetic similarity between normal-sized and neo-bantam counterparts than among true bantams. Individuals from the same defined clusters (Table S2) of bantam origin are generally clustered closely, especially for cluster 3. Some breeds in cluster 1 show considerable overlap with cluster 2, suggesting the overall normal-sized breed relationship, whereas cluster 3 disperses from most of the population in the first component. Particularly, the within cluster relationships of neo-bantams and true bantams are supported by additional population tree analyses (Figure S3.1C-E). For the second component, the true bantams, namely Dutch bantam (cluster 1), Sebright bantam, and Eikenburger bantam (cluster 2) separate from the majority of the traditional native breeds, which indicates definite divergence among breeds. Note that the clustering is based on the origin of bantam, not necessary on the relatedness of large fowls.

3.3.2 Cluster-based GWAS results show different signals

Because of the presupposed heterogeneous background of bantams, we performed genome-wide association studies on the bantam phenotype using autosomal genomic variants in the three bantam clusters independently. Independent GWAS for each cluster was performed accounting for the population structure. The lambda values of all GWAS were close to one (1.063 to 1.132), suggesting the population stratification was controlled. For the association studies with structural variants, we only found one putative bantam associated structural variant in cluster 2, whose effect however needs to be further studied (Figure S3.2). The analyses of the sex chromosomes confirmed that the bantam phenotype is not caused by a variant on sex chromosomes (Figure S3.3C-D). We did not find any association signal around the causative gene (*GHR*) for the sex-linked dwarfism, which supports the inheritance mode of the bantam phenotype. The three GWAS results show autosomal variants statistically associated with bantam phenotypes, however, notably different signals are found among clusters(Figure 3.2A-C). For cluster 1, we found a total of 133 variants surpassing the

threshold ($5x10^{-8}$), 78 of which are annotated with 32 known protein-coding genes or non-coding elements. In cluster 2, in total 28 variants and 11 genes are significantly reported. With respect to cluster 3, 116 variants and 47 genes were denoted as significant. For the association, we found three major consistent signals in cluster 1 and cluster 2. First, we report an interesting association on chromosome 1, located in the *High Mobility Group AT-hook 2* gene (*HMGA2*). In this candidate gene, cluster-specific signals reach the significance of $P=1.1 \times 10^{-16}$ (in cluster 1) and $P= 1.1x10^{-8}$ (in cluster 2). The significant variants are in the upstream and intronic regions of the gene. Other overlapping signals found in clusters 1 and 2 are signals in the *PR/SET domain 16* gene (*PRDM16*) on chromosome 21, as well as a signal proximal 170 to171 Mb on chromosome 1. However, the variants within these peaks show definite heterogeneity among the three clusters.

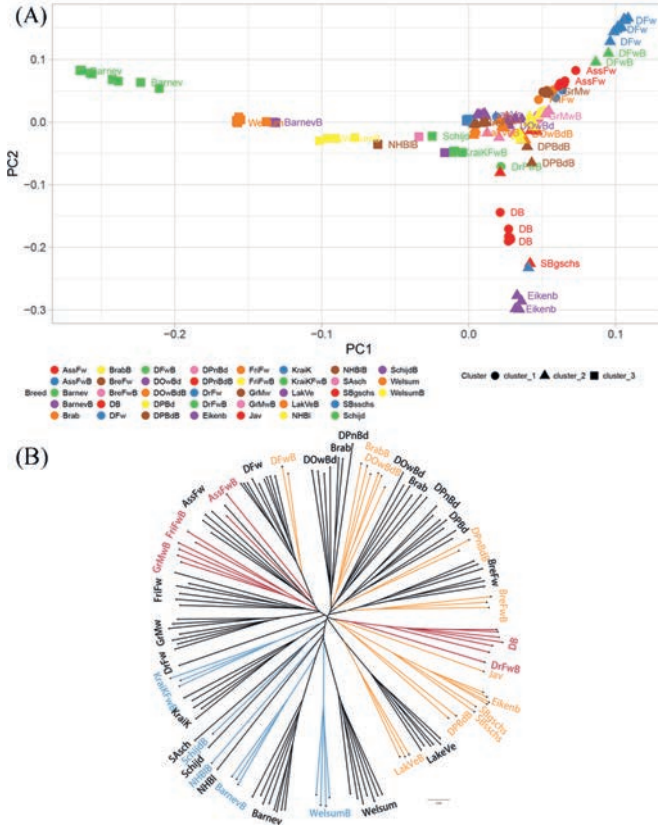

Figure 3.1 Population structure of Dutch chickens. (A) Principal Component Analysis, the breeds of chicken are displayed in different colors and shapes showing the three identified clusters. (B) The unrooted Neighbor-Joining tree of Dutch chicken presents 135 individuals, the bantam individuals have clades and nodes colored according to the phenotype and the clusters: bantams in defined clusters (cluster 1 in red, cluster 2 in yellow, and cluster 3 in blue), while the normal-sized breeds are colored black. The abbreviation of the breed name is used according to **Table S3.1**.

When explicitly looking at each cluster, several unique associated genes are reported (Table S3.3). For instance, in cluster 2 we observed an associated SNP (NC_006089.5:g.16,453,888C>T) passes the Bonferroni significance threshold ($P<3.97x10^{-9}$) that is located in the intergenic region between the myosin IIIA (*MYO3A*) *and G protein-coupled receptor 158* (*GPR158*) genes. We also identified a cluster 3 specific intronic mutation (NC_006089.5:g.1,255,851T>C) in the *Growth Hormone Releasing Hormone Receptor* gene (*GHRHR*). Another example within cluster 3 is the highest associated SNP (rs13643124) on chromosome 4, located in the third intron of *ENSGALG00000047072*, which is orthologous to Bromodomain and WD repeat domain containing 3 (*BRWD3*). Neither this leading SNP nor the *BRWD3* gene was found as a candidate in the analyses of cluster 1 and cluster 2, suggesting distinct genetic determinants.

3.3.3 Meta-analysis and comparison of associated variants and genes across studies

A meta-analysis was performed across the three clusters with the aim to detect shared loci and potentially new ones (Figure 3.2D). We used the meta-analysis to combine the results of the three cluster-based GWA studies and were able to detect shared bantam associated regions among different backgrounds. In total, the meta-analysis resulted in 627 variants overlapping with 129 genes that surpassing the significant threshold ($P<= 5x10^{-8}$), of which 15.9% have not been described by the Ensembl variation set (version 95). In total 145 variants and 47 genes are shared by at least two of the four studies (three cluster-based GWAS and the meta-analysis). In the meta-analysis, the most significant association (NC_006088.5:g.34,326,548G>C) is located within the first intron of *HMGA2* ($P=5.1x10^{-55}$), accompanyied by other 52 variants enriched in this gene, suggesting the important role of *HMGA2* (Table S5). The direction of the allelic effect in the three studies is consistently positive, with the alternative allele (C) statistically associated with the bantam phenotype. The lead variant shows disparate frequency of the associated allele of 93.3%: 0% in bantam against normal-sized in cluster 1, and in cluster 2 the frequency is 60.9%: 3.7%; whereas the frequency in cluster 3 is 27.8%: 0%. Particularly, no variant located in *HMGA2* is significantly associated with the bantam phenotype in cluster 3 (Figure S3.3B). The meta-analysis also showed that an abundant number of associated variants (29 variants) were enriched for *PRDM16*. Interestingly, *HMGA2* and *PRDM16* are the only two genes commonly associated in cluster 1, cluster 2, and the meta-analysis (Figure 3.2E). As for common variants between analyses, three significantly associated SNPs (rs313721485, rs313723493, rs1058489589) are in the upstream and intronic region of *HMGA2*, while another SNP (rs735861847) is located in the first intron of *PRDM16* (Figure 3.2F). Although the aforementioned QTL (around 170-171Mb on chromosome 1) has no specific SNP shared between the clusters, the region stands out in the meta-analysis too. The meta-analysis revealed a

candidate peaks around 171.30 Mb ($P=2.1x10^{-47}$). The reported QTL covers several functional genes, for example, coding for WD Repeat and FYVE Domain Containing 2 (*WDFY2*), serpin family E member 3 (*SERPINE3*), integrator complex subunit 6 (*INTS6*), tripartite motif containing 13 (*TRIM13*), and non-coding elements, e.g., *ENSGALG00000053256* and *ENSGALG00000052822*. By comparison, cluster 1 shows a significant association at 171.30-171.58 Mb, whilst cluster 2 and cluster 3 have candidates around 170.70 Mb and 170.91 Mb, respectively. The subtler differences in the interval between three association studies resulted in a proximal associated region in meta-analysis. The heterogeneity test in the meta-analysis confirmed that 48.1% of the significant variants were heterogeneous. Typically, many variants reach significance in one analysis, while in other analyses they are either not associated or inconclusive. From the Venn diagram (Figure 3.2E-F) cluster 3 does not share any significant gene or variant with the other two clusters, implying heterogeneous genetic backgrounds between the three bantam clusters. In addition, the meta-analysis also identified many unique variants and genes, showing the potential of discovering new genetic loci that might not reach significance in the single cluster GWAS. For example, four missense mutations were identified in the meta-analysis, of which one (NC_006088.5:g. 34,324,401C>A) is expected to alter the 2nd amino acid residue from Serine to Arginine in the aforementioned candidate gene *HMGA2*.

Furthermore, we compared the results of the meta-analysis and a "pooled" GWAS without using the clustering strategy (Figure S3.3A); the latter is directly pooling all cases and controls in one analysis. With the same sample size, the meta-analysis shows higher significance levels than the "pooled" GWAS without the clustering strategy. Moreover, although the major associations were also revealed by the "pooled" GWAS as in the meta-analysis, the majority of the signals failed to be detected using this approach. This suggests that the variants are likely only associated with a subset of the population, and the tests may lose power by simply pooling animals together. These results demonstrate the power of meta-analysis in detecting the potential association between analyses.

With respect to the functional annotation of significant genes across studies (170 genes), we identified GO terms related to development, though the enrichment analysis was not significant (Figure S3.4, Table S6), some of the GO terms are of explicit interest: bone morphogenesis, regulation of skeletal muscle tissue development, bone development, and negative regulation of cellular response to growth factor stimulus.

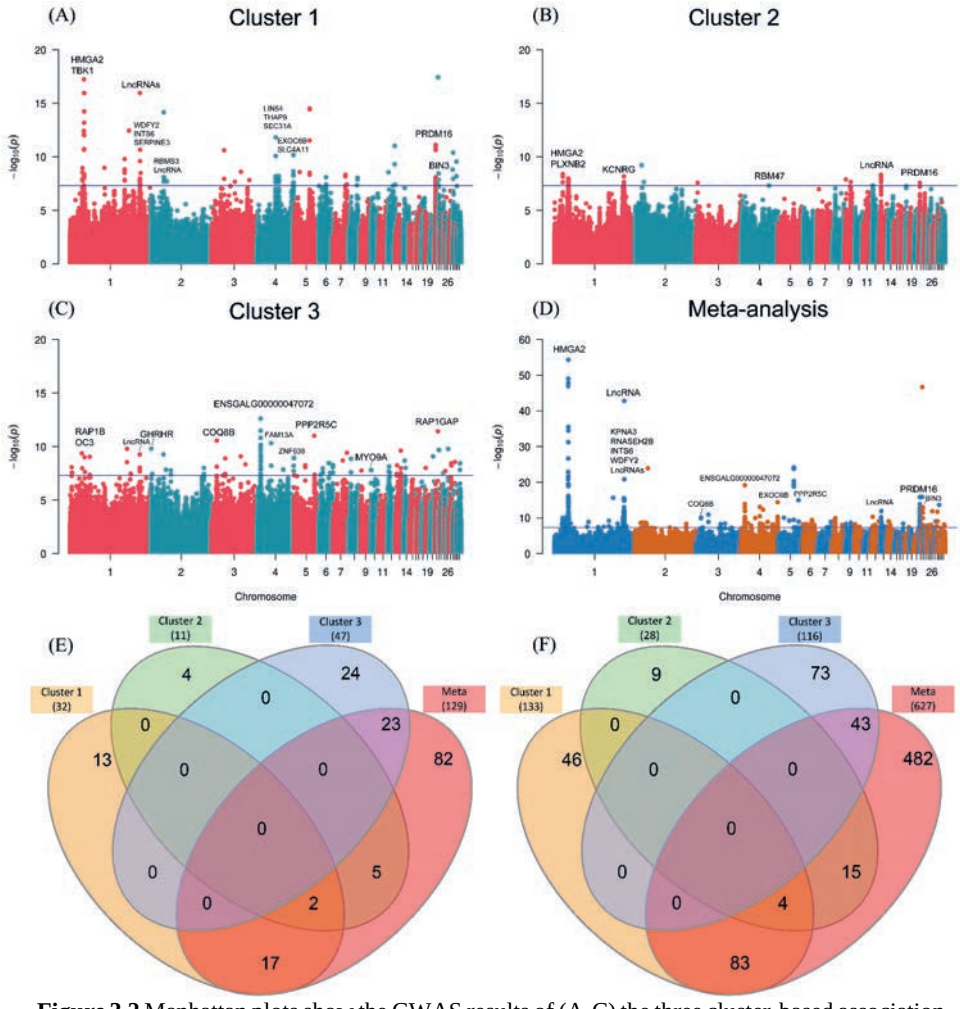

Figure 3.2 Manhattan plots show the GWAS results of (A-C) the three cluster-based association and (D) the meta-analysis. The -log10 P value on the y-axis is plotted by autosomal variants on the x-axis. The blue horizontal line indicates the suggestive cut-off threshold ($P=5x10^{-8}$). The variants are annotated with gene symbols, or long non-coding RNAs (LncRNAs). Detailed gene information can be found in Table S3.4. The Venn diagrams display the comparison between clusters 1 to 3 and the meta-analysis, representing (E) associated genes and (F) significant variants among four association results.

3.3.4 Exploring HMGA2 associated region: Fst and rIBD analyses

To further investigate the bantamization history and the introgression pattern of neo-bantam breeds, we explored the haplotype sharing and genetic differences on chromosome 1 using Fst and relative IBD sharing (rIBD). We computed the Fst and shared IBD segments between neo-bantam and their normal-sized counterpart, as well as that between neo-bantam and the corresponding bantam source. Overall, we observed a generally lower mean Fst (0.03-0.07) between the neo-bantams and their normal-sized counterparts than between the neo-bantams and the bantam sources (0.04-0.22). Similarly, we found more extensive and longer shared IBD segments between neo-bantams and normal-sized counterparts than between neo-bantams and bantam sources (Figure S3.5), in line with the expected close genetic relatedness between the native breeds and neo-bantams. However, when zooming in into the bantam-associated interval containing *HMGA2* on chromosome 1, positive rIBD signals were found in clusters 1 and 2, which suggests that the neo-bantams share more similar haplotypes with bantam sources in this interval than with normal-sized counterparts (Figure 3.3). The regional introgression from the bantam sources to neo-bantams is also supported by a lower regional Fst estimation. As a contrast, the regional negative rIBD and higher Fst displayed in cluster 3 are in accordance with the absence of an association signal. Another example is the regional pattern of Fst and rIBD in the cluster 3 specific interval on chromosome 4 (Figure S3.6). Our results confirm the introgression of these regions in which the neo-bantams are more similar to their bantam sources, suggesting a regional strong introgression from the bantam source rather than from the normal-sized counterpart.

3.3.5 Constructing haplotype "PhyloGWAS" across breeds

Finally, to investigate bantam introgressed haplotypes that might have been selected from segregating ancestral variation, we estimated the genetic relationship among clusters using both information from overall significant loci, and haplotype blocks within intervals. Specifically, the PCA and phylogenetic tree were used to test if the topologies of genetic variants came from confounding effects. Firstly, we analyzed this using all the significant variants (n=755) across the genome. A clear separation between bantams and normal-sized individuals is observed in both the PCA and the phylogenetic tree (Figure 3.4). Interestingly, the associated variants not only separated the case and control individuals but also distinguished the bantams of cluster 1 from the rest of the bantams. More variations were found within the (neo-) bantams than in the normal-sized breeds, supported by the longer branch lengths in the phylogenetic tree and the disperse distribution of bantam breeds in the PCA. Moreover, the topology of all the bantam breeds from cluster 1 demonstrates a stronger genetic relatedness than the other two clusters. These results show that although we observed limited overlap in associated genetic variants between three clusters, there is still a

clear overall similar selection for the bantam phenotype in the neo-bantam breeds. Secondly, we narrowed down to the haplotypes of specific lead variants. The associated haplotype in each cluster confirmed that the three clusters have clearly different association patterns as well as haplotype blocks (Figure S3.7A-C). In particular, the haplotypes in cluster 1 and cluster 2 both showed association patterns in the *HMGA2* related region whereas the haplotypes of cluster 3 showed no association in the corresponding region. Moreover, the regional phylogenies illustrate the presence of multiple haplotypes in clusters. For example, the haplotype around the lead SNP (NC_006088.5:g.34,326,548G>C) comprised in *HMGA2* (Figure S3.8A) displays a general cluster of haplotypes stemming from bantams from cluster 1, with a few other bantam breeds from cluster 2 and even fewer from cluster 3. As this SNP is located in a clear introgressed region, the surrounding haplotype is almost completely associated with the bantam phenotype in cluster 1, while the level of association gradually declines in clusters 2 and 3. The phylogenetic topology in cluster 1 demonstrated that the bantams were grouped in close clades, but we also observed the haplotypes of few bantam individuals (e.g., Dutch Bantam) were grouped next to this lineage showing the haplotype diversity. This implies that even when studying a small haplotype block (2 Kb), the strongly associated SNP in different clusters may be present on multiple haplotypes. The haplotype diversity can be further evidenced by the illustration of LD measured in the three clusters. In agreement with the haplotype patterns, the haplotype blocks in cluster 2 show lower LD but are relatively longer in size when compared with the haplotype blocks of cluster 1 (Figure S3.7D). The approximate intervals with high LD (r^2 >0.9) in cluster 1 and 2 are between 34.32-34.33 Mb and 34.32-34.36 Mb respectively.

This selection on multiple bantam haplotypes across clusters and breeds, considered together with the phenotype related separation shown by overall associated variants, could potentially be explained by the convergent selection on the ancestral variations. The comprehensive allelic heterogeneity is confirmed by similar distinct patterns of other associated variants (Figure S3.8).

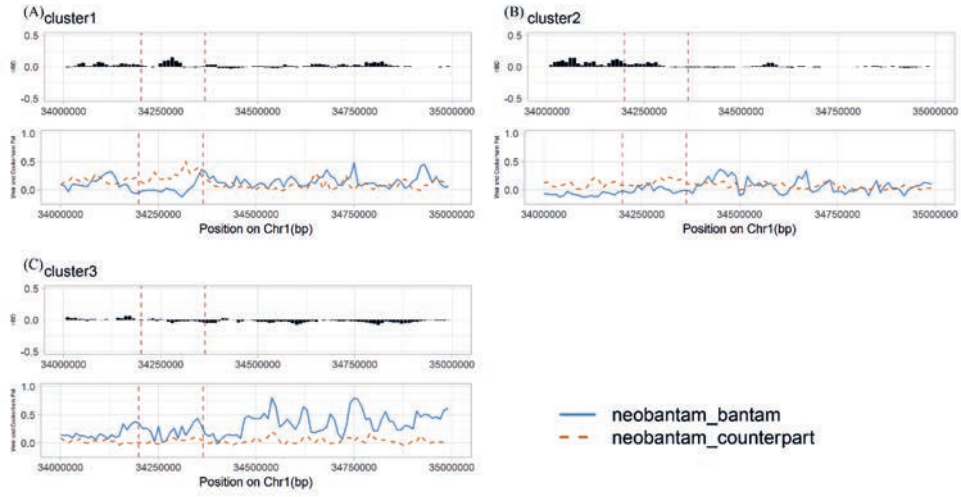

Figure 3.3 Distribution of the rIBD and Fst of the three clusters (A-C) around the HMGA2 corresponding interval (34-35 Mb). The x-axis displays the chromosomal coordinates, while the y-axis shows the value of rIBD and Fst. In each cluster, the upper panel shows the estimation of rIBD. The positive value of rIBD suggests more similarity between neo-bantam and bantam source than between neo-bantam and normal-sized counterpart; the negative rIBD value, on the contrary, shows the high haplotype sharing between neo-bantam and normal-sized counterpart. The lower panel displays the Fst estimation, the blue solid line represents the Fst between neo-bantam and bantam source, while the orange dashed line displays Fst between neo-bantam and normal-sized counterpart.

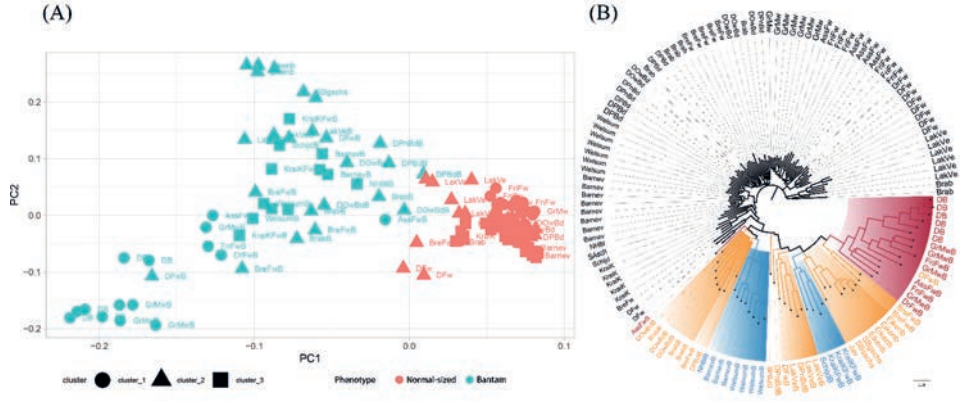

Figure 3.4 PCA and Neighbor-Joining tree of Dutch chickens using all the significant markers. (A) The phenotype of individuals is displayed by colors, and clusters of individuals are shown in different shapes. (B) All individuals are displayed by clades and nodes with different colors (cluster 1 in red, cluster 2 in yellow, and cluster 3 in blue), the normal-sized breeds are colored black. The bantam individuals are highlighted with background colors by the three clusters.

3.4 Discussion

3.4.1 Bantam breeding information enables untangling the complexity of the bantam phenotype

The human-mediated bantamization reshaped the genetic characteristics of neo-bantam chickens through crossbreeding. Here, we focus especially on the historical bantam breeding in the Dutch indigenous breeds. Bantam breeding in the Netherlands has been performed by hobby breeders adhering to breed standards. Despite the absence of an exhaustive crossbreeding scheme, the complexity of the bantam phenotype was revealed by our investigation showing that different (sub-)types of bantam breeds were utilized.

Body size, known as a highly polygenic trait in animals, has distinct forms of the phenotype presented in different breeds. The success of using genome-wide association studies to identify genetic variants in complex traits and diseases has been remarkable (Hardy and Singleton, 2009; Schaid et al., 2018). An appropriate GWAS population is based upon the matching of cases and controls and avoids the cryptic relatedness that might lead to population stratification (Tam et al., 2019). Here, we utilized the unique model of Dutch traditional chicken breeds involving matching counterparts of the normal-sized native breed and neo-bantam breed. Previous studies on dwarfism have focused on specific genetic variants in the genome (Burnside et al., 1992; Agarwal et al., 1994; Boegheim et al., 2017; Wu et al., 2018), whereas diverse backgrounds and heterogeneous phenotypes in different breeds have received little attention. Additionally, the formation of neo-bantam breeds requires us to account for the historical records of bantam crossbreeding and to study the bantam phenotype within specific clusters.

In this study, we integrated within cluster association studies and a meta-analysis across the populations to study the unknown genetics underlying the bantam phenotype. Such an approach has successfully identified genetic loci in previous studies, such as human height (Weedon et al., 2008), bovine stature (Bouwman et al., 2018), and canine hypothyroidism (Bianchi et al., 2015). The clustering in our study is explicitly based on the source of bantam used and shared during crossbreeding, and not necessarily on the genetic relatedness of the normal-sized breeds, which is nevertheless largely consistent with previous studies (Elferink et al., 2012; Bortoluzzi et al., 2018). We focused on the bantam genetic variants shared across various breeds with similar historical bantamization background and used the matching pairs of cases and controls (the normal-sized and its neo-bantam breed), which are breeds with the same appearance but only differ in size. This allowed us to use a relatively small population to detect eligible bantam associated genes. We also obtained many more significant signals in the meta-analysis at detecting bantam associated variants, outcompeting pooling the breeds while treating bantams as one single population.

With breed pooling, cryptic population structure in the genetic background was introduced to the study, therefore variants that should show association in a subset of the population failed to be discovered.

3.4.2 Heterogeneity of bantam and its sources

Our study provides insight into the heterogeneity of genotype-phenotype associations across diverse bantam ancestral clusters. Genetic heterogeneity was observed for the lack of sharing significant variants in the four major association analyses (three cluster-based GWAS and the meta-analysis), especially for cluster 3. The haplotype blocks surrounding *HMGA2* reported in cluster 1 and cluster 2 are significantly associated with bantam phenotype, but this association is not observed in cluster 3. Based on the size of LD blocks observed in clusters 1 and 2 we anticipate that multiple haplotypes are associated comprising the causal variant. Furthermore, the definite heterogeneous genetic architecture was illustrated in both the variant heterogeneity test and regional phylogeny structure, showing the complexity of the bantam trait is comprised of distinct subtypes.

There are three basic sources that can introduce heterogeneity in our study. First, heterogeneity can be caused by a non-standard phenotypic definition. In the case of complex traits, phenotypic determination sometimes is difficult to standardize and define, almost inevitably resulting in phenotypic heterogeneity. Previous studies suggest that dwarfism in chicken is a phenotype involving many forms of variation (Agarwal et al., 1994; Andersson and Georges, 2004; Boegheim et al., 2017; Wu et al., 2018). In agreement with this, we observed differences in the reduction of standard bodyweight across breeds (Figure S3.1A-B). Second, the heterogeneity may result from different ancestral origins (Evangelou and Ioannidis, 2013). In our study, we utilized the bantam historical record as a key basis for the association study. The cryptic ancestral groups are interpreted from the crossbreeding histories and confirmed by the definite differences in association patterns between the three clusters. This is further supported by the introgression signals showing rIBD and Fst fractions across the three clusters are different. Lastly, we observed heterogeneity in the allele effect across different analyses. We performed a heterogeneity test in the meta-analysis to estimate the variance effect between studies (Table S3.4). As described above, we confirmed that multiple variants are associated with only a subset of the population, and the effect of alleles can be found different across clusters. Furthermore, the haplotype analysis demonstrates that one specific haplotype could not completely explain the phenotypic differences among clusters. Within one cluster, even within one breed, the variation in haplotypes cannot present a complete phenotype-specific topology, which is evidence of genetic heterogeneity and haplotype diversity. The haplotype diversity is additionally evidenced by the LD between markers within the associated region (Figure S3.7D). In cluster 1 and 2, the

relatively short size of haplotype blocks and the degree of LD observed in the nearby sites suggested that the genetic variants surrounding the lead variant are not completely fixed in the bantam breeds. This implies the presence of more than one haplotype where the most significant SNPs are located on. The genomic analyses in this study show the fact that the Dutch chicken breeds contain diverse and complex bantam resources. In future studies, in order to control the unknown phenotypic and genetic heterogeneity, a standard phenotypic definition and measurement are desirable, especially for meta-analyses (Evangelou and Ioannidis, 2013).

3.4.3 Overview of candidate genes found in GWAS

Bantam associated genes were investigated for function in the growth of animals. Our results show that bantam is a typical polygenic trait, thus the integrative approach we implemented provides a unique opportunity to study it. The overlap between the meta-analysis and cluster-based GWAS demonstrates two genes in particular: *HMGA2* and *PRDM16*. Both of these genes have been reported to correlate with the growth of myoblasts (Li et al., 2012)(Seale et al., 2008). Variants (i.e., deletion, missense, and UTR variants) in *HMGA2* have been reported to be associated with reduced growth and stature in several other species, including human, mouse, rabbit, and cattle (Zhou et al., 1995; Weedon et al., 2007; Rimbault et al., 2013; Carneiro et al., 2017; Bouwman et al., 2018). *HMGA2* controls the proliferation of myoblasts and muscle development by regulating the expression of IGF2-binding protein 2 (*IGF2BP2*), which subsequently regulates multiple genes important for cell growth (Li et al., 2012). A variant in *HMGA2* was previously reported to be correlated with body weight in chicken (Song et al., 2011), but our study is the first to report the association between *HMGA2* and chicken dwarfism. In our study, most of the variants in *HMGA2* are intronic and upstream variants and not directly affecting the protein coding sequence. The significant variants are in a region that spans from the upstream till the first intron of *HMGA2*, containing signals of introgression and selection from the bantam origin to the neo-bantam, particularly in cluster 1. Similarly, variations detected in *PRDM16* were reported to be associated with growth and fatness traits in chicken and other species (Seale et al., 2008; Wang et al., 2010; Han et al., 2012). It is known that variation in *PRDM16* controls the cell fate switch between skeletal myoblasts and brown fat cells (Seale et al., 2008). Apart from that, the candidate region around 170-171Mb on chromosome 1 stretches across a widely reported proximal 1.5 Mb QTL (170.52 -172.04 Mb (Xie et al., 2012)). The QTL region influences growth and body weight, and contains lncRNAs and microRNAs (e.g., gga-mir-16-1) that are reported to regulate the expression of growth related genes (Wahlberg et al., 2009; Xie et al., 2012; Sheng et al., 2013). In this candidate region, clusters show slightly different refined intervals for the association, and candidate SNPs in each cluster do not overlap. In addition, the predicted consequences of the variants in this QTL are mostly intronic, upstream and downstream variations, which

makes it difficult to directly conclude the consequence on the expression of genes. Our study showed the importance of this QTL in regulating body growth in bantam chickens, the biological function and the genetic heterogeneity around this QLT should be confirmed and investigated in future studies. We found cluster 3 to extensively exhibit a heterogeneous association pattern compared to the analyses of clusters 1 and 2. Specially, a unique signal on chromosome 4 peaks within the gene ENSGALG00000047072, a fruit fly *BRWD3* homologue. In humans, this gene correlates with intellectual disability and macrocephaly and may alter developmental signaling (Field et al., 2007; Chen et al., 2015).

3.4.4 Overall convergent selection and regional introgression

By comparison, the "PhyloGWAS" and haplotype analyses show clear haplotype diversity across the three clusters, yet a potential convergent selection on the overall associated variants. For example, according to the presumed history of cluster 1, Dutch Bantam was repeatedly used as the (in-) direct source of bantam donor, which can be supported by a relatively consensus haplotype around the lead variant shared between the bantams within this cluster (Figure S3.8A-B). In Dutch traditional chickens, it is likely that selection for the bantam phenotype was performed in multiple clusters containing different underlying haplotypes with bantam alleles. As a result, the multiple haplotypes in different clusters and breeds can undergo a convergent selection for the bantam phenotype in the Dutch populations.

Generally, due to the intense crossbreeding and selection for a similar appearance as their normal-sized counterparts, the neo-bantams are genetically closely related to their normal-sized counterparts. Therefore, different from the majority of the genome, the regional high rIBD and low Fst signals in neo-bantams when compared to the bantam source indicate that these bantam-related genomic regions undergo a stronger introgression from the bantam source rather than from the normal-sized counterpart. Moreover, this suggests that most of the genomic contribution of the true bantam breeds is flushed out so that only haplotypes relevant for the bantam phenotype remain in the neo-bantams.

Finally, the intronic and up-stream variants found in the candidate list remain to be prioritized regarding their functionality. Currently, to improve the annotation of the causative alleles and functional regulatory elements, investigations are on the way performed by the international consortium Functional Annotation of Animal Genomes (FAANG) (Andersson et al., 2015), which will refine the causative variants and biological mechanisms that underlie the bantam phenotype.

Taken all together, we conclude that different bantam associated genomic regions are observed in the three clusters of the Dutch chicken population, accompanying by heterogeneity and diverse crossbreeding histories. Within the Dutch chicken populations, neo-bantam breeds were derived from the normal-sized counterpart by

using bantams as the donor for the dwarf phenotype. Therefore, making use of matching pairs of (neo-)bantam and normal-sized breeds provided us with a powerful proxy to understand the bantam phenotype. We used genomic analyses to show that the bantam phenotype is a complex trait caused by multiple underlying genes, which shows heterogeneity across the historical clusters. We report bantam associated genes in these cluster-based studies, including *HMGA2* and *PRDM16*, some of them are reported to correlate with dwarfism in chicken for the first time. Among Dutch bantam breeds, we show the selection for the bantam phenotype is likely subjected to a convergent direction across populations. As a result of crossbreeding, neo-bantams show regional introgression signals from the traditional bantam sources in the associated genomic regions. Overall, the genomic analyses on Dutch bantam breeds and the bantamization history demonstrate how human-mediated crossbreeding diversely reshape the genome and phenotype.

3.5 Data Archiving Statement

Whole genome sequence data were deposited in the European Nucleotide Archive (ENA). The data can be accessed through the three project numbers: (1) PRJEB34245, described 88 traditional chickens from the Netherlands in a previous study (Bortoluzzi et al., 2020a). (2) PRJEB39725, the data of 44 Dutch chickens has been submitted. (3) PRJEB36674, three samples (two Seabright bantams and one Sumatra) were described in a previously published study (Bortoluzzi et al., 2020b).

3.6 Acknowledgement

We would like to thank the China Scholarship Council for the financial support of Zhou Wu (Grant No. 201606350175). The sequencing data generated in this work was supported by the IMAGE Project from the European Union's Horizon 2020 Research and Innovation Program (Grant Agreement No. 677353). We would like to thank the Centre for Genetic Resources, the Netherlands (CGN) of Wageningen University and Research for providing some of the samples. We also sincerely thank the networks of breeders in the Netherlands, who provide information about phenotype and the history of breeds. We thank Hendrik-Jan Megens, Aniek Bouwman, and Henk Bovenhuis for the valuable advice on the data analyses. We would also like to thank Bert Dibbits and Kimberley Laport for experimental support.

3.7 Reference

Agarwal, S. K., Cogburn, L. A., and Burnside, J. (1994). Dysfunctional growth hormone receptor in a strain of sex-linked dwarf chicken: Evidence for a mutation in the intracellular domain. J. Endocrinol. 142, 427–434. doi:10.1677/joe.0.1420427.

Andersson, L. (2001). Genetic dissection of phenotypic diversity in farm animals. *Nat. Rev. Genet.* 2, 130–138. doi:10.1038/35052563.

Andersson, L., Archibald, A. L., Bottema, C. D., Brauning, R., Burgess, S. C., Burt, D. W., et al. (2015). Coordinated international action to accelerate genome-to-phenome with FAANG, the Functional

Annotation of Animal Genomes project. *Genome Biol.* 16, 57. doi:10.1186/s13059-015-0622-4.

Andersson, L., and Georges, M. (2004). Domestic-animal genomics: Deciphering the genetics of complex traits. *Nat. Rev. Genet.* 5, 202–212. doi:10.1038/nrg1294.

Bianchi, M., Dahlgren, S., Massey, J., Dietschi, E., Kierczak, M., Lund-Ziener, M., et al. (2015). A multi-breed genome-wide association analysis for canine Hypothyroidism identifies a shared major risk locus on CFA12. *PLoS One* 10, e0134720. doi:10.1371/journal.pone.0134720.

Boegheim, I. J. M., Leegwater, P. A. J., van Lith, H. A., and Back, W. (2017). Current insights into the molecular genetic basis of dwarfism in livestock. *Vet. J.* 224, 64–75. doi:10.1016/j.tvjl.2017.05.014.

Bortoluzzi, C., Bosse, M., Derks, M. F. L., Crooijmans, R. P. M. A., Groenen, M. A. M., and Megens, H. J. (2020a). The type of bottleneck matters: Insights into the deleterious variation landscape of small managed populations. *Evol. Appl.* 13, 330–341. doi:10.1111/eva.12872.

Bortoluzzi, C., Crooijmans, R. P. M. A., Bosse, M., Hiemstra, S. J., Groenen, M. A. M., and Megens, H. J. (2018). The effects of recent changes in breeding preferences on maintaining traditional Dutch chicken genomic diversity. *Heredity (Edinb).* 121, 564–578. doi:10.1038/s41437-018-0072-3.

Bortoluzzi, C., Megens, H.-J., Bosse, M., Derks, M., Dibbits, B., Lamport, K., et al. (2020b). Parallel genetic origin of foot feathering in birds. *Mol. Biol. Evol.* accepted. doi:10.1093/molbev/msaa092/5818884.

Bosse, M., Megens, H. J., Frantz, L. A. F., Madsen, O., Larson, G., Paudel, Y., et al. (2014). Genomic analysis reveals selection for Asian genes in European pigs following human-mediated introgression. *Nat. Commun.* 5, 4392. doi:10.1038/ncomms5392.

Bouwman, A. C., Daetwyler, H. D., Chamberlain, A. J., Ponce, C. H., Sargolzaei, M., Schenkel, F. S., et al. (2018). Meta-analysis of genome-wide association studies for cattle stature identifies common genes that regulate body size in mammals. *Nat. Genet.* 50, 362–367. doi:10.1038/s41588-018-0056-5.

Browning, B. L., and Browning, S. R. (2013). Improving the accuracy and efficiency of identity-by-descent detection in population data. *Genetics* 194, 459–471. doi:10.1534/genetics.113.150029.

Browning, S. R., and Browning, B. L. (2007). Rapid and accurate haplotype phasing and missing-data inference for whole-genome association studies by use of localized haplotype clustering. *Am. J. Hum. Genet.* 81, 1084–1097. doi:10.1086/521987.

Bruford, M. W., Bradley, D. G., and Luikart, G. (2003). DNA markers reveal the complexity of livestock domestication. *Nat. Rev. Genet.* 4, 900–910. doi:10.1038/nrg1203.

Burnside, J., Liou, S. S., Zhong, C., and Cogburn, L. A. (1992). Abnormal growth hormone receptor gene expression in the sex-linked dwarf chicken. *Gen. Comp. Endocrinol.* 88, 20–28. doi:10.1016/0016-6480(92)90190-U.

Carneiro, M., Hu, D., Archer, J., Feng, C., Afonso, S., Chen, C., et al. (2017). Dwarfism and altered craniofacial development in rabbits is caused by a 12.1 kb deletion at the HMGA2 locus. *Genetics* 205, 955–965. doi:10.1534/genetics.116.196667.

Chang, C. C., Chow, C. C., Tellier, L. C. A. M., Vattikuti, S., Purcell, S. M., and Lee, J. J. (2015). Second-generation PLINK: Rising to the challenge of larger and richer datasets. *Gigascience* 4, 7. doi:10.1186/s13742-015-0047-8.

Chen, W.-Y., Shih, H.-T., Liu, K.-Y., Shih, Z.-S., Chen, L.-K., Tsai, T.-H., et al. (2015). Intellectual disability-associated dBRWD3 regulates gene expression through inhibition of HIRA/YEM-mediated chromatin deposition of histone H3.3. *EMBO Rep.* 16, 528–38. doi:10.15252/embr.201439092.

Chiang, C., Layer, R. M., Faust, G. G., Lindberg, M. R., Rose, D. B., Garrison, E. P., et al. (2015). SpeedSeq: Ultra-fast personal genome analysis and interpretation. *Nat. Methods* 12, 966–968. doi:10.1038/nmeth.3505.

Cole, R. K. (2000). An autosomal dwarfism in the domestic fowl. *Poult. Sci.* 79, 1507–1516. doi:10.1093/ps/79.11.1507.

Dana, N., Megens, H. J., Crooijmans, R. P. M. A., Hanotte, O., Mwacharo, J., Groenen, M. A. M., et al. (2011). East asian contributions to dutch traditional and western commercial chickens inferred from mtDNA analysis. *Anim. Genet.* 42, 125–133. doi:10.1111/j.1365-2052.2010.02134.x.

Danecek, P., Auton, A., Abecasis, G., Albers, C. A., Banks, E., DePristo, M. A., et al. (2011). The variant call format and VCFtools. *Bioinformatics* 27, 2156–2158. doi:10.1093/bioinformatics/btr330.

Elferink, M. G., Megens, H. J., Vereijken, A., Hu, X., Crooijmans, R. P. M. A., and Groenen, M. A. M. (2012). Signatures of selection in the genomes of commercial and non-commercial chicken breeds. *PLoS One* 7, e32720. doi:10.1371/journal.pone.0032720.

Elferink, M. G., van As, P., Veenendaal, T., Crooijmans, R. P. M. A., and Groenen, M. A. M. (2010). Regional differences in recombination hotspots between two chicken populations. *BMC Genet.* 11, 11. doi:10.1186/1471-2156-11-11.

Esther Verhoef, and Rijs, A. (2014). *De kippen encyclopedie*. Rebo Productions.

Evangelou, E., and Ioannidis, J. P. A. (2013). Meta-analysis methods for genome-wide association studies and beyond. *Nat. Rev. Genet.* 14, 379–389. doi:10.1038/nrg3472.

Field, M., Tarpey, P. S., Smith, R., Edkins, S., O'Meara, S., Stevens, C., et al. (2007). Mutations in the BRWD3 gene cause X-linked mental retardation associated with macrocephaly. *Am. J. Hum. Genet.* 81, 367–374. doi:10.1086/520677.

Garrison, E., and Marth, G. (2012). Haplotype-based variant detection from short-read sequencing. *arXiv Prepr.* Available at: http://arxiv.org/abs/1207.3907 [Accessed February 14, 2018].

Han, R., Wei, Y., Kang, X., Chen, H., Sun, G., Li, G., et al. (2012). Novel SNPs in the PRDM16 gene and their associations with performance traits in chickens. *Mol. Biol. Rep.* 39, 3153–3160. doi:10.1007/s11033-011-1081-y.

Hardy, J., and Singleton, A. (2009). Genomewide association studies and human disease. *N. Engl. J. Med.* 360, 1759–1768. doi:10.1056/NEJMra0808700.

Heberle, H., Meirelles, V. G., da Silva, F. R., Telles, G. P., and Minghim, R. (2015). InteractiVenn: A web-based tool for the analysis of sets through Venn diagrams. *BMC Bioinformatics* 16, 169. doi:10.1186/s12859-015-0611-3.

Hulsegge, B., Calus, M. P. L., Windig, J. J., Hoving-Bolink, A. H., Maurice-van Eijndhoven, M. H. T., and Hiemstra, S. J. (2013). Selection of SNP from 50K and 777K arrays to predict breed of origin in cattle. *J. Anim. Sci.* 91, 5128–5134. doi:10.2527/jas.2013-6678.

Joshi, N., and Fass, J. (2011). Sickle: A sliding-window, adaptive, quality-based trimming tool for FastQ files (Version 1.33) [Software]. *Available at https://github.com/najoshi/sickle.*, 2011.

Layer, R. M., Chiang, C., Quinlan, A. R., and Hall, I. M. (2014). LUMPY: A probabilistic framework for structural variant discovery. *Genome Biol.* 15, R84. doi:10.1186/gb-2014-15-6-r84.

Li, H., and Durbin, R. (2009). Fast and accurate short read alignment with Burrows-Wheeler transform. *Bioinformatics* 25, 1754–1760. doi:10.1093/bioinformatics/btp324.

Li, H., Handsaker, B., Wysoker, A., Fennell, T., Ruan, J., Homer, N., et al. (2009). The Sequence Alignment/Map format and SAMtools. *Bioinformatics* 25, 2078–2079. doi:10.1093/bioinformatics/btp352.

Li, Z., Gilbert, J. A., Zhang, Y., Zhang, M., Qiu, Q., Ramanujan, K., et al. (2012). An HMGA2-IGF2BP2 Axis Regulates Myoblast Proliferation and Myogenesis. *Dev. Cell* 23, 1176–1188. doi:10.1016/j.devcel.2012.10.019.

McLaren, W., Gil, L., Hunt, S. E., Riat, H. S., Ritchie, G. R. S., Thormann, A., et al. (2016). The Ensembl Variant Effect Predictor. *Genome Biol.* 17, 122. doi:10.1186/s13059-016-0974-4.

Mi, H., Muruganujan, A., Huang, X., Ebert, D., Mills, C., Guo, X., et al. (2019). Protocol Update for large-scale genome and gene function analysis with the PANTHER classification system (v.14.0). *Nat. Protoc.* 14, 703–721. doi:10.1038/s41596-019-0128-8.

Mignon-Grasteau, S., Boissy, A., Bouix, J., Faure, J. M., Fisher, A. D., Hinch, G. N., et al. (2005). Genetics of adaptation and domestication in livestock. in *Livestock Production Science* (Elsevier), 3–14. doi:10.1016/j.livprodsci.2004.11.001.

Okonechnikov, K., Conesa, A., and García-Alcalde, F. (2016). Qualimap 2: Advanced multi-sample quality control for high-throughput sequencing data. *Bioinformatics* 32, 292–294. doi:10.1093/bioinformatics/btv566.

Panagiotou, O. A., Ioannidis, J. P. A., Hirschhorn, J. N., Abecasis, G. R., Frayling, T. M., McCarthy, M. I., et al. (2012). What should the genome-wide significance threshold be? Empirical replication of borderline genetic associations. *Int. J. Epidemiol.* 41, 273–286. doi:10.1093/ije/dyr178.

Paradis, E., and Schliep, K. (2019). Ape 5.0: An environment for modern phylogenetics and evolutionary analyses in R. *Bioinformatics* 35, 526–528. doi:10.1093/bioinformatics/bty633.

Parker, H. G., VonHoldt, B. M., Quignon, P., Margulies, E. H., Shao, S., Mosher, D. S., et al. (2009). An expressed fgf4 retrogene is associated with breed-defining chondrodysplasia in domestic dogs. *Science (80-.).* 325, 995–998. doi:10.1126/science.1173275.

Pease, J. B., Haak, D. C., Hahn, M. W., and Moyle, L. C. (2016). Phylogenomics Reveals Three Sources of Adaptive Variation during a Rapid Radiation. *PLoS Biol.* 14, e1002379. doi:10.1371/journal.pbio.1002379.

Pedersen, B. S., and Quinlan, A. R. (2018). Mosdepth: Quick coverage calculation for genomes and exomes. *Bioinformatics* 34, 867–868. doi:10.1093/bioinformatics/btx699.

Pedersen, B. S., and Quinlan, A. R. (2019). Duphold: scalable, depth-based annotation and curation of high-confidence structural variant calls. *Gigascience* 8. doi:10.1093/gigascience/giz040.

Rimbault, M., Beale, H. C., Schoenebeck, J. J., Hoopes, B. C., Allen, J. J., Kilroy-Glynn, P., et al. (2013). Derived variants at six genes explain nearly half of size reduction in dog breeds. *Genome Res.* 23, 1985–1995. doi:10.1101/gr.157339.113.

Schaid, D. J., Chen, W., and Larson, N. B. (2018). From genome-wide associations to candidate causal variants by statistical fine-mapping. *Nat. Rev. Genet.* 19, 491–504. doi:10.1038/s41576-018-0016-z.

Seale, P., Bjork, B., Yang, W., Kajimura, S., Chin, S., Kuang, S., et al. (2008). PRDM16 controls a brown fat/skeletal muscle switch. *Nature* 454, 961–967. doi:10.1038/nature07182.

Sheng, Z., Pettersson, M. E., Hu, X., Luo, C., Qu, H., Shu, D., et al. (2013). Genetic dissection of growth traits in a Chinese indigenous × commercial broiler chicken cross. BioMed Central doi:10.1186/1471-2164-14-151.

Song, C., Gu, X., Feng, C., Wang, Y., Gao, Y., Hu, X., et al. (2011). Evaluation of SNPs in the chicken HMGA2 gene as markers for body weight gain. *Anim. Genet.* 42, 333–336. doi:10.1111/j.1365-2052.2010.02141.x.

Sutter, N. B., Bustamante, C. D., Chase, K., Gray, M. M., Zhao, K., Zhu, L., et al. (2007). A single IGF1 allele is a major determinant of small size in dogs. *Science (80-.).* 316, 112–115. doi:10.1126/science.1137045.

Tam, V., Patel, N., Turcotte, M., Bossé, Y., Paré, G., and Meyre, D. (2019). Benefits and limitations of genome-wide association studies. *Nat. Rev. Genet.* 20, 467–484. doi:10.1038/s41576-019-0127-1.

Tarasov, A., Vilella, A. J., Cuppen, E., Nijman, I. J., and Prins, P. (2015). Sambamba: Fast processing of NGS alignment formats. *Bioinformatics* 31, 2032–2034. doi:10.1093/bioinformatics/btv098.

Turner, S. (2018). qqman: an R package for visualizing GWAS results using Q-Q and manhattan plots. *J. Open Source Softw.* 3, 731. doi:10.1101/005165.

Wahlberg, P., Carlborg, Ö., Foglio, M., Tordoir, X., Syvänen, A. C., Lathrop, M., et al. (2009). Genetic analysis of an F2 intercross between two chicken lines divergently selected for body-weight. *BMC Genomics* 10. doi:10.1186/1471-2164-10-248.

Wandelt, R., and Wolters, J. (1998). “Handbuch der Zwerghuhnrassen: die Zwerghuhnrassen der Welt,”

in (Bottrop: Verlag Wolters), 14–15.

Wang, J., Li, Z. J., Lan, X. Y., Hua, L. S., Huai, Y. T., Huang, Y. Z., et al. (2010). Two novel SNPs in the coding region of the bovine PRDM16 gene and its associations with growth traits. *Mol. Biol. Rep.* 37, 571–577. doi:10.1007/s11033-009-9816-8.

Weedon, M. N., Lango, H., Lindgren, C. M., Wallace, C., Evans, D. M., Mangino, M., et al. (2008). Genome-wide association analysis identifies 20 loci that influence adult height. *Nat. Genet.* 40, 575–583. doi:10.1038/ng.121.

Weedon, M. N., Lettre, G., Freathy, R. M., Lindgren, C. M., Voight, B. F., Perry, J. R. B., et al. (2007). A common variant of HMGA2 is associated with adult and childhood height in the general population. *Nat. Genet.* 39, 1245–1250. doi:10.1038/ng2121.

Weir, B. S., and Cockerham, C. C. (1984). Estimating F-Statistics for the analysis of population structure. *Evolution (N. Y).* 38, 1358. doi:10.2307/2408641.

Wickham, H. (2016). *Ggplot2: Elegant Graphics for Data Analysis*. doi:10.1007/978-3-319-24277-4.

Willer, C. J., Li, Y., and Abecasis, G. R. (2010). METAL: Fast and efficient meta-analysis of genomewide association scans. *Bioinformatics* 26, 2190–2191. doi:10.1093/bioinformatics/btq340.

Wu, Z., Derks, M. F. L., Dibbits, B., Megens, H. J., Groenen, M. A. M., and Crooijmans, R. P. M. A. (2018). A novel loss-of-function variant in transmembrane protein 263 (TMEM263) of autosomal dwarfism in chicken. *Front. Genet.* 9, 193. doi:10.3389/fgene.2018.00193.

Xie, L., Luo, C., Zhang, C., Zhang, R., Tang, J., Nie, Q., et al. (2012). Genome-wide association study identified a narrow chromosome 1 region associated with chicken growth traits. *PLoS One* 7, 30910. doi:10.1371/journal.pone.0030910.

Yu, G., Wang, L. G., Han, Y., and He, Q. Y. (2012). ClusterProfiler: An R package for comparing biological themes among gene clusters. *Omi. A J. Integr. Biol.* 16, 284–287. doi:10.1089/omi.2011.0118.

Zeder, M. A. (2012). *Pathways to animal domestication*. doi:10.1017/CBO9781139019514.013.

Zhou, X., Benson, K. F. F., Ashar, H. R. R., and Chada, K. (1995). Mutation responsible for the mouse pygmy phenotype in the developmentally regulated factor HMGI-C. *Nature* 376, 771–774. doi:10.1038/376771a0.

Zhou, X., and Stephens, M. (2012). Genome-wide efficient mixed-model analysis for association studies. *Nat. Genet.* 44, 821–824. doi:10.1038/ng.2310.

3.8 Supplementary materials

The complete supplementary material for this article can be found online at:

https://osf.io/927kp/?view_only=195fd6cdd3124652b2b63820c361e6f5

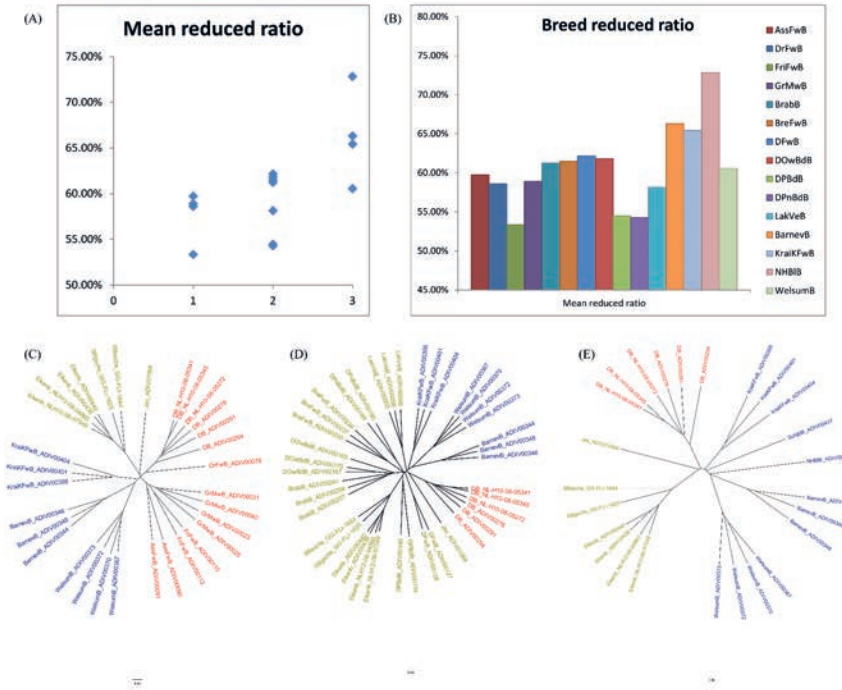

Figure S3.1 The breed reduced body weight and the phylogenic structure of the three clusters. The Breed standard bodyweight of Dutch chicken is collected (Supplementary file 1) and the breed reduced body weight of each breed was summarized in three clusters. Figure (A) shows the mean ratio of reduced body weight (shown in the y-axis) summarized according to three clusters (displayed by the x-axis). Figure (B) shows the reduced ratio of breeds. The figures (C-D) show the NJ-tree topology of neo-bantams of each cluster and the bantams source in the complete dataset, namely Dutch bantam (cluster 1), Java bantam and Sebright bantam (cluster 2); true bantams in cluster 3 were not sampled in this study, therefore three representative neo-bantams that possess diversification are used to represent the group. The color scheme is based on the cluster, red nodes show individuals from cluster 1, yellow shows cluster2, and cluster 3 is in blue nodes.

Figure S3.2 The association studies of structural variations for three clusters on GGA1 and GGA4 respectively (online).

Figure S3.3 Manhattan plot of GWAS results of the “pooled” analysis, HMGA2 analysis in cluster 3, and sex-linked analysis (online).

Figure S3.4 The enrichment analysis of Gene Ontology (GO) terms (online).

Figure S3.5 The histogram shows the comparison of the count of IBD fragments in the three clusters (online).

Figure S3.6 Distribution of rIBD and Fst estimation on GGA4 the cluster 3 specific region (online).

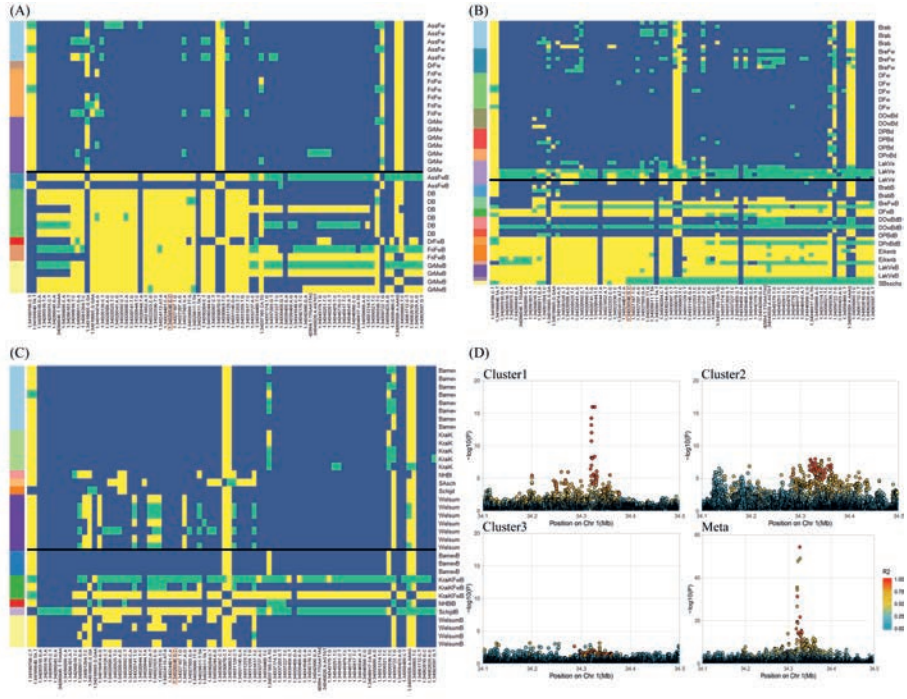

Figure S3.7 The haplotype of genomic associated sites in three clusters. (A-C) The horizontal axis represents the significant variant sites surrounding GGA1:34-35Mb ordered by chromosome and position, each row represents one individual, the breed name is on the right vertical axis and annotated by the left colored boxes. The bantam and normal-sized breeds are separated by a black horizontal line. The highlighted SNP in the orange box on the horizontal axis is the most significant peak variant (NC_006088.5:g.34326548G>C) found in the meta-analysis. (D) Manhattan plot shows the computed linkage disequilibrium (r^2) between markers in the three clusters (cluster 1 to 3) and meta-analysis. The value of r^2 was calculated for each variant against the peak SNP (NC_006088.5:g.34326548G>C). The colors of points indicate the values of r^2, ranging from 0 (blue) to 1 (red).

Figure S3.8 NJ-tree topology of haplotype and PCA structure (online page 9-10).

Table S3.1 The Dutch chicken population breeds and Clusters (online).

Table S3.2 The presumed bantam origin of each bantam breed (online).

Table S3.3 Significant genes associated with bantam phenotype (online).

Table S3.4 List of significant variants including shared ones and ones uniquely found in one cluster (online).

Table S3.5 The significant genes in meta-analysis and the number of variants enriched in the gene (online).

Table S3.6 Enrichment of Gene Ontology (online).

Supplementary file 3.1 Information on the bodyweight of Dutch chicken breeds (online).

4

Detection of differentially expressed genes in bantam chickens

Zhou Wu[1], Martien A.M. Groenen[1], Richard P.M.A. Crooijmans[1]

[1] Animal Breeding and Genomics, Wageningen University &Research, Wageningen, the Netherlands

In preparation

Abstract

To obtain insight in the gene expression influencing the reduced growth in bantam chicken, a type of dwarfism. RNA-Seq data was generated and derived from chicken embryos of contrasting sizes, which were sampled at two developmental stages: an early (E5) and a later (E13) stage. After detecting differentially expressed genes (DEGs) in different chicken breeds at each stage, we identified genes involved in growth related signaling pathways (e.g., *FGF*, *COL*), biological processes like myogenesis and osteogenesis, as well as genes reported previously as bantam candidates (e.g., *RNASEH2B*). We were able to identify the DEGs associated with bantam phenotype as early as embryonic stage E5. Overall, DEGs compared between breeds showed limited overlap, supporting the expected heterogeneity contributing to the bantam phenotype. The DEGs and signaling pathways identified in this study provide new insights into the molecular basis underlying growth reduction in chickens.

Keywords: RNA-seq, differentially expressed genes, chicken, dwarfism, bantam, embryonic development

4.1 Introduction

Dwarfism is a growth reduction condition leading to short stature, that can be found in many species. Bantam phenotype, characterized by the exquisite form of growth reduction in poultry, is one of the most important genetic resources in indigenous chickens, which has become popular and prevalent across the world. In the Netherlands, crossbreeding to create bantam forms of the local breeds, has been used extensively since the end of the 19th century (Esther Verhoef and Rijs, 2014). The crossbred bantams (neo-bantams) were created by mating the local traditional breeds with existing bantam breeds, followed by backcrossing. This resulted in counterparts of traditional breeds that share the same features but differ in size. Typically, the bantams in the Netherlands show approximately 50% to 60% reduction in body weight (Wu et al., 2020). Moreover, there is a significant difference between the bantams and normal-sized breeds with regards to the size of eggs and chicks at hatch. Recently, we identified genes and genetic variants associated with bantam phenotype by using genome-wide association studies (GWAS) based on whole genome sequence data (Wu et al., 2020). We have shown that the bantams of the Netherlands can be subdivided into subtypes characterized by heterogeneous bantam introgression backgrounds. However, gene expression profiles and signaling pathways that modulate embryonic development in bantams remain to be understood.

The molecular mechanisms underlying dwarfism are controlled by coordinated development of bone and skeletal muscle during growth. Dwarfism that is heritable can result from genetic mutations triggering protein alterations and signaling or hormonal disruptions (Boegheim et al., 2017). One example of these signaling pathways can be seen in the genetic basis of achondroplasia, the most common form of dwarfism in humans (Shiang et al., 1994; Richette et al., 2008). The mutations in the fibroblast growth factor receptor-3 gene (*FGFR3*) induce disturbance of endochondral ossification (Richette et al., 2008). Another example is the genetic mutations in the growth hormone receptor gene (*GHR*) resulting in the sex-linked dwarfism in chickens (Agarwal et al., 1994; Tahara et al., 2009). As part of the GH-GHR-IGF1 axis, the affected GHR signaling transduction can reduce skeletal muscle growth, leading to short stature (Lin et al., 2012; Luo et al., 2016). Understanding the gene expression associated with growth reduction in bantam embryos will expand our knowledge about myogenesis and osteogenesis in chicken.

In this study, we performed differential gene expression analyses between different bantams and normal-sized samples at two developmental stages using RNA-seq data. Analyses were explicitly performed at the developmental stage E5 (early stage) and E13 (later stage) to identify differentially expressed genes (DEGs) in growth variation. In particular, we also compared between respective bantam counterparts, i.e., a Dutch traditional breed exhibiting both normal-sized and bantam phenotypes, to provide

insights into the breed specific DEGs and signaling pathways involved in bantam phenotypic and genetic heterogeneity.

4.2 Materials and Methods

4.2.1 Sample collection and RNA-seq data

In order to understand the gene expression underlying the bantam phenotype, chicken embryonic samples of contrasting sizes were sampled at two time points. The two sampling time points are embryonic day 5 (E5) and day 13 (E13) of incubation, corresponding to the Hamburger Hamilton Stage 26 and 39, respectively. We collected tissues from the upper-body and right leg with the removal of head and organs from the samples. Animal material was cut in pieces and transferred to RNAlater (QIAGEN) for stabilization. Tissues from the upper-body and the right leg were grinded in liquid nitrogen and subsequently used for RNA isolation. In total, we generated RNA-seq data of 31 samples representing 8 breeds. We collected 15 samples for E5, and 16 samples for E13. The table of samples can be found in Table S4.1. There are two types of bantam breeds sampled in this study each with 2 animals per breed. First, traditional/true bantams, representing the Dutch Bantam (DB) and the Sebright Bantam (SB), are bantam breeds for which no large counterpart exists. The second type are the neo-bantam breeds; Frisian fowl bantam (FriFwB), Dutch Polish Bearded bantam (DPBdB) and Schijndelaar Bantam (SchijdB), for which we also sampled the corresponding normal-sized counterpart breeds as controls. The three neo-bantam breeds in this study represent the three heterogeneous bantam backgrounds identified in a prior bantam GWAS analysis (Wu et al., 2020; chapter 3). The neo-bantam breeds in combination with their non-bantam counterparts form the three breed pairs for DEGs identification for specific breed. Moreover, according to the historical classification, FriFw(B) belong to country fowl, DPBd(B) are ornamental fowls, and Schijd(B) belong to the past productive type, representing diverse management purposes of the Dutch breeds in the dataset.

RNA-seq data was generated by paired-end 150 bp Illumina sequencing. The reads were mapped to the chicken reference genome, GRCg6a, using STAR v2.4.0 (Dobin et al., 2013). We used featureCounts for the quantification of transcript abundance (Liao et al., 2014). The Ensembl gene set (version 95) was used as the genetic feature. The expression count matrix was obtained and pre-filtered by using the DESeq2 package (Love et al., 2014). The schematic outline of the analyses in this study is shown in Figure 4.1.

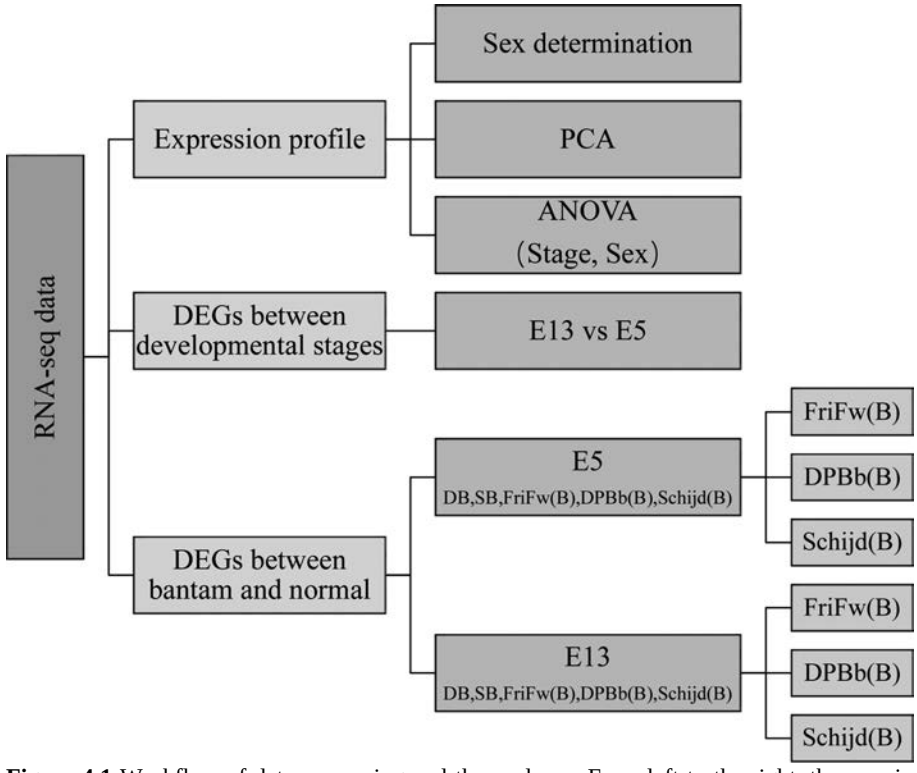

Figure 4.1 Workflow of data processing and the analyses. From left to the right, three main analyses were conducted to study the RNA-seq data generated by this study. Breed names in the green and yellow boxes are in abbreviation, representing the normal size breeds and their neo-bantam counterpart breeds (indicated by the "B" in bracket). For instance, FriFw(B) represent the DEGs identification between Frisian Fowl and its neo-bantam counterpart Frisian Fowl Bantam.

4.2.2 Sex determination

Because all the samples were collected at embryonic stages, the sex of the samples is unknown and requires prior determination. In order to reduce the influence of the dynamic gene expression level between samples and stages, we determined the sex by comparing the number of specifically expressed genes on the sex chromosomes (Z and W). We excluded the recombining pseudo-autosomal regions by filtering for the Z and W paired paralogous genes with >80% identity. As a result, we excluded 21 and 28 paralogous genes from the gene set on Z and W chromosomes respectively. The gene expression level was then pre-filtered to remove genes with unexpressed or extremely low expression level by filtering out genes with, on average, less than one count per individual. Then for each individual, the number of expressed genes (count > 0) on sex chromosomes were summarized. We used the number of expressed genes on the W chromosome to discriminate between males and females, while accounting for the number of expressed genes on the Z chromosome of the same individual:

$$ratio\ of\ gene\ expressed = \frac{number\ of\ expressed\ genes\ on\ W / All\ genes\ on\ W}{number\ of\ expressed\ genes\ on\ Z / All\ genes\ on\ Z}$$

where a female (ZW) sample is expected to have a ratio of gene expressed (W/Z) close to one, and a male sample (ZZ) should have a value close to 0 (due to complex characterization of the pseudo-autosomal regions in chicken (Nam and Ellegren, 2008; Zhou et al., 2014), this value is not expected to be equal to 0 in ZZ samples). In addition, we used the plotPCA function in DESeq2 (Love et al., 2014) to perform a PCA analysis decomposing the variation of gene expression level on the W chromosome of all individuals.

4.2.3 Expression profile and effect of developmental stage and sex

In the expression profile analysis, we examined the pairwise correlation between samples across all genes. The expression count matrix was first normalized by using the counts per million function (cpm) in edgeR (Robinson et al., 2009), then log2 transformed. The pairwise correlation coefficient between samples was calculated following the "spearman" method.

To examine the factors that potentially influence the expression profile, we performed the one-way analysis of variance (ANOVA) to detect the effect of the developmental stage and the sex of samples. To consider the variance of each gene across samples for similar dynamic range, gene expression data was transformed using the variance stabilizing transformation implemented in DESeq2. We performed a principal component analysis (PCA) including all 31 samples from the two developmental stages (E5 and E13) and of both genders using the plotPCA function in DESeq2. We subsequently applied the ANOVA test to the two top principal component axes in order to test the effect of developmental stage and the sex of samples. We used the one-way ANOVA implemented in the R package stats (R Core Team, 2019).

4.2.4 Detection of differentially expressed genes

We detected DEGs associated with bantam phenotype by comparing the gene expression between the bantam and normal-sized samples. The R package DESeq2 was used for normalization and detection of DEGs (Love et al., 2014). Detection of DEGs was performed with a multi-factor design using sex as an additional fixed effect variable in the model. An internal normalization implemented in DESeq2 was performed to account for differences in read depth and expression patterns. First, we detected the DEGs using all samples of eight breeds at the two developmental stages respectively, which correspond to Hamburger Hamilton Stage 26 (E5) and HH 39 (E13). Secondly, for each developmental stage, DEGs were detected for the three specific breed pairs: FriFwB vs FriFw, DPBdB vs DPBd, and SchijdB vs Schijd. The P values were adjusted using the "BH" method (Benjamini and Hochberg, 1995), and the significant threshold of adjusted P value was set at 0.05. The fold changes (FC) of

expression and the “up-” or “down-regulated” levels were determined by comparing the bantams against the normal-sized samples. Due to the limited number of individuals in the breed specific comparisons, the FC for these breed specific DEGs was carefully interpreted. In addition, the same procedure was used to identify DEGs between the embryonic stages, E13 and E5, to identify DEGs associated with developmental dynamics.

4.2.5 Gene ontology enrichment analysis of DEGs

The functional annotation of the DEGs was performed using the Gene Ontology (GO) enrichment. We used the human orthologous genes for GO enrichment using ClusterProfiler (Yu et al., 2012). The DEGs detected between bantam and normal-sized phenotypes at each developmental stage were used for the functional annotation analysis. The DEGs identified between two development stages were also analyzed. The P values were adjusted using the “BH” method (Benjamini and Hochberg, 1995), and $P > 0.05$ was considered significantly overrepresented. We also tested the overrepresentation of pathways additionally using the reactome pathways database (Jassal et al., 2020).

4.3 Results

4.3.1 RNA sequence data

We sequenced the RNA of 31 samples representing 8 breeds from two developmental stages (Table S4.1). At each developmental stage, we collected samples from true bantams (two breeds), neo-bantams (three breeds) and the corresponding normal-sized counterparts (three breeds). On average, 89.11% of the sequence reads was aligned to the reference genome (GRCg6a) representing approximately 32 million uniquely mapped reads. We observed around nineteen thousand expressed genes (count > 0) after pre-filtering to remove genes with exceptionally low average value in the count matrix.

4.3.2 Sex determination using transcriptomic data

We considered and examined the effect of sex across the samples due to the sex differences in the growth of chicken embryos (Burke and Sharp, 1989). To determine the sex of the animals we employed two methods. The first to infer the sex of the embryos, is by inferring the gene expressed ratio on the sex chromosomes (W and Z). After filtering, we used 845 genes on the Z chromosome and 51 genes on the W chromosome for subsequent analyses. Results showed the samples of different sex had distinct number of expressed genes on W chromosome (Figure S4.1), which enabled us to utilize this to determine the sex of samples. Based on that, we found a discriminant pattern of gene expressed ratio (W/Z) between females (ZW) and males (ZZ) (Figure 4.2A). This result was further supported by the second method where we used a Principal Component Analysis (PCA) determining the sex based on the

expression pattern of genes on the W chromosome (Figure 4.2B). For the PCA, the first component explaining 78% of variance clearly separates the two genders despite the stage and the phenotype of the samples. The inferred sex was assigned for all individuals and used in the subsequent analyses. Of the 31 samples, 18 samples were assigned as male (ZZ) and 13 as females (ZW) (Table S4.1).

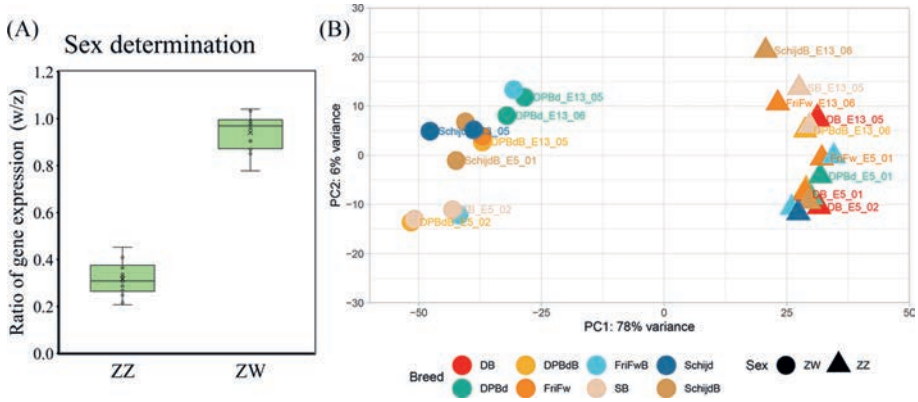

Figure 4.2 Sex determination of the samples. (A) The ratio of gene expression (W/Z) between females (ZW) and males (ZZ). (B) PCA plot displays the expression pattern of all samples using the genes located on the W chromosome, the inferred sex of the samples is shown by a circle (female) or a triangle (male).

4.3.3 Expression profile shows the effect of developmental stage and sex

As for the expression profile, the correlation of all genes across samples demonstrated a stage-specific pattern (Figure 4.3A-B). First, samples from the same developmental stage clustered together despite their phenotype or sex. The PCA using all genes across the genome revealed a further divergent pattern of separation by stage and sex. For the first component (71% variance), samples were separated by the two developmental stages (E5 and E13); while for the second component (10% variance), samples were distinguished by the sex of the samples. This is supported by the ANOVA results (Figure 4.3C-D), which shows that the samples from E5 and E13 are significantly different along PC1 ($P=2.2x10^{-16}$), whereas the expression between females and males is significantly different for PC2 ($P=2.2x10^{-16}$). These results identified a clear stage-specific pattern in the expression profile. Furthermore, the sex of samples can also influence the expression profile as a secondary factor.

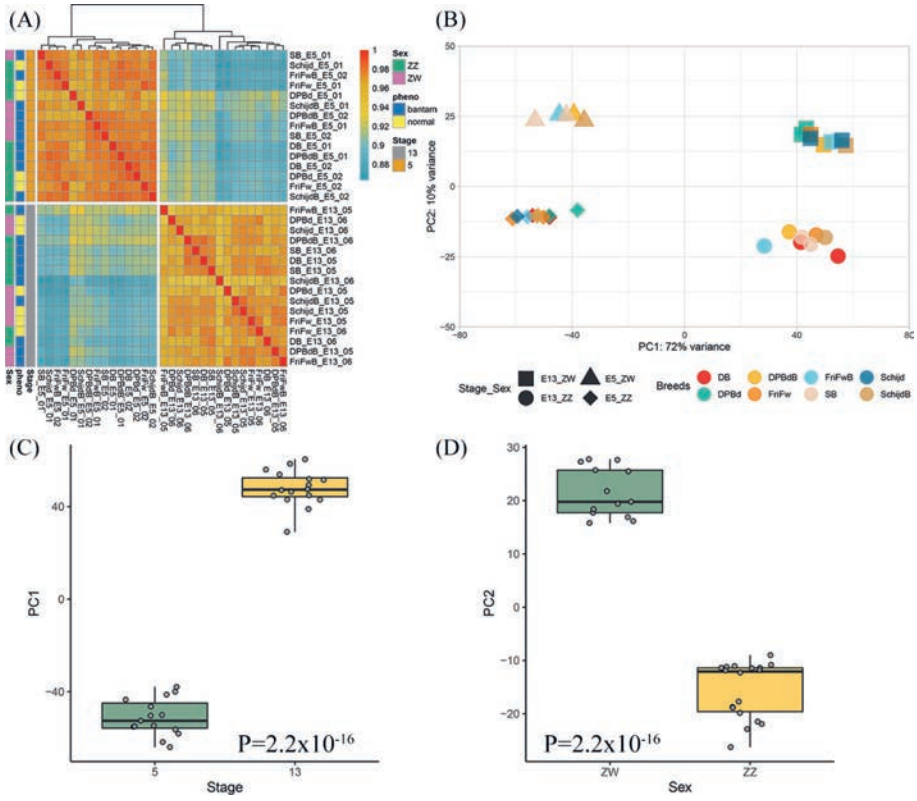

Figure 4.3 Gene expression profile across the two stages and samples. (A) The correlation heatmap shows expression pattern of 31 samples across all genes. The sex, phenotype (i.e., bantam or normal-sized), and stage of samples are shown on the left of the figure. (B) PCA shows the overall gene expression pattern of 31 samples. The breed of the samples was shown in different colors, while the shapes display different stages combined with sex. (C-D) The variance of the two factors (stage and sex) along the first two principal components (PCs). The PCs represent the gene expression across the genome, including the autosomes and the sex chromosomes.

4.3.4 Identification of DEGs between developmental stages

When comparing the gene expression between the two developmental stages E5 and E13, we detected 832 DEGs (Table S4.2). A GO enrichment analysis presented a large number of enriched terms regarding muscle development and differentiation process, including muscle organ development, muscle system process, skeletal muscle tissue development and regulation of ossification (Table S4.3). In terms of the biological process and cellular component, we found many genes involved in the formation of myofibril (42 genes) and sarcomere (40 genes), supported by the overrepresentation of GO terms associated with muscle development. In particular, 52 DEGs comprised the GO term "muscle organ development" ($P = 2.13x10^{-19}$). In addition, the term "skeletal muscle tissue development" was found to be enriched ($P = 5.32x10^{-13}$),

supported by 22 up-regulated and 5 down-regulated DEGs. We further observed the muscle structure development pathway to be enriched with 47 DEGs, including the gene encoding Insulin-like Growth Factor 1 (*IGF-I*). In addition to *IGF-I*, 11 other DEGs were found to be associated with the "regulation of Insulin-like Growth Factor (IGF) transport and uptake by Insulin-like Growth Factor Binding Proteins (IGFBPs)" pathway, which is responsible for the binding and targeting of IGFs in human (Jassal et al., 2020). Expression of *IGF-I* is upregulated at stage E13 compared to E5 by more than 10-fold ($P = 8.44x10^{-25}$).

4.3.5 Identification of DEGs between the bantam and normal-sized phenotypes

To detect the DEGs involved in the differentiation of body size, we compared the gene expression between the two phenotypes, bantam and normal size, at time point E5 and E13, respectively. We first performed an overall DEGs detection at every stage using all eight breeds, comparing the bantam breeds (true and neo-bantams) against the non-bantam samples. In addition, to better understand specific transcriptomic differences for the breeds that exist in both small and normal size, we subsequently identified DEGs within the three pairs of counterparts at each stage.

4.3.5.1 DEGs detected at stage E5

At embryonic stage E5, we detected DEGs among the eight breeds. In total 10 genes were significantly differently expressed between bantam and non-bantam individuals, of which 9 were down-regulated and 1 up-regulated (Table S4.2). In particular, the gene encoding Ribonuclease H2 subunit B (*RNASEH2B*) showed 1.27-fold decreased expression in bantam samples compared to non-bantam ones ($P = 0.02$) (Figure 4.4). Of the true bantams, Dutch Bantam (DB) showed significantly lower expression levels compared to the controls at this stage. When looking at DEGs detected in the specific breed pairs, we identified a higher number of DEGs and more down-regulated than up-regulated genes. The numbers of DEGs identified between FriFwB vs FriFw are 65 up-regulated and 257 down-regulated genes; between DPBdB vs DPBd are 79 up-regulated and 215 down-regulated genes; between SchijdB vs Schijd are 4 down-regulated genes and no up-regulated. For the SchijdB vs Schijd comparison, not many DEGs were detected, which might be explained by the single individual sampled for Schijd leading to the restricted power at detection. The GO enrichment analysis combining all these genes resulted in the top overrepresented GO terms related to muscle development, such as muscle organ development, myofibril, and structural constituent of muscle (Figure S4.2, Table S4.3). In particular, we showed six paralogues encoding chains of different types of collagen that were down-regulated, which are involved in the gonadotropin-releasing hormone (GnRH) pathway. For instance, genes encoding collagen type VI and IX alpha subunits (e.g., *COL6A2* and *COL9A1*) exhibited significantly lower expression in bantam samples. Moreover, in bantam samples, we observed many down-regulated genes involved in the term

"muscle tissues development". For instance, the expression of both myogenin (*MYOG*) and myogenic differentiation 1 (*MYOD1*) is over 2.5-fold decreased in bantam samples compared to normal-sized samples. In addition, the gene insulin like growth factor 2 mRNA binding protein 1 (*IGF2BP1*) exhibited 1.65-fold increased expression in the DPBdB samples (P = 0.02).

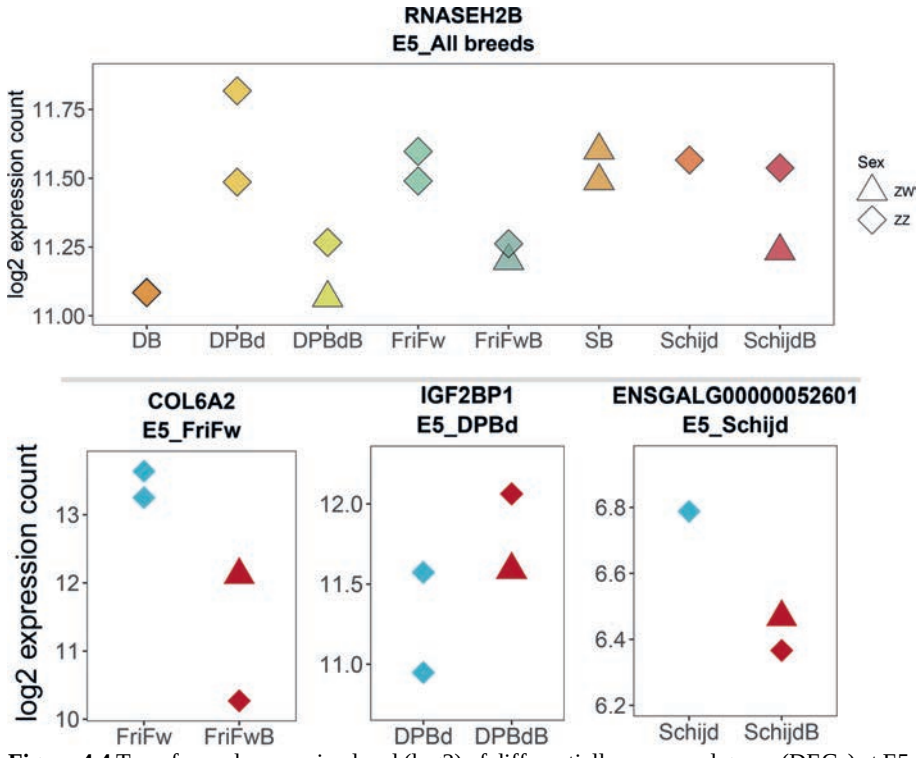

Figure 4.4 Transformed expression level (log2) of differentially expressed genes (DEGs) at E5. The upper panel displays gene expression among all the 8 breeds tested at developmental stage E5. The lower panel shows the DEGs detected in the specific breed pairs. The sex of samples is displayed by different shapes.

4.3.5.2 DEGs detected at Stage E13

A similar analysis approach as described above, resulted for embryonic stage E13 in 4 up- and 7 down-regulated genes in the bantams compared to normal-sized samples (Table S4.2). In the GO annotation results, the top significant terms include cell fate commitment and pattern specification process, collagen-containing extracellular matrix, myofibril, response to BMP and bone morphogenesis (Figure S4.2, Table S4.3). Two differently expressed genes were involved in osteogenesis, i.e., gene *TBX2* and *TBX4* encoding members of a conserved gene family T-box transcription factor, which were down-regulated in bantams with 2.11-fold and 3.50-fold change, respectively. The true bantams, DB and SB, showed similar levels of expression as

the three neo-bantam breeds in the *TBX4* gene, which is down-regulated compared to normal-sized samples (Figure 4.5).

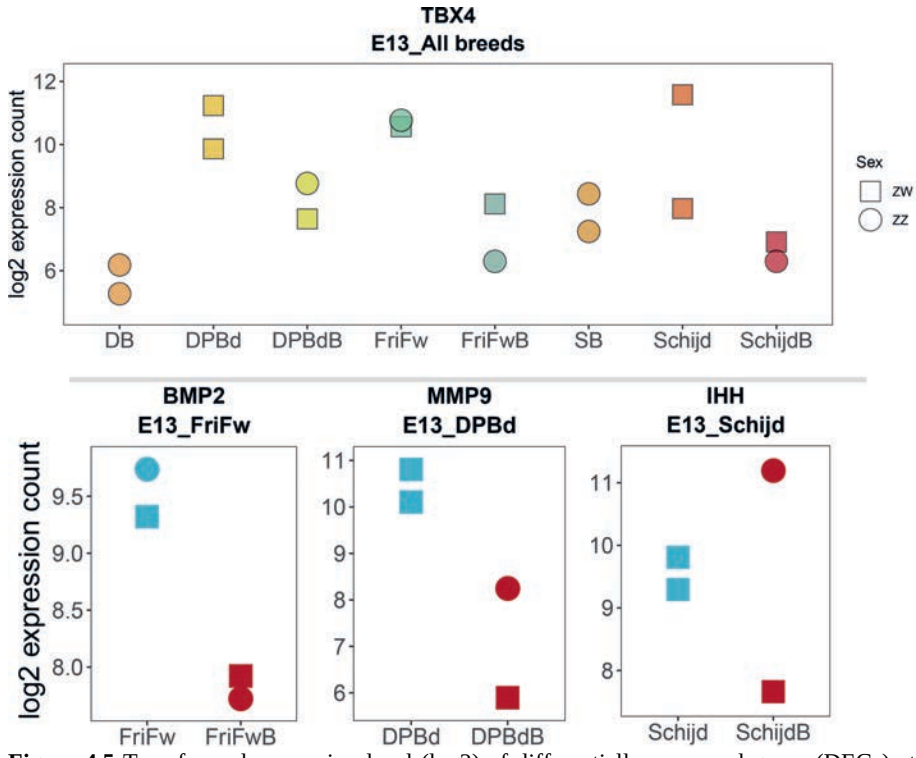

Figure 4.5 Transformed expression level (log2) of differentially expressed genes (DEGs) at E13. The upper panel displays gene expression among all the 8 breeds tested at developmental stage E13. The lower panel shows the DEGs detected in the breed pairs. Different shapes display the sex of the samples.

The DEGs detected in the specific breed pair comparisons resulted in 262 up-regulated and 236 down-regulated genes in FriFwB vs FriFw; 89 up-regulated and 26 down-regulated in DPBdB vs DPBd; 29 up-regulated and 28 down-regulated in SchijdB vs Schijd. In the GO-term analysis we found genes overrepresented for GO terms influencing bone development, including bone morphogenesis, mineralization, ossification, and cartilage development. It is to be noted, genes encoding the bone morphogenetic proteins, *BMP2* and *BMP4*, and genes encoding fibroblast growth factor and its binding protein or receptor (*FGF10*, *FGFBP2*, and *FGFR2*), all exhibited around 2-fold lower expression in bantam samples compared to normal-sized samples for the FriFwB vs FrFw comparison. Genes encoding proteins of the matrix metalloproteinase (MMP) family, *MMP9*, *MMP10*, and *MMP13*, were detected to be downregulated in DPBdB samples relative to DPBd. Among these three genes, *MMP9* showed a substantial decreased expression in DPBdB with 4.71-fold change. In addition, the Indian hedgehog (*IHH*) gene showed decreased expression in

the bantams of SchijdB with over 2-fold change. Moreover, besides the differences in expression of *IHH* between bantam and non-bantam we also observed a clear difference in expression between males and females in spite of the body size. The difference between the two sexes suggests that the expression of *IHH* might also have a sex-specific pattern at E13.

4.4 Discussion

In this study, we used RNA-seq data to compare the gene expression of chicken breeds with dwarf phenotype (bantam) against the normal-sized breeds. With the RNA-seq data of 31 samples representing 8 Dutch chicken breeds and two developmental stages, the expression profile analysis showed a developmental stage-specific pattern. The expression of all genes across breeds can be distinguished and separated by the two developmental stages, E5 and E13. This shows that within the developmental stages the gene expression patterns were very similar. The effect of the developmental stage, therefore, needs to be taken into account when detecting growth related differently expressed genes (DEGs). Furthermore, we also showed the presence of a significant sex effect on the expression patterns. These results clearly show that both developmental stage and sex should be taken into account when analyzing DEGs between the bantam and non-bantam phenotypes.

By comparing the gene expression between the two developmental stages, we anticipated that for embryonic development there are significant temporal differences regarding the physiological aspects that involved the myogenesis and osteogenesis of the embryo. During the development of embryonic growth, the bones and muscles begin to form at early stage, e.g., E5, involving the process of ossification and myogenesis. The appearance of epiphyseal growth plate can be observed in the chicken embryo as early as 2-5 day at embryonic age (Hamburger and Hamilton, 1992), which is responsible for the initial and elongation of bone development, and the defects in which can lead to deficient cartilage formation and thus growth disorder (Leach et al., 2007). Whereas, at later embryonic stages, the embryo is at a high speed of growing and developing. For instance, the *IGF-I* expression level showed significantly increased at stage E13 compared to E5, suggesting the considerable increased of embryonic tissues differentiation and musculoskeletal development (Figure S4.3A) (Liu et al., 2016; Ouyang et al., 2017).

We focused on the DEGs identified between bantam and normal-sized phenotypes at stage E5 and E13. A large number of DEGs between bantam and non-bantam chickens can be observed at both E5 and E13, and the bantam samples exhibited more down-regulated DEGs than up-regulated ones at stage E5. The DEGs identified at both stages were annotated with GO terms significantly enriched for muscle and bone development. These muscle and bone development pathways are relatively less overrepresented at stage E13. To further discover the roles of the identified DEGs,

those associated with bantam at each stage (E5 or E13) were compared to the bantam associated genes identified in our previous GWAS (Wu et al., 2020; chapter3). In total, it showed eight genes that were identified in both GWAS and RNA-seq studies (Figure 4.6). Two genes were found to be shared in the gene sets of E5, E13 and GWAS, which are *COL9A1* and *KRT7*. Over a hundred genes (106) were shared by the DEGs identified from E5 and E13, but these were not identified in our GWAS. In addition, the gene set derived from the GWAS shares three genes with E5; *RNASEH2B*, interleukin 1 receptor accessory protein like 2 (*IL1RAPL2*) and protein phosphatase 1 regulatory subunit 12B (*PPP1R12B*), and three genes with E13; Homeobox B9 (*HOXB9*), bridging integrator (*BIN1*), and *ENSGALG00000010854*. Of special interest is the significant down-regulation of the *RNASEH2B* gene in bantam samples at embryonic stage E5. In previous studies, the *RNASEH2B* gene has been reported to be located in a growth related QTL on chromosome 1 (Zhang et al., 2010; Xie et al., 2012), and it was suggested as one of the bantam candidates in our previous GWAS study (Wu et al., 2020; chaper 3). This gene is known to degrade the RNA which is thought to regulate DNA replication, and *RNASEH2B* knockout mice exhibit smaller embryos compared to the controls (Hiller et al., 2012). The affected *RNASEH2B* expression supports its functional role in the development of bantam chickens during embryonic growth.

Several genes involved in myogenesis, muscle tissue development and contraction were downregulated in the bantam samples. For instance, we found in total twelve paralogous genes encoding different types of collagen (COL 1, 3, 6, 8, 9, 12, and 18) to be down regulated in the bantam samples. Interestingly, the *COL9A1* gene was also identified as a bantam candidate gene in our previous GWAS analysis (Wu et al., 2020; chapter 3). The expression of this gene is downregulated at both stages, providing further transcriptomic evidence for the genetic association. In human, collagen formation or degradation has been shown to be closely associated with body growth (Vihervuori et al., 1997). Genetic mutations in collagen encoding genes can lead to human muscular disorders (e.g., *COL6As*) or diseases associated with short stature like the Marshall syndrome, which is associated with *COL11A1* or *COL2A1* gene (Lampe and Bushby, 2005; Guo et al., 2017; Bolduc et al., 2019; Wang et al., 2019). Down-regulated genes involved in myogenesis including *MYOG*, *MYOD1*, and *MYLs*. Myogin plays a role as a muscle-specific transcription factor enhancing myogenesis, and it is important for skeletal muscle development (Chen et al., 2011).

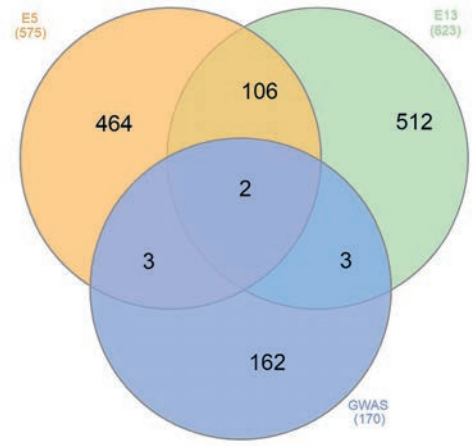

Figure 4.6 Venn diagram shows the overlapping between the gene sets identified by differential expression analyses related to bantam at E5 and E13, as well as gene set derived from a prior bantam GWAS analysis (a total of 170 genes were retrieved from the three cluster-based GWA studies and a meta-analysis).

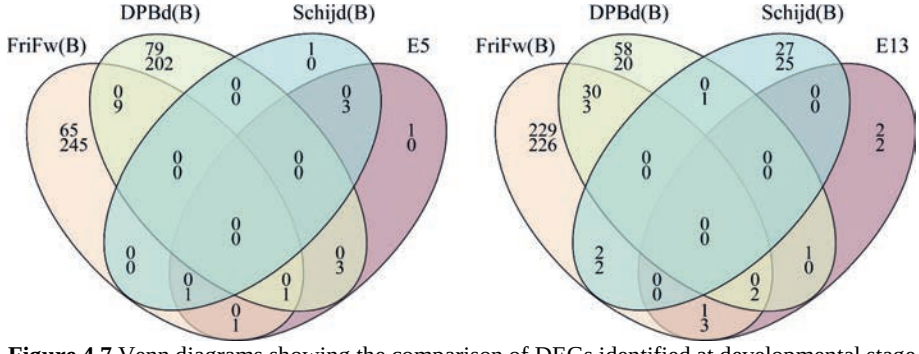

Figure 4.7 Venn diagrams showing the comparison of DEGs identified at developmental stage E5 (left) and E13 (right), the upper number stands for the number of up-regulated genes, and the lower number is the down-regulated genes. At each stage, the four gene sets are identified DEGs for FriFw(B), DPBd(B), Schijd(B) and among all breeds.

We further showed overrepresentation of genes involved in bone development, like bone morphogenesis, mineralization, ossification and cartilage development. Genes encoding *MMP9*, *MMP10*, and *MMP13*, which have been described to be expressed during endochondral ossification (Ortega et al., 2004), showed reduced expression in bantams. In addition, genes from the FGF/FGFR gene family, together with FGFBPs showed decreased expression in the bantams compared to normal-sized samples. Members of the FGF/FGFR gene family extensively moderate chondrogenesis and osteogenesis during skeletal development (Marie et al., 2019). Dwarfisms in many species are caused by mutations in FGFs/FGFRs. For instance, the dominant achondroplasia in human is caused by mutations in *FGFR3* (Shiang et al., 1994), and the short-legged dwarfism in several dog breeds (e.g., Corgi) is associated with the

expression of *FGF4* (Parker et al., 2009). Therefore, expression changes in those genes of the FGF signaling pathway are likely to affect the growth of animals through influencing the skeletal growth and bone formation, especially ossification (Eswarakumar et al., 2002; Marie et al., 2019). In addition, the down-regulated transcription factor *TBX4* was reported in previous chicken studies, showing that *TBX4* is expressed specifically in hindlimb buds, which suggests an essential role for this gene in the initiation of hindlimb development (Rodriguez-Esteban et al., 1999; Takeuchi et al., 2003). Furthermore, expression of *TBX4* also control the activation of the FGF and Wnt signaling pathways (Takeuchi et al., 2003).

As for the members of the BMP family, these are considered to affect almost all aspects of bone, cartilage and joint formation (Salazar et al., 2016). In our study, *BMP2* and *BMP4* both showed reduced expression in bantam embryos. In human studies, genetic alterations (e.g., deletions) in *BMP2* and *BMP4* both cause syndromes including short stature (Reis et al., 2011; Tan et al., 2017). In the Chinese Yuanbao bantam chicken, the gene expression of another member of this family, *BMP10*, was suggested to potentially control the dwarf body size (Wang et al., 2016). Interestingly, the FGF signaling interacts with BMP and IHH signaling in a complex manner. First, FGF (e.g., FGF9 and FGF18) can regulate osteogenesis (Marie et al., 2019). FGF and BMP signaling cooperate to modulate osteogenesis in osteoblasts. Functionally, FGF (e.g., *FGF2*) can directly enhance BMP (e.g., *BMP2*) function as well as positively control BMP function through inhibition of its antagonist noggin (e.g., *FGF9*) (Warren et al., 2003; Fakhry et al., 2005; Marie et al., 2019). Whereas for chondrogenesis, there have been studies showed that in the mature growth plate, the FGF signaling pathway negatively regulates IHH signaling and is antagonized by the BMP signaling (Minina et al., 2002; Marie et al., 2019). BMP and IHH signals act in parallel to induce chondrocyte proliferation, whereas FGF signaling suppress chondrocyte proliferation (Minina et al., 2002). At E13, the expression of the *IHH* gene exhibited a reduction in female Schijndelaar bantam samples compared to the Schijndelaar controls. IHH is known as a regulator for bone and cartilage development (Wu et al., 2001). Deletion of this gene has been reported as the causative variant for the creeper trait in chicken, an autosomal dominant semi-lethal mutation. Homozygous embryos are lethal while the heterozygous ones are characterized as the short-legged dwarf chicken. Furthermore, IHH plays a significant role in bone morphology and development underlying bone dysplasia in human and mouse (St-Jacques et al., 1999; Gao et al., 2009).

The DEGs identified in the three specific breed pairs counterpart and in all breeds showed limited overlap (Figure 4.7). The breed-specific DEGs showed the most overlap between the breed comparisons of FriFwB vs FriFw and DPBdB vs DPBd at both stages, suggesting similar genes and molecular mechanisms are involved in the bantam formation of these two breeds, which is in line with our previous GWAS

results. Of special note is the small number of DEGs identified in all breeds at the two developmental stages. This implies between different breeds genes involved in bantam phenotype have unique and different expression patterns, therefore treating these bantam breeds in a simply homogenous manner will constrain the power to identify DEGs. This observation further supports the genetic and/or phenotypic heterogeneity we discovered between the three bantam clusters in the previous GWAS analysis, which were represented deliberately by the three neo-bantam breeds in this study. Moreover, this result suggests that the genetic heterogeneity can be studied and further investigated in the context of gene expression as well, which in turn can provides insights into the biological mechanisms underlying phenotypic heterogeneity of dwarfism (Zeggini and Ioannidis, 2009). Suppose such mechanism may function through the precise allelic effect and complex signaling pathways, the future analyses of heterogeneity between bantam breeds can be studied with the temporospatial dynamics of musculoskeletal development or cell differentiation and proliferation in a diverse fashion (Minina et al., 2002; Marie et al., 2019).

Finally, the expression of the *IGF-I* and *HMGA2* genes was not significantly different between bantam and non-bantam samples (Figure S4.3). However, we found a considerable number of genes involved in the regulation of IGF-I transport and signaling to be differentially expressed. For instance, the down-regulated gene *IGF2BP1* encoding a binding protein that can regulate the mRNA translation by binding to mRNAs of these genes (e.g., *IGF2I*). Moreover, mice embryos with deficient IGF2BP1 protein exhibit growth retardation (Hansen et al., 2004); a continuous expression of *IGF2BP1* after hatch increases body size in ducks (Zhou et al., 2018). Although the expression of *IGF-I* is not affected at the two analyzed developmental stages, the differentially expressed genes encoding the protein in the GH-IGF axis and other protein that plays a role in the signaling pathway may contribute to the bantam phenotype.

To summarize, in this study we used RNA-seq data to study differential gene expression between the contrasting body sizes, bantam and normal-sized chicken embryos. Overall, DEGs compared between breeds or developmental stages showed limited overlap, but genes involved in certain overlapping signaling pathways (e.g., FGF) or biological processes (myogenesis and osteogenesis) were substantially identified. Although the comprehensive understanding of how these signaling pathways interact with each other to regulate a short stature phenotype remain largely unknown, this study provided further insights into the genes involved in the growth reduction in chickens.

4.5 Acknowledgements

We would like to thank the breeder associations and the Nederlands Pluimveemuseum for their support during sampling. We sincerely thank Bert Dibbits, Kimberley Laport,

and Chiara Bortoluzzi for the experimental support. Special thanks to Langqing Liu and Siyuan Xing for helpful discussions on the data analysis. ZW has received financial support from the China Scholarship Council (Grant No. 201606350175).

4.6 References

Agarwal, S. K., Cogburn, L. A., and Burnside, J. (1994). Dysfunctional growth hormone receptor in a strain of sex-linked dwarf chicken: Evidence for a mutation in the intracellular domain. *J. Endocrinol.* 142, 427–434. doi:10.1677/joe.0.1420427.

Benjamini, Y., and Hochberg, Y. (1995). Controlling the False Discovery Rate: A Practical and Powerful Approach to Multiple Testing. doi:10.1111/j.2517-6161.1995.tb02031.x.

Boegheim, I. J. M., Leegwater, P. A. J., van Lith, H. A., and Back, W. (2017). Current insights into the molecular genetic basis of dwarfism in livestock. *Vet. J.* 224, 64–75. doi:10.1016/j.tvjl.2017.05.014.

Bolduc, V., Reghan Foley, A., Solomon-Degefa, H., Sarathy, A., Donkervoort, S., Hu, Y., et al. (2019). A recurrent COL6A1 pseudoexon insertion causes muscular dystrophy and is effectively targeted by splice-correction therapies. *JCI Insight* 4. doi:10.1172/jci.insight.124403.

Burke, W. H., and Sharp, P. J. (1989). Sex differences in body weight of chicken embryos. *Poult. Sci.* 68, 805–810. doi:10.3382/ps.0680805.

Chen, L., Huang, H. W., Gu, S. H., Xu, L., Gu, Y. D., and Xu, J. G. (2011). The study of myogenin expression in denervated human skeletal muscles. *J. Int. Med. Res.* 39, 378–387. doi:10.1177/147323001103900205.

Dobin, A., Davis, C. A., Schlesinger, F., Drenkow, J., Zaleski, C., Jha, S., et al. (2013). STAR: Ultrafast universal RNA-seq aligner. *Bioinformatics* 29, 15–21. doi:10.1093/bioinformatics/bts635.

Esther Verhoef, and Rijs, A. (2014). *De kippen encyclopedie*. Rebo Productions.

Eswarakumar, V. P., Monsonego-Ornan, E., Pines, M., Antonopoulou, I., Morriss-Kay, G. M., and Lonai, P. (2002). The IIIc alternative of Fgfr2 is a positive regulator of bone formation.

Fakhry, A., Ratisoontorn, C., Vedhachalam, C., Salhab, I., Koyama, E., Leboy, P., et al. (2005). Effects of FGF-2/-9 in calvarial bone cell cultures: Differentiation stage-dependent mitogenic effect, inverse regulation of BMP-2 and noggin, and enhancement of osteogenic potential. *Bone* 36, 254–266. doi:10.1016/j.bone.2004.10.003.

Gao, B., Hu, J., Stricker, S., Cheung, M., Ma, G., Law, K. F., et al. (2009). A mutation in Ihh that causes digit abnormalities alters its signalling capacity and range. *Nature* 458, 1196–1200. doi:10.1038/nature07862.

Guo, L., Elcioglu, N. H., Wang, Z., Demirkol, Y. K., Isguven, P., Matsumoto, N., et al. (2017). Novel and recurrent COL11A1 and COL2A1 mutations in the Marshall-Stickler syndrome spectrum. *Hum. Genome Var.* 4, 1–4. doi:10.1038/hgv.2017.40.

Hamburger, V., and Hamilton, H. L. (1992). A series of normal stages in the development of the chick embryo. *Dev. Dyn.* 195, 231–272. doi:10.1002/aja.1001950404.

Hansen, T. V. O., Hammer, N. A., Nielsen, J., Madsen, M., Dalbaeck, C., Wewer, U. M., et al. (2004). Dwarfism and Impaired Gut Development in Insulin-Like Growth Factor II mRNA-Binding Protein 1-Deficient Mice. *Mol. Cell. Biol.* 24, 4448–4464. doi:10.1128/mcb.24.10.4448-4464.2004.

Hiller, B., Achleitner, M., Glage, S., Naumann, R., Behrendt, R., and Roers, A. (2012). Mammalian RNase H2 removes ribonucleotides from DNA to maintain genome integrity. *J. Exp. Med.* 209, 1419–1426. doi:10.1084/jem.20120876.

Jassal, B., Matthews, L., Viteri, G., Gong, C., Lorente, P., Fabregat, A., et al. (2020). The reactome pathway knowledgebase. *Nucleic Acids Res.* 48, D498–D503. doi:10.1093/nar/gkz1031.

Lampe, A. K., and Bushby, K. M. D. (2005). Collagen VI related muscle disorders. *J. Med. Genet.* 42, 673–685. doi:10.1136/jmg.2002.002311.

Leach, R. M., Richards, M. P., Praul, C. A., Ford, B. C., and McMurtry, J. P. (2007). Investigation of the insulin-like growth factor system in the avian epiphyseal growth plate. *Domest. Anim. Endocrinol.* 33, 143–153. doi:10.1016/j.domaniend.2006.04.010.

Liao, Y., Smyth, G. K., and Shi, W. (2014). FeatureCounts: An efficient general purpose program for assigning sequence reads to genomic features. *Bioinformatics* 30, 923–930. doi:10.1093/bioinformatics/btt656.

Lin, S., Li, H., Mu, H., Luo, W., Li, Y., Jia, X., et al. (2012). Let-7b regulates the expression of the growth hormone receptor gene in deletion-type dwarf chickens. *BMC Genomics* 13, 306. doi:10.1186/1471-2164-13-306.

Liu, Y., Guo, W., Pu, Z., Li, X., Lei, X., Yao, J., et al. (2016). Developmental changes of Insulin-like growth factors in the liver and muscle of chick embryos. *Poult. Sci.* 95, 1396–1402. doi:10.3382/ps/pew043.

Love, M. I., Huber, W., and Anders, S. (2014). Moderated estimation of fold change and dispersion for RNA-seq data with DESeq2. *Genome Biol.* 15, 550. doi:10.1186/s13059-014-0550-8.

Luo, W., Lin, S., Li, G., Nie, Q., and Zhang, X. (2016). Integrative analyses of miRNA-mRNA interactions reveal let-7b, miR-128 and MAPK pathway involvement in muscle mass loss in sex-linked dwarf chickens. *Int. J. Mol. Sci.* 17, 276. doi:10.3390/ijms17030276.

Marie, P. J., Hurley, M., and Ornitz, D. M. (2019). "Fibroblast growth factor (FGF) and FGF receptor families in bone," in *Principles of Bone Biology* (Elsevier), 1113–1140. doi:10.1016/B978-0-12-814841-9.00045-2.

Minina, E., Kreschel, C., Naski, M. C., Ornitz, D. M., and Vortkamp, A. (2002). Interaction of FGF, Ihh/Pthlh, and BMP signaling integrates chondrocyte proliferation and hypertrophic differentiation. *Dev. Cell* 3, 439–449. doi:10.1016/S1534-5807(02)00261-7.

Nam, K., and Ellegren, H. (2008). The Chicken (Gallus gallus) Z Chromosome Contains at Least Three Nonlinear Evolutionary Strata. *Genetics* 180, 1131–1136. doi:10.1534/genetics.108.090324.

Ortega, N., Behonick, D. J., and Werb, Z. (2004). Matrix remodeling during endochondral ossification. *Trends Cell Biol.* 14, 86–93. doi:10.1016/j.tcb.2003.12.003.

Ouyang, H., Wang, Z., Chen, X., Yu, J., Li, Z., and Nie, Q. (2017). Proteomic analysis of chicken skeletal muscle during embryonic development. *Front. Physiol.* 8, 281. doi:10.3389/fphys.2017.00281.

Parker, H. G., VonHoldt, B. M., Quignon, P., Margulies, E. H., Shao, S., Mosher, D. S., et al. (2009). An expressed fgf4 retrogene is associated with breed-defining chondrodysplasia in domestic dogs. *Science (80-.).* 325, 995–998. doi:10.1126/science.1173275.

R Core Team (2019). R: A language and environment for statistical computing. Available at: https://www.r-project.org/.

Reis, L. M., Tyler, R. C., Schilter, K. F., Abdul-Rahman, O., Innis, J. W., Kozel, B. A., et al. (2011). BMP4 loss-of-function mutations in developmental eye disorders including SHORT syndrome. *Hum. Genet.* 130, 495–504. doi:10.1007/s00439-011-0968-y.

Richette, P., Bardin, T., and Stheneur, C. (2008). Achondroplasia: From genotype to phenotype. *Jt. Bone Spine* 75, 125–130. doi:10.1016/J.JBSPIN.2007.06.007.

Robinson, M. D., McCarthy, D. J., and Smyth, G. K. (2009). edgeR: A Bioconductor package for differential expression analysis of digital gene expression data. *Bioinformatics* 26, 139–140. doi:10.1093/bioinformatics/btp616.

Rodriguez-Esteban, C., Tsukul, T., Yonel, S., Magallon, J., Tamura, K., and Izpisua Belmonte, J. C. (1999). The T-box genes Tbx4 and Tbx5 regulate limb outgrowth and identity. *Nature* 398, 814–818. doi:10.1038/19769.

Salazar, V. S., Gamer, L. W., and Rosen, V. (2016). BMP signalling in skeletal development, disease and repair. *Nat. Rev. Endocrinol.* 12, 203–221. doi:10.1038/nrendo.2016.12.

Shiang, R., Thompson, L. M., Zhu, Y. Z., Church, D. M., Fielder, T. J., Bocian, M., et al. (1994). Mutations in the transmembrane domain of FGFR3 cause the most common genetic form of dwarfism, achondroplasia. *Cell* 78, 335–342. doi:10.1016/0092-8674(94)90302-6.

St-Jacques, B., Hammerschmidt, M., and McMahon, A. P. (1999). Indian hedgehog signaling regulates proliferation and differentiation of chondrocytes and is essential for bone formation. *Genes Dev.* 13, 2072–2086. doi:10.1101/gad.13.16.2072.

Tahara, K., Tsukada, A., Hanai, T., Okumura, K., Yamada, K., Murai, A., et al. (2009). Identification of Two Types of Growth Hormone Receptor Mutations in Two Strains of Sex-linked Dwarf Chickens. *J. Poult. Sci.* 46, 249–256. doi:10.2141/jpsa.46.249.

Takeuchi, J. K., Koshiba-Takeuchi, K., Suzuki, T., Kamimura, M., Ogura, K., and Ogura, T. (2003). Tbx5 and Tbx4 trigger limb initiation through activation of the Wnt/Fgf signaling cascade. *Development* 130, 2729–2739. doi:10.1242/dev.00474.

Tan, T. Y., Gonzaga-Jauregui, C., Bhoj, E. J., Strauss, K. A., Brigatti, K., Puffenberger, E., et al. (2017). Monoallelic BMP2 variants predicted to result in haploinsufficiency cause craniofacial, skeletal, and cardiac features overlapping those of 20p12 deletions. *Am. J. Hum. Genet.* 101, 985–994. doi:10.1016/j.ajhg.2017.10.006.

Vihervuori, E., Turpeinen, M., Siimes, M. A., Koistinen, H., and Sorva, R. (1997). Collagen formation and degradation increase during growth hormone therapy in children. *Bone* 20, 133–138. doi:10.1016/S8756-3282(96)00332-8.

Wang, M. S., Huo, Y. X., Li, Y., Otecko, N. O., Su, L. Y., Xu, H. B., et al. (2016). Comparative population genomics reveals genetic basis underlying body size of domestic chickens. *J. Mol. Cell Biol.* 8, 542–552. doi:10.1093/jmcb/mjw044.

Wang, P., Teng, Z., Liu, X., Liu, X., Kong, C., and Lu, S. (2019). A new single nucleotide polymorphism affects the predisposition to thoracic ossification of the posterior longitudinal ligament. *J. Orthop. Surg. Res.* 14, 438. doi:10.1186/s13018-019-1481-6.

Warren, S. M., Brunet, L. J., Harland, R. M., Economides, A. N., and Longaker, M. T. (2003). The BMP antagonist noggin regulates cranial suture fusion. *Nature* 422, 625–629. doi:10.1038/nature01545.

Wu, Q. Q., Zhang, Y., and Chen, Q. (2001). Indian hedgehog is an essential component of mechanotransduction complex to stimulate chondrocyte proliferation. *J. Biol. Chem.* 276, 35290–35296. doi:10.1074/jbc.M101055200.

Wu, Z., Bortoluzzi, C., Derk1, M. F. L., Liu, L., Bosse, M., Hiemstra, S. J., et al. (2020). Heterogeneity of a dwarf phenotype in Dutch traditional chicken breeds revealed by genomic analyses. *submitted*.

Xie, L., Luo, C., Zhang, C., Zhang, R., Tang, J., Nie, Q., et al. (2012). Genome-wide association study identified a narrow chromosome 1 region associated with chicken growth traits. *PLoS One* 7, 30910. doi:10.1371/journal.pone.0030910.

Yu, G., Wang, L. G., Han, Y., and He, Q. Y. (2012). ClusterProfiler: An R package for comparing biological themes among gene clusters. *Omi. A J. Integr. Biol.* 16, 284–287. doi:10.1089/omi.2011.0118.

Zeggini, E., and Ioannidis, J. P. A. A. (2009). Meta-analysis in genome-wide association studies. *Pharmacogenomics* 10, 191–201. doi:10.2217/14622416.10.2.191.

Zhang, H., Zhang, Y. D., Wang, S. Z., Liu, X. F., Zhang, Q., Tang, Z. Q., et al. (2010). Detection and fine mapping of quantitative trait loci for bone traits on chicken chromosome one. *J. Anim. Breed. Genet.* 127, 462–468. doi:10.1111/j.1439-0388.2010.00871.x.

Zhou, Q., Zhang, J., Bachtrog, D., An, N., Huang, Q., Jarvis, E. D., et al. (2014). Complex evolutionary trajectories of sex chromosomes across bird taxa. *Science (80-.).* 346, 1246338. doi:10.1126/science.1246338.

Zhou, Z., Li, M., Cheng, H., Fan, W., Yuan, Z., Gao, Q., et al. (2018). An intercross population study reveals genes associated with body size and plumage color in ducks. *Nat. Commun.* 9, 2648. doi:10.1038/s41467-018-04868-4.

4.7 Supplementary materials

The complete supplementary material for this article can be found online at:

https://osf.io/kqs38/?view_only=f358194594754333bbbda7aa7ab3bee0

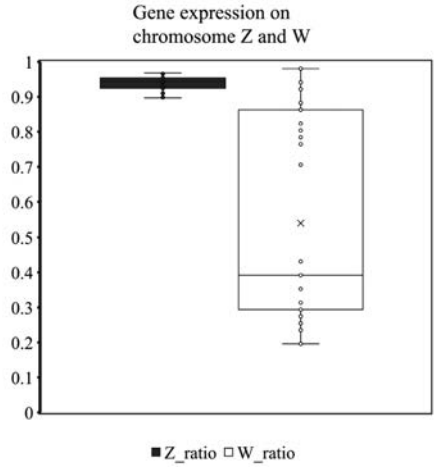

Figure S4.1 The ratio of genes expressed on the chromosomes Z and W. The box plots show the of number of genes expressed on the Z or W chromosome of each individual divided by the total number of genes on this chromosome.

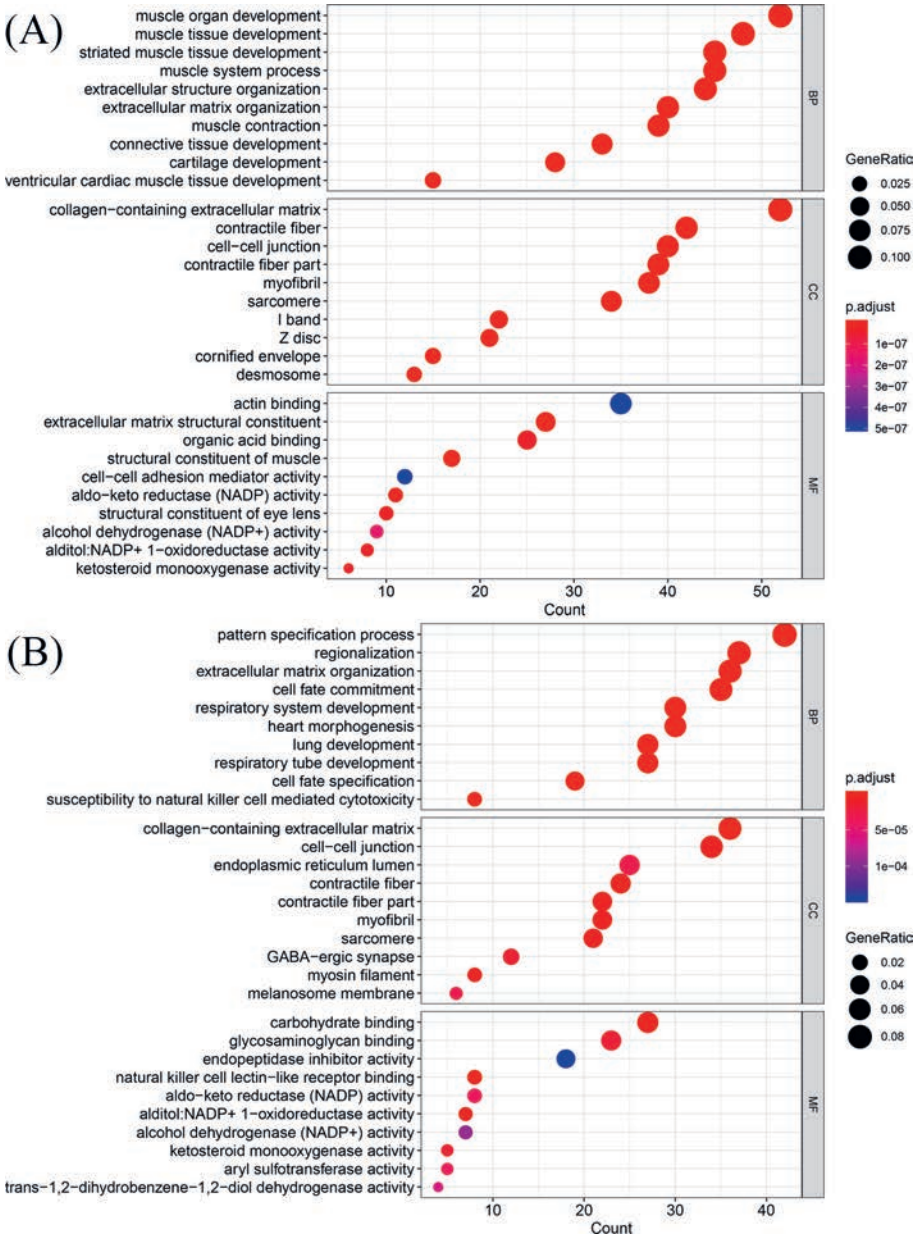

Figure S4.2 The enrichment analysis of Gene Ontology (GO) terms using DEGs identified at (A) stage E5 and (B) E13. The three GO categories, BP, CC and MF are shown by the three facets in each plot, with colored circle as the adjusted P value, the x-axis as the count of the terms, and the size of the circle as the gene ratio.

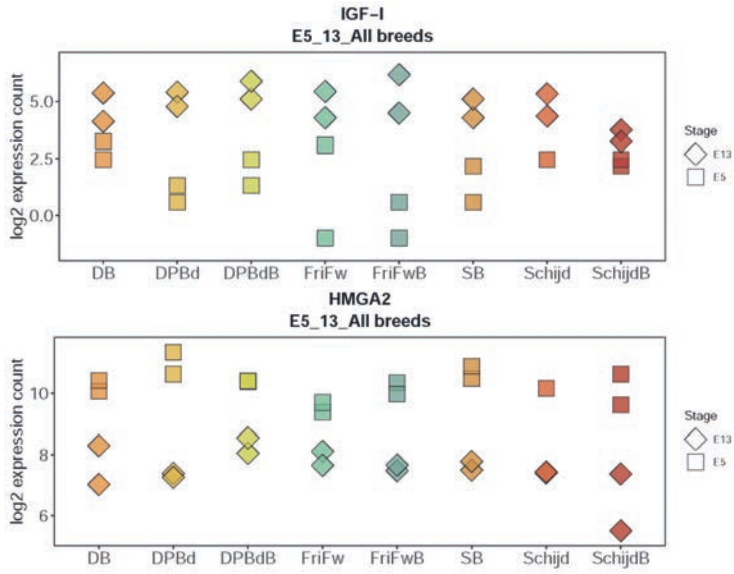

Figure S4.3 Transformed expression level (log2) of genes at the two stages among all breeds. The upper panel displays the gene expression of *IGF-I*, while the lower one shows the expression of *HMGA2*. Different shapes display the two developmental stages of sample, and colors display the 8 breeds.

Table S4.1 Sample list used for transcriptomic data with sex imputed for individuals.

ID	Breed_name*	Stage**	Phenotype	Sex
DB_E5_01	DB	5	bantam	ZZ
DB_E5_02	DB	5	bantam	ZZ
DPBdB_E5_01	DPBdB	5	bantam	ZZ
DPBdB_E5_02	DPBdB	5	bantam	ZW
DPBd_E5_01	DPBd	5	normal	ZZ
DPBd_E5_02	DPBd	5	normal	ZZ
FriFwB_E5_01	FriFwB	5	bantam	ZW
FriFwB_E5_02	FriFwB	5	bantam	ZZ
FriFw_E5_01	FriFw	5	normal	ZZ
FriFw_E5_02	FriFw	5	normal	ZZ
SB_E5_01	SB	5	bantam	ZW
SB_E5_02	SB	5	bantam	ZW
SchijdB_E5_01	SchijdB	5	bantam	ZW
SchijdB_E5_02	SchijdB	5	bantam	ZZ
Schijd_E5_01	Schijd	5	normal	ZZ
DB_E13_05	DB	13	bantam	ZZ
DB_E13_06	DB	13	bantam	ZZ
DPBdB_E13_05	DPBdB	13	bantam	ZW
DPBdB_E13_06	DPBdB	13	bantam	ZZ
DPBd_E13_05	DPBd	13	normal	ZW
DPBd_E13_06	DPBd	13	normal	ZW
FriFwB_E13_05	FriFwB	13	bantam	ZZ
FriFwB_E13_06	FriFwB	13	bantam	ZW
FriFw_E13_05	FriFw	13	normal	ZW
FriFw_E13_06	FriFw	13	normal	ZZ
SB_E13_05	SB	13	bantam	ZZ
SB_E13_06	SB	13	bantam	ZZ
SchijdB_E13_05	SchijdB	13	bantam	ZW
SchijdB_E13_06	SchijdB	13	bantam	ZZ
Schijd_E13_05	Schijd	13	normal	ZW
Schijd_E13_06	Schijd	13	normal	ZW

*****The breeds shown are Frisian Fowl (FriFw) and Frisian Fowl Bantam (FriFwB), Dutch Polish Bearded (DPBd) and Dutch Polish Bearded Bantam (DPBdB), as well as Schijndelaar (Schijd) and Schijndelaar Bantam (SchijdB). And the two true bantams, Dutch Bantam (DB) and Sebright Bantam (SB).

******Stage: embryonic day for sampling, E5 and E13 correspond to Hamburger Hamilton Stage 26 and 39, respectively.

Table S4.2 List of DEGs identified between two stages or between bantam and normal-sized at each stage (online).

Table S4.3 Enrichment of Gene Ontology (online).

5

Genomic insight into the influence of selection, geography, and crossbreeding on population structure

Zhou Wu[1], Mirte Bosse[1], Christina M. Rochus[1], Martien A.M. Groenen[1], Richard P.M.A. Crooijmans[1]

[1] Animal Breeding and Genomics, Wageningen University & Research, Wageningen, the Netherlands

In preparation

Abstract

The population structure of indigenous breeds is usually complex. Local chicken breeds offer an interesting proxy to understand the complexity of population structure due to the human-mediated development of diverse morphology and variety. We studied diverse Dutch chicken breeds to investigate the population structure using whole-genome sequence data.

Looking at the genetic differences between breeds, the Dutch chicken breeds demonstrate a complex and admixed subdivided structure. The dissection of this complexity highlighted the influence of selection adhering to management purposes, as well as the role of geographic distance within subdivided breed clusters. Identification of genetic differentiation signatures showed genomic regions associated with diversifying phenotypic selection between breeds, including dwarf size (bantam) and feather color. In addition, by a case study of a recent bantam crossbreeding we demonstrated the hybrid history of the breed and offer a genomic perspective on the effect of crossbreeding. This study demonstrates the complex population structure of Dutch chicken, offering insight into the genomic basis and the factors involved in the formation of this complexity.

5.1 Introduction

Following the process of domestication, chicken populations, during subsequent agriculture revolutions worldwide, have been diversified with distinct morphological features. During this process, chicken populations have been selectively bred for specific types of management, which led to genetic differentiation and population subdivision. Based on human interventions, chicken populations can be generally classified into commercial breeds and local indigenous breeds. The commercial breeds were bred under the specialized and extensive selection for either egg-laying (layers) or meat production (broilers) (Rubin et al., 2010). Whereas breeding for local traditional breeds was contingent on diverse and complex mechanisms which lack strict supervision, such as migration, random drift, geographic dispersal followed by environmental adaptation, and selective breeding adhering to breed characteristics (Woelders et al., 2006; Wilkinson et al., 2012; Bortoluzzi et al., 2018; Zhang et al., 2018). For instance, several studies showed that geographic dispersal distances can lead to genetic differentiation in local indigenous populations (Yang et al., 2017; Nie et al., 2019), as well as in pure breeds (Parker et al., 2017). The most extreme influence of geographic pattern can lead to isolation and speciation which is known as allopatry (Zink, 1997; Wang et al., 2020).

Various factors or forces influencing population structure may coincide with each other and/or outcompete one another, which was subsequently comprised in the complexity of population structure. To understand the complex structure of populations, many studies have been performed to untangle the differentiation between populations by initially looking for genomic regions with divergent genetic signals. Identification of genetic differentiation serves as a good starting point to understand the genetic basis underlying phenotypic variation. Phenotypes like body stature, comb type, and coat/plumage pattern may reflect the history of selection (Hillel et al., 2003; Sheppy, 2011; Imsland et al., 2012; Rochus et al., 2018; Wu et al., 2020). Genomic analytical approaches, like signatures of selection by identifying genomic regions with pronounced differentiation between populations or breeds, enable us to understand the differentiation and complex structure in the population.

In the Netherlands, historic chicken resources have received attention and admiration from the 16th century onwards, and continued to be managed in diverse forms (Woelders et al., 2006; Dana et al., 2011). The long tradition of breed development resulted in various organizations (private and governmental) making efforts to utilize and preserve the native breeds as well as their genetic resources (Woelders et al., 2006). Dutch chicken breeds were defined mostly based on geographic location (e.g., Groningen Mew Fowl) and phenotypic characteristics (e.g., Dutch Polish Bearded). These breeds are comprised of many subdivisions determined by the management types of the breeds and historical clustering, which was profiled in many relevant

studies (Hillel et al., 2003; Dana et al., 2011; Elferink et al., 2012; Bortoluzzi et al., 2018). This historical clustering includes the past-productive breeds developed for rapid production (especially egg production), ornamental breeds used for fancy breeding, and country fowls represented by primitive traditional breeds. At the same time, the Dutch traditional chicken breeds contain a unique variety of bantam forms (a dwarf phenotype with 50-60% reduced body weight). Besides the *traditional* or *true* bantam breeds, Dutch chicken breeds exhibit an important history of bantam crossbreeding, so-called bantamization. The bantamization process utilized donors from existing bantams and/or neo-bantams of local breeds to create corresponding neo-bantams, the dwarf counterparts of native 'large' chickens (Esther Verhoef and Rijs, 2014; Bortoluzzi et al., 2018; Wu et al., 2020). As a common practice, bantam crossbreeding was followed by repeated backcrossing, which has proven to effectively dilute the contribution from bantam ancestries (Bortoluzzi et al., 2018; Wu et al., 2020). From a genomic perspective, because of backcrossing, the introgressed genomic segments are expected to be broken and recombined over time. Therefore, the genomic composition of neo-bantams is expected to contain only a few genomic segments derived from the original bantam donors, apart from loci that contribute to the bantam phenotype. The introgressed contribution of bantam donors in the neo-bantams should reach equilibrium due to purifying and artificial selection (e.g., backcrossing) (Gompert et al., 2017).

In this study, we focused on multiple factors that may play a significant role in recent breed formation revealing the complex population structure of the Dutch traditional chicken breeds. In particular, we used whole genome sequence data, representing the genetic basis of various breeds. We revealed a complex population structure and admixture between breeds, resulting from management type, geographic distribution, and phenotypic selection. Lastly, by using a case of a recent crossbreeding in Drenthe Fowl bantam we demonstrated the recent hybrid history of this breed and offer a genomic perspective to show the effect of selective breeding.

5.2 Results and Discussion

5.2.1 Complex and admixed population structure

In total, we assessed the population structure of 136 chickens from 37 breeds using whole-genome sequence data (Figure 5.1). The Dutch traditional chicken breeds are grouped into three historical clusters according to the conventional management classification. Breeds within the same cluster have similar management and breeding aims and consist of past-productive fowl (CL1), ornamental breeds (CL2), and country fowl (CL3). As shown in Table S5.1, CL1 is represented by 24 individuals from 6 breeds, CL2 comprises 38 samples from 10 breeds, and CL3 is represented by 65 chickens from 18 breeds. Besides these clusters, 9 individuals from the Lakenvelder breed and its bantam counterpart were included in the analyses as well

(CL4), for the breed has a unique genetic composition relative to the others (Bortoluzzi et al., 2018). For almost every Dutch traditional breed there is a corresponding bantam counterpart (neo-bantam) included in each cluster, with the exception in the Chaam Fowl. Additionally, the two true bantam breeds, the Dutch Bantam and Eikenburger bantam, are allocated to the cluster of country fowl. We employed three approaches to assess whether the genetic population structure matches the historical clustering: a principal component analysis (PCA) decomposing genomic variants, a Neighbor-Joining Tree (NJ-tree) illustrating the Reynold's distance between breeds, and an admixture analysis estimating the proportion of ancestry.

The principal component analysis revealed that at PC1 (eigenvalue = 10.06) three breeds and their bantam counterparts were separated from the other breeds, WelSummer (WelSum), Barnevelder (Barnev), and North Hollands Blue (NHBl) (Figure 5.1B). These breeds are considered as the past-productive breeds in the Netherlands, therefore confirming the clustering. The second principal component (PC2, eigenvalue = 6.21) separated the two true bantam breeds, Dutch bantam (DB) and Eikenburger bantam (Eikenb), from the other breeds. However, the remaining breeds, including ornamental breeds and country fowl, clustered closely together in the PCA plot, suggesting an underlying genetic relationship. The unique population structure is supported by the unrooted NJ-tree as presented in Supplementary Figure S5.1. The historical clustering of breeds is generally demonstrated in the population phylogeny, the branch length of each breed shows the diversification between them. We observed that most Dutch native breeds and their bantam counterparts are closely clustered. Nevertheless, the close breed relationship was found between intermingled breeds, such as between breeds of ornamental fowl (i.e., Brabanter (Brab) and Dutch Owl bearded (DOwBd)) and of the country fowl cluster (i.e., Frisian Fowl (FriFw), Assendelft Fowl (AssFw) and Groningen Mew (GrMw)). This pattern of the close relationship between intermingled breeds has been reported before based on SNP-array data (Bortoluzzi et al., 2018), suggesting a profound genetic similarity and potential gene flow between these breeds. One explanation for this observation is the similar selection for management types and morphological traits within clusters. Another exception is seen for Drenthe Fowl bantam (DrFwB), where the neo-bantam shows a closer relationship with Dutch Bantam rather than with its large counterpart, DrFw.

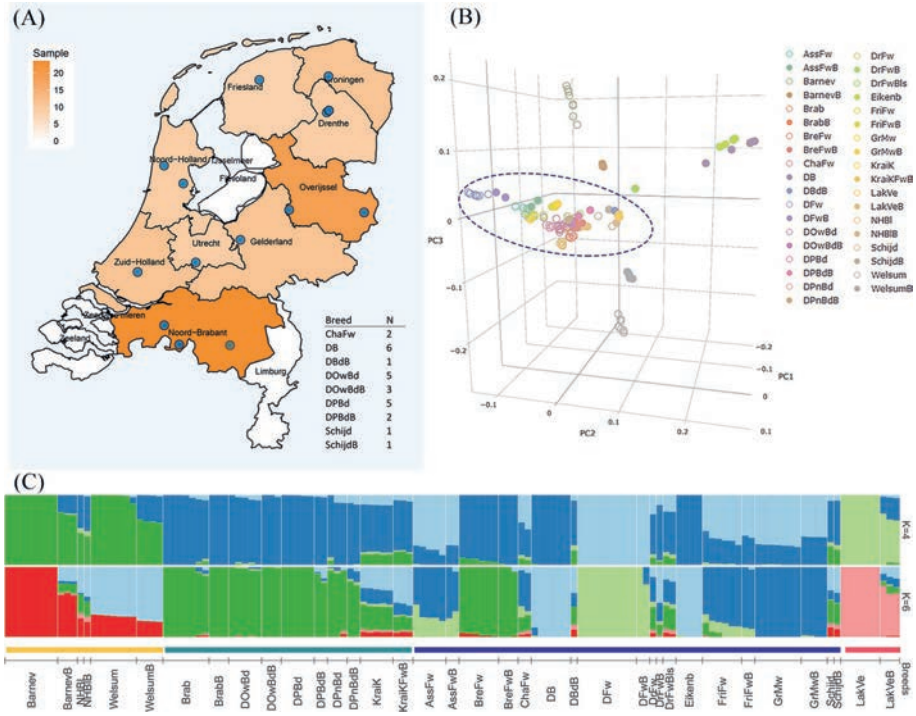

Figure 5.1 The population structure in Dutch chicken breeds. (A) The map shows the provinces in the Netherlands where the breeds originated. The blue circles on the map represent the known region of origin of the samples, whereas those breeds without any clear geographic information are listed in table format at the bottom-right. (B) Principal Component Analysis showing the first three principal components. (C) Admixture analyses with K = 4 and 6. The ancestry coefficients of each individual are shown by vertical bars. The horizontal bars display the different clusters, CL1 (yellow), CL 2 (green), CL3 (purple), and CL4 (Lakenvelder and its bantam) (red). The abbreviation of breed names can be found in **Table S5.1**.

The ADMIXTURE analysis complements the other two approaches. The results of ADMIXTURE (Figure 5.1C) subdivided the clusters, showing varied proportions of presumed ancestry. In agreement with the PCA and phylogenetic analyses, the clustering of past-productive breeds (CL1) and the group of Lakenvelder (CL4) is clearly separated at both K= 4 and 6, whereas the breeds of ornamental purpose (CL2) and country fowl (CL3) seemed to be more related. Strong admixture signals for breeds such as Twentse Fowl (KraiK), Schijndelaar (Schijd) and Drenthe Fowl (DrFw), as well as their bantams, showed population subdivision at K=6, implying their complex ancestry. Compared with other breeds, the country fowls showed varying levels of admixture. Among them, the Dutch Bantam and Eikenburger were distinguished from the rest, conforming to the second principal component in the PCA. In addition, the Kraienkoppe Fowl (BreFw) and its bantam, belonging to country fowl, share a large proportion of genetic ancestry with the ornamental chickens (CL2). By considering the history and features of the breed, we anticipated

that the relatedness may be derived from the shared characteristics of these breeds, like the shared form of a crest (Dana et al., 2011) or from the common bantam source. This relatedness is less likely associated with a geographic factor since BreFw(B) and breeds from CL2 are not located at a significantly close geographical distance compared to other breeds.

Taken together, the population structure of Dutch traditional chickens suggests a clear substructure showing a complex ancestry. The influence of breed management on the substructure is pronounced. The genetic relationships between the three clusters may reflect that the selection for breed standards and management categories can be a major force subdividing the population structure and reshaping the characteristics of breeds during breed formation. Compared to other animals with more refined and specialized purebreds (e.g., dogs), the indigenous chicken breeds are expected to have diverse genetic variations within the breeds and there is usually extensive gene flow between local regions among breeds with similar characteristics (Dana et al., 2011; Luo et al., 2020). As a result, a pattern of complex population structure and signatures of admixture are observed within the chicken population, accompanied by some distinguished substructure.

5.2.2 Isolation-By-Distance

In order to study the role of geographic dispersal in the population structure and the genetic differences between the breeds, we performed an Isolation-By-Distance (IBD) test to assess the correlation between genetic and geographic distances. The IBD test was performed for the dataset with all the Dutch breeds, as well as in the three historical clusters of breeds: past-productive (CL1); ornamental (CL2); country fowl (CL3).

The result of the IBD test among the overall Dutch chicken breeds showed a nonsignificant pattern of IBD (mantel r = -0.09, P = 0.99), suggesting no clear correlation between genetic and geographical distance across the population (Figure 5.2A). While looking at IBD patterns within historical clusters, a positive correlation was observed in CL1 (mantel r = 0.73, P = $1x10^{-4}$) and CL3 (mantel r = 0.33, P = $1x10^{-4}$), while breeds in CL2 showed a positive but rather weak correlation (mantel r = 0.13, P = 0.034) (Figure 5.2B-D). The significant correlation between the genetic and geographical distances within clusters suggests that the breeds at increasing geographical distance are also accompanied by increased genetic differences.

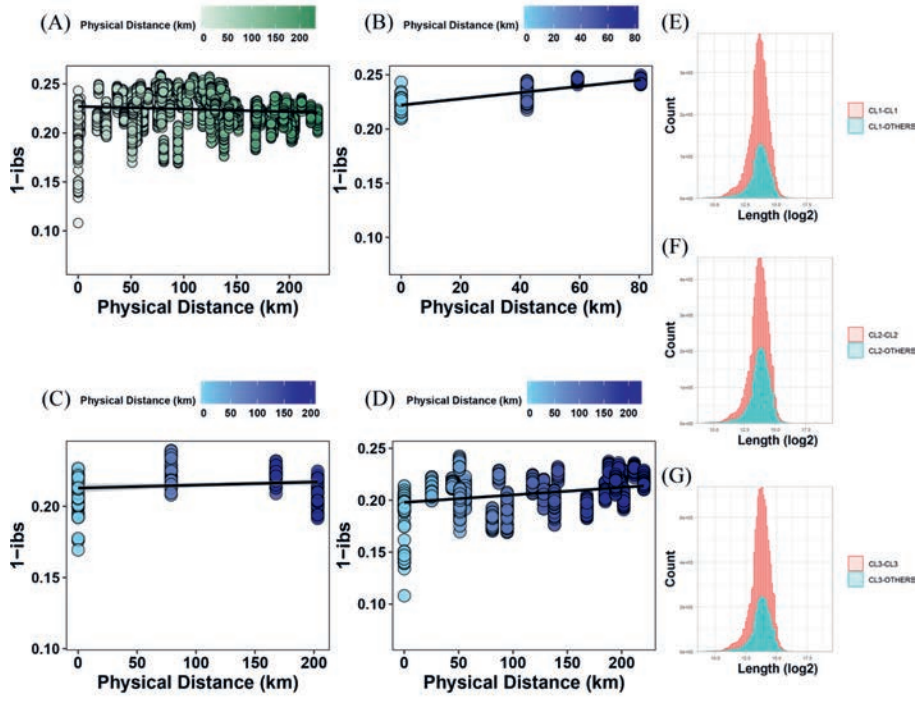

Figure 5.2 The correlation between genetic distance (1-ibs) and geographic distances (in Km) (A) among all breeds from the Dutch population, (B-D) and those in CL1, 2 and 3. (E-G) Distribution of shared identity-by-descent blocks identified within each subdivided cluster (red) and between clusters (green).

We observed that genetic distance is correlated with geographic distance only within the clusters, which is likely due to gene flow within each cluster and the management "barrier" between clusters. Given the limited dispersal distance between chickens in the Netherlands (maximum 227 Km), strong artificial selective breeding may dramatically pose a human-driven "barrier" reshaping the genetic landscape over geographic distance. Nevertheless, when we look at dispersal distance within each cluster, breeds that shared management purposes are also distributed evenly across the country at a maximum distance of 200 Km (with the exception of CL1 at a maximum dispersal distance of 80 Km), suggesting that the geographic distance plays a role in the genetic difference within clusters. The exception in CL1 showed limited geographical dispersal across those breeds, which can be partially explained by the assumption that homogenous specialization of past-productive purpose was popular only regionally. Although the productive specializations of breeds from CL1 are generally homogenous, i.e., for egg production, it is to be noted that breeds could have sub-divergent purposes, e.g., North Holland Blue was kept for dual purpose for both egg-laying and production of meat (Esther Verhoef and Rijs, 2014). This divergence

within this cluster may subsequently have contributed to the genetic differentiation, therefore confounding with geographical distance. When compared across clusters, the management purposes are different and unique, even for breeds from different clusters at a close geographic distance, and gene flow between them therefore will be limited resulting in a higher genetic distance. As a consequence, the exclusive exchange of genetic materials within subdivided management groups leads to a "barrier" between clusters.

To test our hypothesis of a management based "barrier", we examined haplotype sharing (identity-by-descent) across breeds within and between clusters. Haplotype sharing of identity-by-descent fragments has been used to reveal recent relatedness and demographic history between individuals in previous studies (Bosse et al., 2014; Parker et al., 2017). Within the three clusters, the haplotype sharing patterns were consistent. We found extensively shared haplotypes between individuals within clusters rather than between individuals belonging to different clusters (Figure 5.2 E-G). The limited haplotype sharing between clusters further confirmed the distant genetic relationship between management groups and is likely due to restricted recent gene flow. Moreover, the haplotype sharing within clusters demonstrated some recent common ancestry and genetic exchange within clusters, rather than a deep phylogenetic split with restricted gene flow.

Overall, we observed a stronger effect of management than of geographic distance on the subdivision of the Dutch traditional chicken breeds. In other words, the breeds in the same management cluster tend to show higher genetic similarity, outcompeting and masking the geographic separation at a population level. During the last century, selective breeding to maintain the breed characteristics of the traditional breeds has been intense in the Netherlands (Dana et al., 2011; Bortoluzzi et al., 2018). Based on the historical management purposes of the breeds, these breed characteristics can be complicated because of the dynamic and changing breeding goal. One example is the coexistence of maintaining management types while breeding for the bantam trait. These diverse purposes are sometimes confounded or competing, which complicates the overall genetic layout. Future study with the aim to disentangle the underlying interaction of factors involved in the complex population structure (e.g., between clusters CL2 and CL3) is needed. Moreover, it is common practice to include morphological variation (e.g., color varieties) in the breeding goal for indigenous chicken breeds. It is important to note that the number of individuals from each breed in this study is relatively small, and more widespread sampling across the country, including more morphological varieties, is desired.

5.2.3 Detection of genomic regions with differentiation between breeds

One of the causes of the complex genetic population structure of Dutch traditional chicken breeds is selective breeding adhering to desired traits and/or management

types. The breed features shared between multiple breeds have resulted from extensive crossbreeding and recycling of the genetic basis of these phenotypes. Of many desired phenotypic features, selection has been focused on downsizing the local breeds and to increase morphological varieties, especially color varieties, over the past decades. To identify genomic regions underlying unique and shared traits, we tested the dataset comprising of the 37 breeds for genetic differentiation of all kinds of breed specific or breed overlapping traits. We employed the FLK approach (extended LK test) using both the single variant and haplotype information. The single variant approach FLK was used to detect genomic regions comprising genetic differentiation between populations, such as signatures of selection, meanwhile accounting for the hierarchical structure of the populations (Bonhomme et al., 2010). Likewise, the haplotype-based approach, hapFLK, was used to detect differences in haplotype frequencies.

We observed a total of 387 significant signals (FDR 5%) in 299 genes across the genome by using the FLK test, suggesting potential genetic differentiation of the population (Figure 5.3). Using the genes identified by the FLK test, we did not find any GO term that was significantly overrepresented, which is expected because these breeds were selected for multiple phenotypes rather than one single trait. Compared with previously reported candidate genes associated with the bantam phenotype (Wu et al., 2020; chapter 3), eight bantam candidate genes overlapped with selective sweep signals of FLK. These signals confirm that the bantam related genomic regions were part of a strong selection regime. Interestingly, we found selective sweeps overlapping with the genes encoding High Mobility Group AT-hook 2 (*HMGA2*) and the PR/SET domain 16 (*PRDM16*). These genes have been reported to moderate body growth or short stature in diverse organisms (Weedon et al., 2007; Seale et al., 2008; Han et al., 2012; Rimbault et al., 2013; Bouwman et al., 2018), further supporting the strong association signals in our bantam GWAS analysis phenotype (Wu et al., 2020; chapter 3). Although we did not find hapFLK signals reaching the significance threshold (Figure S5.2); suggestive signals were observed which supplement the signals discovered by FLK analysis. The hapFLK signals revealed signals surrounding the genes *ENSGALG00000052273* and *ENSGALG00000049778* on chromosome 4, encoding two long non-coding RNAs (lncRNAs). In addition, a strong selective sweep is observed around 170.72 Mb on chromosome 1, proximal to the QTL reported to be associated with growth and body weight (170.52 -172.04 Mb) (Xie et al., 2012). Given the bantam phenotype is one of the most prominent phenotypes in the Dutch population, the identified genomic regions associated with body growth and size variation are of great interest. This QTL region is composed of several genes, encoding potassium channel regulator (*KCNRG*), tripartite motif containing 13 (*TRIM13*) and the microRNAs, *gga-mir-15a* and *gga-mir-16-1* (Figure S5.2B). Focusing on chromosome 1, we integrated the results of FLK with hapFLK and

observed two suggestive signatures surrounding the genes encoding SRY-box 10 (*SOX10*), and SRY-box 5 (*SOX5*). According to previous studies and OMIA (https://omia.org/home/) database for chicken, a deletion upstream of the *SOX10* gene is associated with dark brown feather color in chickens (Gunnarsson et al., 2011), while a copy number variation in the *SOX5* gene is responsible for the shape of the comb through the epistatic interaction with the *MNR2* gene (Imsland et al., 2012). Feather color and comb shape are both phenotypes related directly with breed standards, and thus especially important for chickens kept for ornamental purposes and fancy breeding. These signatures of selection at these two genes suggest morphological diversification among Dutch breeds, reflecting the breeding interest associated with phenotypic variation. In particular, we confirmed that comb shape and plumage color are very variable within and among breeds. For instance, there are over 20 different feather plumage varieties recorded in Dutch Bantam (Esther Verhoef and Rijs, 2014). However, due to the limited sample size and incomplete phenotypic records, we were unable to validate these selective signatures. It is further important to note that our interpretation of the signatures of selection are based on previous knowledge from the online catalogue OMIA, which may be improved when the annotation of the phenotype database is better understood (e.g., through Functional Annotation of Animal Genomes (FAANG) (Giuffra and Tuggle, 2019)).

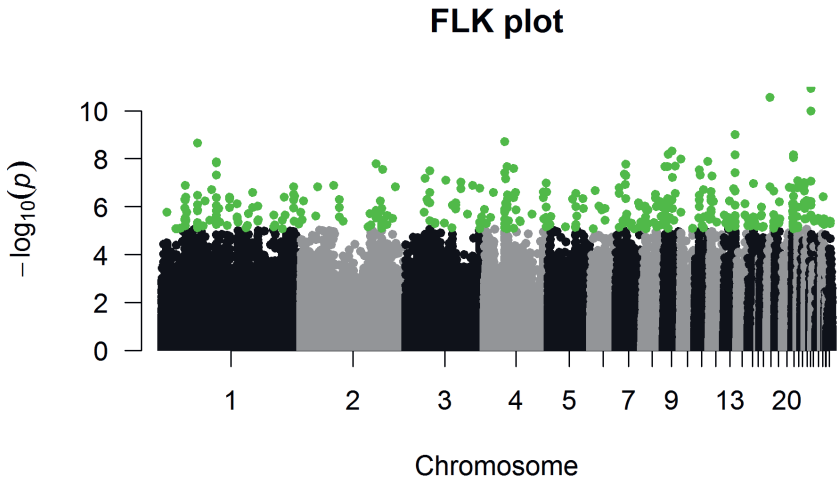

Figure 5.3 Manhattan plot of FLK across the genome detected in Dutch chicken breeds. Significant variants (FDR>5%) of FLK are indicated with green dots.

5.2.4 The impact of recent crossbreeding: A case study in Drenthe Fowl Bantam

We have addressed the selective signatures related to introducing desired phenotypes and especially the strong selection at bantam associated loci. Therefore, we take a

neo-bantam breed as a case study to show the hybrid nature of these genomes and the consequences of crossbreeding to introduce desired traits. The bantam-oriented crossbreeding to introduce the bantam phenotype to native breeds is an excellent model to understand the introgression of bantam.

Drenthe Fowl bantam (DrFwB) as a corresponding neo-bantam counterpart of the traditional breed Drenthe Fowl (DrFw), has a recently developed history in the bantam crossbreeding process. According to the bantamization record, the DrFwB was created by mating DrFw with existing bantam breeds, particularly Dutch Bantam (DB) (Esther Verhoef and Rijs, 2014). The relatively recent crossbreeding for DrFwB is an ongoing trajectory, which has resulted in a unique genomic characteristic of the breed. Unlike the other neo-bantam breeds that share a similar crossbreeding history with the same presumed bantam donors (e.g., GrMwB), DrFwB shows a closer genetic distance with the bantam donor DB (0.199), whereas it is more distantly related to its normal-sized counterpart DrFw (0.213). This unique relationship is supported by the admixture signal of DrFwB (Figure 5.1C). One possible explanation is that the crossbreeding to create DrFwB is relatively recent, and the subsequent backcrossing has not yet played its role to effectively dilute the other components of the bantam donor. In many studies of introgression from an evolutionary perspective, the focus was on the introgression event that happened many generations ago, often spanning thousands of years (Patterson et al., 2012; Bosse et al., 2014; Wang et al., 2020). The three breeds (i.e., the donor breeds DrFw and DB, and the derived breed DrFwB) provided us with an excellent proxy to investigate the recent event of hybridization which leaves many “hitchhiking” segments derived from the donor in the recipient genome. The removal of these genomic segments requires time to effectively take place by backcrossing, which enables us to estimate the effect of this ongoing process.

To understand crossbreeding in the context of bantamization, we used the genetic haplotype sharing (identity-by-descent) method to address the contribution of bantam ancestry towards the neo-bantam breed, which is from DB to DrFwB. Based on the number and length of identity-by-descent fragments between bantam donor and recipient, we observed abundant segments of shared haplotypes between DB and DrFwB (Figure S5.3). In contrast, a smaller number of haplotype blocks is shared between the breed counterparts, DrFw and DrFwB.

To further detect the haplotype sharing signals across the genome, regional haplotype sharing is summarized by relative identity-by-descent (rIBD) after normalization (Figure 5.4). In general, almost all chromosomes contained regions similar to either the counterpart (DrFw) or the true bantam (DB) donors, suggesting overall signals of haplotype sharing across the genome (Figure S5.4). However, when focusing on specific chromosomes (e.g., chromosome 1), we observed large and consecutive

stretches of rIBD in DrFwB displaying higher similarity with DB. As a confirmation of the relative haplotype sharing signals captured by rIBD, we examined the region around the *HMGA2* gene underlying the bantam phenotype based on the results of our bantam association study (Wu et al., 2020; chapter 3). As expected, the haplotype blocks around the *HMGA2* gene are almost completely shared between DB and DrFwB, which confirms the shared signals are at the bantam related region. This result supports the bantamization history of the breed, that these segments surrounding the *HMGA2* gene are likely introgressed from DB or the co-ancestral population.

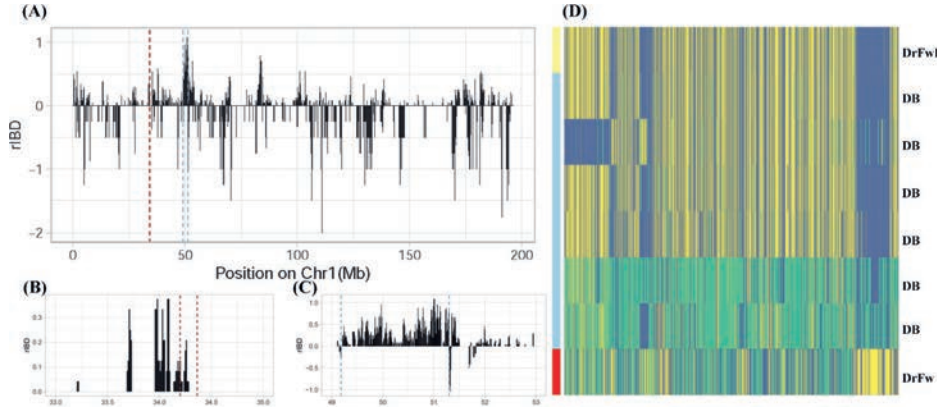

Figure 5.4 The relative haplotype sharing and the genotypes of individuals from DrFwB, DrFw, and DB. (A) Distribution of relative identity-by-descent (rIBD)on chromosome 1, showing the relative fraction of haplotype blocks shared between DrFwB and DB (positive rIBD) and DrFwB and DrFw (negative rIBD). (B) The *HMGA2* related interval is highlighted by the red dashed lines. (C) The DB introgressed region (49.2-51.3Mb) is indicated by the blue dashed lines. (D) Individual genotypes of the representative DB introgressed region (50.7-51.0 Mb) are visualized for each locus: homozygous reference allele (blue), homozygous alternative allele (yellow), heterozygous locus (green).

Interestingly, we noticed a large region containing extensive and consecutive DB haplotypes between 49.2-51.3 Mb on chromosome 1, which outcompeted the bantam associated locus (around the *HMGA2* gene) in terms of length and sequence similarity. The function of genes in this region is overrepresented in the oxygen transport process (e.g., oxygen binding and haptoglobin binding). We inferred and compared the localized haplotypes between DrFwB with both the counterpart (DrFW) and the bantam donor (DB). Within this introgressed region, the distribution of genotypes of 2000 variants demonstrates that the sequence of DrFwB is highly homozygous and highly similar to the sequences from DB individuals (three out of six) (Figure 5.4D). While in DB, the haplotypes were observed to be diverse within the breed, suggesting the corresponding region is not completely fixed among individuals. In particular, two individuals were extensively comprised of heterozygous loci, which is more similar to the normal-sized DrFw. This regional haplotype diversity in DB individuals implies that there is no evidence showing specific selection for this region. One possible

explanation for the consecutive introgressed signals in the genome of DrFwB is genetic drift. The DB introgressed haplotypes in DrFwB may be a result of genetic drift, which was subsequently retained in the genome due to the short time since bantamization and/or the lack of recombination. The shared haplotypes represented by only some of the DB chickens further suggests that chance played a role in determining this region was passed on from the DB donor to the DrFwB recipient.

To partially obtain a view of the outcome of this ongoing procedure of crossbreeding, we compared this region with another neo-bantam breed, Groningen Mew Bantam (GrMwB). GrMwB is believed to have a similar bantam crossbreeding origin (from DB) but that has been established for a relatively longer period (Figure S5.5). We first detected the bantam associated signal (around *HMGA2*) in its genome, confirming the consecutive selection for the bantam trait. Then we observed that haplotype blocks in the corresponding region around 49.2-51.3 Mb are completely shared between GrMwB and its normal counterpart, GrMw. This result showed a reverse pattern as seen in DrFwB. In addition, since positive selection and genetic drift are both expected to change the frequency of certain alleles or haplotypes, it is to be noted that the observation of some of the fixed introgression signals may suggest potential selection or a coincided "hitchhiking effect", which can be favorable for performance or morphology. However, it lacks direct evidence and additional observation to support the possibility that the DB introgressed regions are under selection.

The current study has provided insight in the complex population structure of Dutch chicken breeds and the factors that influence this complexity. The complex population structure can be attributed to selection for management standards and phenotypic differentiation, like crossbreeding processes to introduce the bantam trait. We also obtained evidence for the role that geographic dispersal plays in the distribution of breeds within the subdivided populations. We detected a large set of signatures of selection suggesting diversifying selection in these breeds, including bantam related selection and breed standard phenotypes selection. Finally, the DrFwB case study showed the power of genomic data to understand the recent demographic history and ongoing breed development.

5.3 Materials and Methods

5.3.1 Whole-genome sequencing and processing of genetic variants

The chickens sampled for whole-genome sequencing included a total of 136 individuals from 37 breeds, in which the neo-bantam and the normal-sized counterparts were considered as different breeds (Table S5.1). Paired-end sequencing (PE125) was performed on the Illumina HiSeq 3,000 platform, with insert sizes of 350 bp. The processing of whole genome sequence data was conducted following an in-house analysis pipeline. In brief, raw sequencing reads were trimmed by Sickle (Joshi and Fass, 2011) then mapped to the latest chicken reference assembly, build GRCg6a

(GenBank Accession: GCA_000002315.5) using BWA-MEM (V0.7.17) (Li and Durbin, 2009). Duplicated reads were marked and removed using sambamba V0.6.3 (Tarasov et al., 2015). Whole-genome SNPs and Insertion and Deletion (InDels) were genotyped using Freebayes (Garrison and Marth, 2012). After filtering for base quality and genotype quality, we further processed the variants with the following criteria: minor allele frequency (MAF) >1% and call-rate >80%.

The raw data of whole genome sequencing, including novel and published data, has been submitted to the European Nucleotide Archive (ENA). The data of 88 traditional chicken breeds from the Netherlands can be accessed through the project number: PRJEB34245, described in a previous study (Bortoluzzi et al., 2020).The data of 44 Dutch chicken breeds has been described in previous work under accession number: PRJEB39725 (Wu et al., 2020). Additional data of four samples (2 DrFwBls and 2 ChaFw) will be submitted.

5.3.2 Haplotype sharing (Identity-by-descent) detection

We used the genotype phasing program Beagle (version 5.0) (Browning and Browning, 2007) to construct the haplotypes for all individuals using a sliding window size of 0.02 cM and 0.01 cM overlap between adjacent windows with 12 iterations. The chromosomal genetic distances were based on Elferink et al. (2010). However, in this genetic map, not all chromosomes are covered. Therefore, only the chromosomes with a reported genetic map were included in this analysis, and uninformative chromosomes (GGA16 and GGA30-33), linkage groups without chromosomal location, and the sex chromosomes (Z and W) were excluded. An exception is the genetic map for GGA25 which was derived from an earlier study by Groenen et al. (2009) because it was missing in the study of Elferink et al. (2010).

The haplotype of individuals was used for detection of Identity-by-descent segments using Refined-ibd (Browning and Browning, 2013). This analysis aims to detect Identity-by-descent segments derived from the same population rather than from a single common ancestor. The segments of Identity-by-descent were detected using the following requirements: window size of 0.06 cM, length=0.03 cM, trim for length < 0.001 cM, and LOD score > 3. To infer the relative fraction of haplotype sharing in regions across the genome, we computed the relative Identity-by-descent (rIBD) frequency following Bosse et al. (2014). The rIBD in this study was calculated between the DrFwB and the two donors (the bantam donor, DB; and the normal-sized donor, DrFw) in bins of 10 Kb. And the rIBD in different bins of the genome was essentially compared and plotted by chromosome (see below for more details).

5.3.3 Population structure analysis

The population structure analyses were performed using three approaches: a principal component analysis (PCA), a population phylogeny constructed using Reynold's

distance, and an admixture analysis. (1) The PCA was computed using PLINK (V1.9) (Chang et al., 2015) with autosomal variants, and visualized using the R package "plotly" (Sievert, 2020). (2) The pairwise Reynolds' genetic distances between breeds were computed as in Fariello et al. (2013) and the phylogenetic tree is fitted using the Neighbor-Joining algorithm. We visualized the genetic distance by using FigTree V1.4.4 (http://tree.bio.ed.ac.uk/software/figtree/). The phylogenetic relationship was used in the FLK and hapFLK analysis. (3) We used the genetic analysis software ADMIXTURE to estimate ancestry in the individuals (Alexander et al., 2009). The software was run with different numbers of ancestral populations, and representative output of K=4 and K=6 is presented in this study.

5.3.4 Isolation-by-distance (IBD) test

The geographical distance is determined by haversine distance given the longitude and latitude of the location of the origin of the breeds using the "geosphere" package (Robert J Hijmans, E Williams, 2015) in R V3.6.1. The individual pairwise genetic distance was computed by 1-ibs distance using the autosomal whole-genome variants with the command (--distance square 1-ibs) in PLINK (V1.9). Because of the unknown geographic location for 9 of the 37 breeds, these were excluded from the IBD test. These 9 breeds are listed in table format in Figure 5.1A. We performed a mantel test and determined the level of significance with permutation for 9999 times. We tested the IBD with individuals from all populations, and also examined it within groups based on historical clustering, the groups of Dutch breeds were profiled in Elferink et al. (2012) and Bortoluzzi et al. (2018): CL1 past-productive, CL2 ornamental, CL3 country fowl, CL4 Lakenvelder and Lakenvelder bantam. Because CL4 only contained Lakenvelder and its bantam, we excluded it for the IBD test. In order to show the haplotype similarity within clusters and between clusters, the detection of identity-by-descent segments was performed in each cluster accordingly. The count and the length of identity-by-descent segments between individuals were visualized for comparisons within the cluster and that between this cluster and the rest.

5.3.5 FLK and hapFLK

The FLK and hapFLK analyses were conducted to detect the signatures of selection between different populations (Bonhomme et al., 2010; Fariello et al., 2013). The autosomal variants were pre-processed before computing FLK and hapFLK. To save computational time, we filtered out the variants with MAF < 8% and linkage equilibrium pruning (r^2 >0.3). In total, we ended up with 2.30 million variants covering the genome. The hierarchical structure (Reynolds' distance matrix) of the populations was accounted for in the genomic scans for selection signatures. For the single-marker analysis, we performed the FLK test on all variants by chromosome. As for the haplotype-based FLK (hapFLK) test, we set the number of haplotype

groups in the population to K=15, as suggested by the authors, where the P-values were derived by scaling the hapFLK statistic to a chi-square distribution as described in Boitard et al. (2016). The significant signals were determined at a false discovery rate (FDR) of 5%.

We annotated the variants if they are within 5 Kb up- or downstream distance to a gene or regulatory element (Ensembl gene sets version 95). Selective sweeps annotated with more than one significant variant were considered for further investigation. First, we compared the genes with the Online Mendelian Inheritance in Animals (OMIA) dataset, searching for "likely known" causative genes for Mendelian traits in chicken (https://omia.org/home/). Second, a Gene Ontology enrichment analysis was employed using PANTHER v.11 (Mi et al., 2019) based on the chicken to human one-to-one orthologues. Gene enrichment analysis was then performed by using the package clusterProfiler (Yu et al., 2012).

5.3.6 Haplotype sharing in the case study

In the case study of Drenthe Fowl bantam chicken, haplotype sharing was measured by identity-by-descent among the three breeds (Dutch Bantam, Drenthe Fowl, and Drenthe fowl bantam). The pairwise identity-by-descent segments between two breeds were estimated by bins of 10 Kb and then normalized by the possible count between these two breeds (nIBD). The relative fraction of identity-by-descent (rIBD) was computed by comparing the nIBD between DB and DrFwB ($nIBD_{DB\_DrFwB}$) with the nIBD between DrFw and DrFwB ($nIBD_{DrFw\_DrFwB}$). A positive rIBD shows more haplotype sharing between DB and DrFwB than between DrFw and DrFwB, whereas a negative rIBD shows more haplotype sharing between the counterparts (i.e., DrFw and DrFwB) correspondingly. In order to compare the rIBD pattern in another neo-bantam breed with a similar crossbreeding history, we selected individuals from GrMwB and GrMw breeds to show the introgression signals. To keep the samples comparable, we chose one individual from each breed, and the average coverage of the samples should be adequate and as good as the coverage of DrFwB. Likewise, we computed the rIBD between DB, GrMwB, and GrMw. The DB introgressed regions were highlighted at visualization.

5.4 Acknowledgments

We would like to thank the Centre for Genetic Resources, the Netherlands (CGN) of WUR for providing the samples used in this study. We also thank the networks of breeders in the Netherlands, who provided phenotype information of the breeds. The sequencing data generated in this work was supported by the IMAGE Project from the European Union's Horizon 2020 Research and Innovation Program (Grant Agreement No. 677353). We would like to thank the China Scholarship Council for the financial support to ZW (Grant No. 201606350175).

5.5 Author Contribution Statement

ZW and RPMAC conceived and designed the study. ZW analyzed the data and wrote the manuscript. MB, MAMG provided valuable input on the design of this study. CMR provided useful suggestions on the FLK and hapFLK analyses. CMR, MB, MAMG, and RPMAC provided valuable suggestions and comments to improve the manuscript.

5.6 References

Alexander, D. H., Novembre, J., and Lange, K. (2009). Fast model-based estimation of ancestry in unrelated individuals. *Genome Res.* 19, 1655–1664. doi:10.1101/gr.094052.109.

Boitard, S., Boussaha, M., Capitan, A., Rocha, D., and Servin, B. (2016). Uncovering adaptation from sequence data: Lessons from genome resequencing of four cattle breeds. *Genetics* 203, 433–450. doi:10.1534/genetics.115.181594.

Bonhomme, M., Chevalet, C., Servin, B., Boitard, S., Abdallah, J., Blott, S., et al. (2010). Detecting selection in population trees: The Lewontin and Krakauer test extended. *Genetics* 186, 241–262. doi:10.1534/genetics.110.117275.

Bortoluzzi, C., Bosse, M., Derks, M. F. L., Crooijmans, R. P. M. A., Groenen, M. A. M., and Megens, H. J. (2020). The type of bottleneck matters: Insights into the deleterious variation landscape of small managed populations. *Evol. Appl.* 13, 330–341. doi:10.1111/eva.12872.

Bortoluzzi, C., Crooijmans, R. P. M. A., Bosse, M., Hiemstra, S. J., Groenen, M. A. M., and Megens, H. J. (2018). The effects of recent changes in breeding preferences on maintaining traditional Dutch chicken genomic diversity. *Heredity (Edinb).* 121, 564–578. doi:10.1038/s41437-018-0072-3.

Bosse, M., Megens, H. J., Frantz, L. A. F., Madsen, O., Larson, G., Paudel, Y., et al. (2014). Genomic analysis reveals selection for Asian genes in European pigs following human-mediated introgression. *Nat. Commun.* 5, 4392. doi:10.1038/ncomms5392.

Bouwman, A. C., Daetwyler, H. D., Chamberlain, A. J., Ponce, C. H., Sargolzaei, M., Schenkel, F. S., et al. (2018). Meta-analysis of genome-wide association studies for cattle stature identifies common genes that regulate body size in mammals. *Nat. Genet.* 50, 362–367. doi:10.1038/s41588-018-0056-5.

Browning, B. L., and Browning, S. R. (2013). Improving the accuracy and efficiency of identity-by-descent detection in population data. *Genetics* 194, 459–471. doi:10.1534/genetics.113.150029.

Browning, S. R., and Browning, B. L. (2007). Rapid and accurate haplotype phasing and missing-data inference for whole-genome association studies by use of localized haplotype clustering. *Am. J. Hum. Genet.* 81, 1084–1097. doi:10.1086/521987.

Chang, C. C., Chow, C. C., Tellier, L. C. A. M., Vattikuti, S., Purcell, S. M., and Lee, J. J. (2015). Second-generation PLINK: Rising to the challenge of larger and richer datasets. *Gigascience* 4, 7. doi:10.1186/s13742-015-0047-8.

Dana, N., Megens, H. J., Crooijmans, R. P. M. A., Hanotte, O., Mwacharo, J., Groenen, M. A. M., et al. (2011). East asian contributions to dutch traditional and western commercial chickens inferred from mtDNA analysis. *Anim. Genet.* 42, 125–133. doi:10.1111/j.1365-2052.2010.02134.x.

Elferink, M. G., Megens, H. J., Vereijken, A., Hu, X., Crooijmans, R. P. M. A., and Groenen, M. A. M. (2012). Signatures of selection in the genomes of commercial and non-commercial chicken breeds. *PLoS One* 7, e32720. doi:10.1371/journal.pone.0032720.

Elferink, M. G., van As, P., Veenendaal, T., Crooijmans, R. P. M. A., and Groenen, M. A. M. (2010). Regional differences in recombination hotspots between two chicken populations. *BMC Genet.* 11, 11. doi:10.1186/1471-2156-11-11.

Esther Verhoef, and Rijs, A. (2014). *De kippen encyclopedie*. Rebo Productions.

Fariello, M. I., Boitard, S., Naya, H., SanCristobal, M., and Servin, B. (2013). Detecting signatures of selection through haplotype differentiation among hierarchically structured populations. *Genetics* 193, 929–941. doi:10.1534/genetics.112.147231.

Garrison, E., and Marth, G. (2012). Haplotype-based variant detection from short-read sequencing. *arXiv Prepr.* Available at: http://arxiv.org/abs/1207.3907 [Accessed February 14, 2018].

Giuffra, E., and Tuggle, C. K. (2019). Functional Annotation of Animal Genomes (FAANG): Current Achievements and Roadmap. *Annu. Rev. Anim. Biosci.* 7, 65–88. doi:10.1146/annurev-animal-020518-114913.

Gompert, Z., Mandeville, E. G., and Buerkle, C. A. (2017). Analysis of Population Genomic Data from Hybrid Zones. *Annu. Rev. Ecol. Evol. Syst* 48, 207–236. doi:10.1146/annurev-ecolsys-110316.

Groenen, M. A. M., Wahlberg, P., Foglio, M., Cheng, H. H., Megens, H. J., Crooijmans, R. P. M. A., et al. (2009). A high-density SNP-based linkage map of the chicken genome reveals sequence features correlated with recombination rate. *Genome Res.* 19, 510–519. doi:10.1101/gr.086538.108.

Gunnarsson, U., Kerje, S., Bed'hom, B., Sahlqvist, A.-S. S., Ekwall, O., Boichard, M. T., et al. (2011). The Dark brown plumage color in chickens is caused by an 8.3-kb deletion upstream of SOX10. *Pigment Cell Melanoma Res.* 24, 268–274. doi:10.1111/j.1755-148X.2011.00825.x.

Han, R., Wei, Y., Kang, X., Chen, H., Sun, G., Li, G., et al. (2012). Novel SNPs in the PRDM16 gene and their associations with performance traits in chickens. *Mol. Biol. Rep.* 39, 3153–3160. doi:10.1007/s11033-011-1081-y.

Hillel, J., Groenen, M. A. M., Tixier-Boichard, M., Korol, A. B., David, L., Kirzhner, V. M., et al. (2003). Biodiversity of 52 chicken populations assessed by microsatellite typing of DNA pools. 35. Available at: http://www.gsejournal.org/content/35/6/533 [Accessed April 30, 2018].

Imsland, F., Feng, C., Boije, H., Bed'hom, B., Fillon, V., Dorshorst, B., et al. (2012). The Rose-comb mutation in chickens constitutes a structural rearrangement causing both altered comb morphology and defective sperm motility. *PLoS Genet.* 8, e1002775. doi:10.1371/journal.pgen.1002775.

Joshi, N., and Fass, J. (2011). Sickle: A sliding-window, adaptive, quality-based trimming tool for FastQ files (Version 1.33) [Software]. *Available at https://github.com/najoshi/sickle.*, 2011.

Li, H., and Durbin, R. (2009). Fast and accurate short read alignment with Burrows-Wheeler transform. *Bioinformatics* 25, 1754–1760. doi:10.1093/bioinformatics/btp324.

Luo, W., Luo, C., Wang, M., Guo, L., Chen, X., Li, Z., et al. (2020). Genome diversity of Chinese indigenous chicken and the selective signatures in Chinese gamecock chicken. *Sci. Rep.* 10, 14532. doi:10.1038/s41598-020-71421-z.

Mi, H., Muruganujan, A., Huang, X., Ebert, D., Mills, C., Guo, X., et al. (2019). Protocol Update for large-scale genome and gene function analysis with the PANTHER classification system (v.14.0). *Nat. Protoc.* 14, 703–721. doi:10.1038/s41596-019-0128-8.

Nie, C., Almeida, P., Jia, Y., Bao, H., Ning, Z., Qu, L., et al. (2019). Genome-Wide Single-Nucleotide Polymorphism Data Unveil Admixture of Chinese Indigenous Chicken Breeds with Commercial Breeds. *Genome Biol. Evol.* 11, 1847–1856. doi:10.1093/gbe/evz128.

Parker, H. G., Dreger, D. L., Rimbault, M., Davis, B. W., Mullen, A. B., Carpintero-Ramirez, G., et al. (2017). Genomic Analyses Reveal the Influence of Geographic Origin, Migration, and Hybridization on Modern Dog Breed Development. *Cell Rep.* 19, 697–708. doi:10.1016/j.celrep.2017.03.079.

Patterson, N., Moorjani, P., Luo, Y., Mallick, S., Rohland, N., Zhan, Y., et al. (2012). Ancient admixture in human history. *Genetics* 192, 1065–1093. doi:10.1534/genetics.112.145037.

Rimbault, M., Beale, H. C., Schoenebeck, J. J., Hoopes, B. C., Allen, J. J., Kilroy-Glynn, P., et al. (2013). Derived variants at six genes explain nearly half of size reduction in dog breeds. *Genome Res.* 23, 1985–1995. doi:10.1101/gr.157339.113.

Robert J Hijmans, E Williams, C. V. (2015). Geosphere: spherical trigonometry.R package. Available at: https://cran.r-project.org/web/packages/geosphere/.

Rochus, C. M., Tortereau, F., Plisson-Petit, F., Restoux, G., Moreno-Romieux, C., Tosser-Klopp, G., et al. (2018). Revealing the selection history of adaptive loci using genome-wide scans for selection: An example from domestic sheep. *BMC Genomics* 19. doi:10.1186/s12864-018-4447-x.

Rubin, C. J., Zody, M. C., Eriksson, J., Meadows, J. R. S., Sherwood, E., Webster, M. T., et al. (2010). Whole-genome resequencing reveals loci under selection during chicken domestication. *Nature* 464, 587–591. doi:10.1038/nature08832.

Seale, P., Bjork, B., Yang, W., Kajimura, S., Chin, S., Kuang, S., et al. (2008). PRDM16 controls a brown fat/skeletal muscle switch. *Nature* 454, 961–967. doi:10.1038/nature07182.

Sheppy, A. (2011). The colour of domestication and the designer chicken. in *Optics and Laser Technology* (Elsevier), 295–301. doi:10.1016/j.optlastec.2009.02.003.

Sievert, C. (2020). *Interactive Web-Based Data Visualization with R, plotly, and shiny*. doi:10.1201/9780429447273.

Tarasov, A., Vilella, A. J., Cuppen, E., Nijman, I. J., and Prins, P. (2015). Sambamba: Fast processing of NGS alignment formats. *Bioinformatics* 31, 2032–2034. doi:10.1093/bioinformatics/btv098.

Wang, M.-S., Thakur, M., Peng, M.-S., Jiang, Y., Frantz, L. A. F., Li, M., et al. (2020). 863 genomes reveal the origin and domestication of chicken. *Cell Res.*, 1–9. doi:10.1038/s41422-020-0349-y.

Weedon, M. N., Lettre, G., Freathy, R. M., Lindgren, C. M., Voight, B. F., Perry, J. R. B., et al. (2007). A common variant of HMGA2 is associated with adult and childhood height in the general population. *Nat. Genet.* 39, 1245–1250. doi:10.1038/ng2121.

Wilkinson, S., Wiener, P., Teverson, D., Haley, C. S., and Hocking, P. M. (2012). Characterization of the genetic diversity, structure and admixture of British chicken breeds. *Anim. Genet.* 43, 552–563. doi:10.1111/j.1365-2052.2011.02296.x.

Woelders, H., Zuidberg, C. A., and Hiemstra, S. J. (2006). Animal genetic resources conservation in The Netherlands and Europe: Poultry perspective. *Poult. Sci.* 85, 216–222. doi:10.1093/ps/85.2.216.

Wu, Z., Bortoluzzi, C., Derk1, M. F. L., Liu, L., Bosse, M., Hiemstra, S. J., et al. (2020). Heterogeneity of a dwarf phenotype in Dutch traditional chicken breeds revealed by genomic analyses. *submitted*.

Xie, L., Luo, C., Zhang, C., Zhang, R., Tang, J., Nie, Q., et al. (2012). Genome-wide association study identified a narrow chromosome 1 region associated with chicken growth traits. *PLoS One* 7, 30910. doi:10.1371/journal.pone.0030910.

Yang, B., Cui, L., Perez-Enciso, M., Traspov, A., Crooijmans, R. P. M. A., Zinovieva, N., et al. (2017). Genome-wide SNP data unveils the globalization of domesticated pigs. *Genet. Sel. Evol.* 49, 71. doi:10.1186/s12711-017-0345-y.

Yu, G., Wang, L. G., Han, Y., and He, Q. Y. (2012). ClusterProfiler: An R package for comparing biological themes among gene clusters. *Omi. A J. Integr. Biol.* 16, 284–287. doi:10.1089/omi.2011.0118.

Zhang, M., Han, W., Tang, H., Li, G., Zhang, M., Xu, R., et al. (2018). Genomic diversity dynamics in conserved chicken populations are revealed by genome-wide SNPs. *BMC Genomics* 19, 598. doi:10.1186/s12864-018-4973-6.

Zink, R. M. (1997). "Phylogeographic studies of North American birds," in *Avian Molecular Evolution and Systematics*, 301–324. doi:10.1016/b978-012498315-1/50017-0.

5.7 Supplementary materials

The supplementary materials can be found at online repository through: https://osf.io/ec652/?view_only=183b449e45ea4dc085a6c6a6b2567c9f

Table S5.1 Dutch chicken breeds and groups.

Breed (abbrev.)	Breed name (in English)	Cluster	N
Barnev	Barnevelder	CL1	8
BarnevB	Barnevelder Bantam	CL1	3
NHBl	North Holland Blue	CL1	1
NHBlB	North Holland Blue Bantam	CL1	1
Welsum	Welsummer	CL1	7
WelsumB	Welsummer Bantam	CL1	4
Brab	Brabanter	CL2	7
BrabB	Brabanter Bantam	CL2	3
DOwBd	Dutch Owl Bearded	CL2	5
DOwBdB	Dutch Owl Bearded Bantam	CL2	3
DPBd	Dutch Polish Bearded	CL2	5
DPBdB	Dutch Polish Bearded Bantam	CL2	2
DPnBd	Dutch Polish non-Bearded	CL2	3
DPnBdB	Dutch Polish non-Bearded Bantam	CL2	2
KraiK	Twentse Fowl	CL2	5
KraiKFwB	Twentse Fowl Bantam	CL2	3
AssFw	Assendelft Fowl	CL3	5
AssFwB	Assendelft Fowl Bantam	CL3	2
BreFw	Kraienkoppe Fowl Bantam	CL3	6
BreFwB	Kraienkoppe Fowl	CL3	3
ChaFw	Chaam Fowl	CL3	2
DB	Dutch Bantam	CL3	6
DBdB	Dutch Booted Bantam	CL3	1
DFw	Dutch Fowl	CL3	9
DFwB	Dutch Fowl Bantam	CL3	2
DrFw	Drenthe Fowl	CL3	1
DrFwB	Drenthe Fowl Bantam	CL3	1
DrFwBls	Drenthe Fowl Rumpless	CL3	2
Eikenb	Eikenburger Bantam	CL3	4
FriFw	Frisian Fowl	CL3	6
FriFwB	Frisian Fowl Bantam	CL3	2
GrMw	Groninger Mew	CL3	7
GrMwB	Groninger Mew Bantam	CL3	4
Schijd	Schijndelaar	CL3	1
SchijdB	Schijndelaar Bantam	CL3	1
LakVe	Lakenvelder	CL4	6
LakVeB	Lakenvelder Bantam	CL4	3

Figure S5.1 Unrooted Neighbor-Joining Tree (NJ-tree) illustrates Reynold's distance between breeds (online).

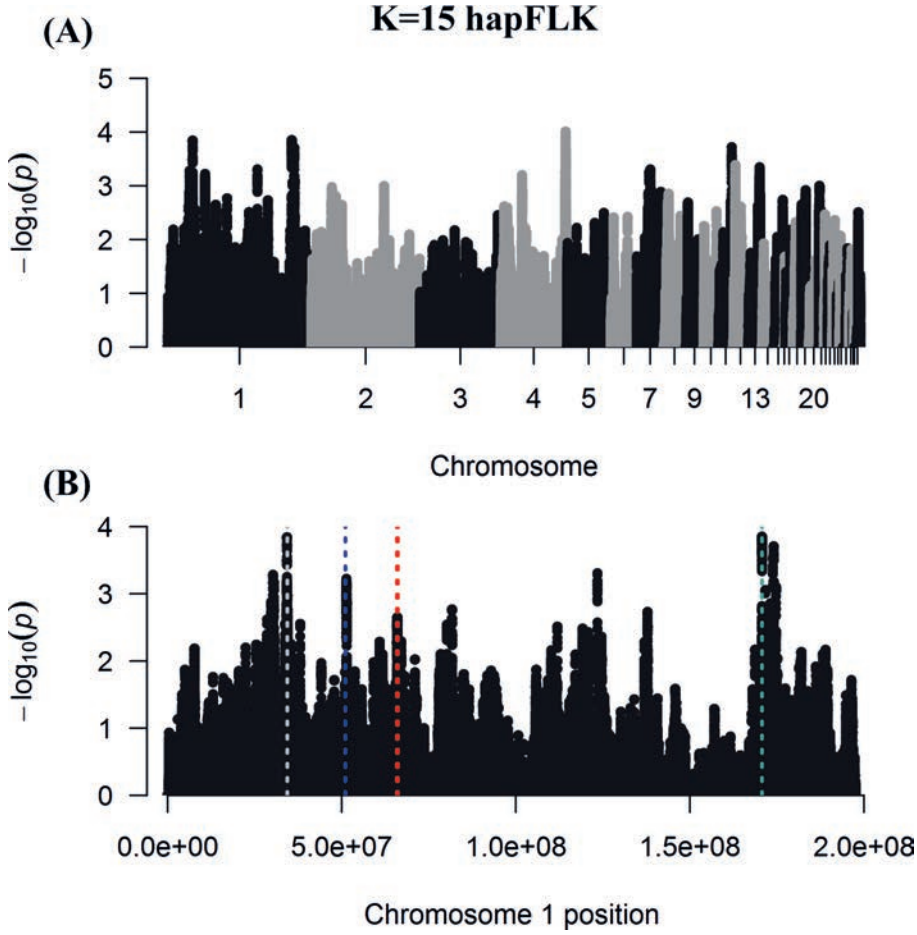

Figure S5.2 Manhattan plot of hapFLK results (A) across the genome. (B) The plot of hapFLK signals on chromosome 1 (GGA1), showing suggestive signatures of selection, highlighting genes *HMGA2* (grey), *SOX10* (blue), *SOX5* (red), as well as *gga-mir-15a* and *gga-mir-16-1* (green).

Figure S5.3 Distribution of shared identity-by-descent blocks identified between breeds (online).

Figure S5.4 The distribution of regions of rIBD across the genome, showing the relative fraction of the haplotype sharing between DrFwB and DB and that between DrFwB and DrFw (online).

Figure S5.5 Distribution of relative identity-by-descent (rIBD) on chromosome 1, showing the relative fraction of haplotype blocks shared between GrMwB and DB (positive rIBD) and GrMwB and GrMw (negative rIBD) (online).

6
General Discussion

6.1 Introduction

Body size variation occurs in many organisms. One of the extreme forms is short stature also known as dwarfism. In genomics, one ultimate goal of forward genetics is to understand a certain phenotype including the underlying genetic and genomic basis. This thesis focused on two types of dwarfism in chickens, autosomal dwarfism (adw) and bantam, aiming to reveal the genes and genetic variants underlying the reduction of growth. The results presented in this thesis have provided further insights into the complexity of the phenotypic differences, genetic heterogeneity and the human-mediated hybridization process for the dwarf/bantam. Genetic mappings have resulted in the discovery of novel candidate genes, such as *TMEM263* and *HMGA2*, which have not been reported to be responsible for dwarfism in chickens in previous studies. Heterogeneity of bantam has subsequently been found in phenotypic and genetic (in variants or haplotypes) aspects. Furthermore, I showed how the regulation of gene expression and signaling pathways may contribute to the embryonic development in bantam chickens. Finally, I addressed how population structure of Dutch chicken breeds was influenced in a complex manner by multiple factors, such as selective breeding for diverse purposes (e.g., management type, morphological characteristics or bantamization) and geographic dispersal isolation.

In this general discussion, I address the opportunities and challenges with regards to genomic analyses of dwarfism (i.e., population genomics and genetic mapping methods), the utilization of dwarf traits in poultry breeding, and the advent of biotechnology, with a special focus on the CRISP-Cas genome-editing system. First, I discuss how the genetic nature of local traditional breeds may influence the option of methodological approaches and analytical strategies employed in genomic analysis. Then, I place the findings of this thesis into an evolutionary perspective and discuss the similarity between natural and artificial selection, and how to translate the knowledge into the study of bantam crossbreeding history. I further discuss questions that remain unanswered in genetic mapping where I highlight the importance of accounting for (phenotypic and genetic) heterogeneity. To show genome-editing as an alternative solution to validate the function of the adw candidate gene, *TMEM263*, I explicitly present an assay to create a knock-out in an easier accessible animal model, zebrafish. Finally, I discuss the implementation of how to utilize dwarf phenotypes in poultry industry.

6.2 Working with local traditional breeds

In the context of animal production, local traditional or indigenous breeds have not been intensively used or commercialized for the world food production. Nevertheless, the phenotypic and genetic diversity harbored by these breeds offers a valuable opportunity to bridge the genotype-phenotype gap. Considered the historical

formation of traditional breeds, what differs from commercial lines is that these breeds have experienced a series of selection and forces that are related to various purposes. This has resulted in the subdivision of local populations that usually contain several phenotypically diverse breeds, and which can be clustered into a few subgroups. In this section, I discuss the challenges researchers have to face when working with local traditional breeds in genomic analyses, including the deconstruction of the subdivision among local traditional breeds and the determination of hybrid origin of breeds. I explicitly address these challenges by using the Dutch traditional chicken breeds as a model system.

6.2.1 Subdivided population: two clustering approaches

The essence of population subdivision is the differentiation between clusters of breeds and the convergence within clusters. In this thesis, I employed two approaches according to different rules and factors to determine the subdivided clusters in Dutch traditional chicken breeds. The first clustering approach, used in chapter 3, is based on the recorded bantam breeds used for the introgression of the bantam trait. By assessing the historical records, we identified three bantam clusters with heterogeneous ancestral sources tracing back to: *cluster 1*, Dutch bantam; *cluster 2*, Sebright and Java bantam; and *cluster 3*, bantams mainly with a South East Asian background. This information enabled us to perform the genetic mapping of bantam associated variants in heterogeneous clusters. In chapter 5, I used another clustering approach substantially exploring the population structure of Dutch traditional chicken breeds. Multiple and complex factors that influence the subdivide pattern were identified. I attributed the complex structure among breeds to management standards, geographic distribution, as well as phenotypic selection and crossbreeding. Among others, the conventional classification on the management basis enabled me to define three groups of breeds, representing (1) country fowl, (2) ornamental breeds, and (3) breeds with past-productive characteristics. I showed that some factors can be (partially) confounded with each other or outcompete one another. In particular, I hypothesize that the management-based barrier among Dutch traditional chicken breeds outcompetes the geographic barrier on a population level.

Interestingly, when comparing the two clustering approaches used in the different chapters, namely based on bantam ancestries and management standards, there is a general consensus on the subgroups that individuals are assigned to. I showed that although the two clustering approaches are based on different determinants, the assignments of breeds are still significantly correlated between the two clustering methods as shown in Figure 6.1 ($P< 2.2x10^{-16}$, spearman's correlation coefficient = 0.78). This observation suggests that the general management of Dutch neo-bantam breeds is partially confounded by the selective breeding for the bantam phenotype. This consensus highlights the complexity of a population structure made up by

multiple factors and the underlying relatedness between approaches. Although it is clear that clustering approaches to be applied strictly depend on the objectives of the study. As I highlight here, it is equally important to take into account the population substructure.

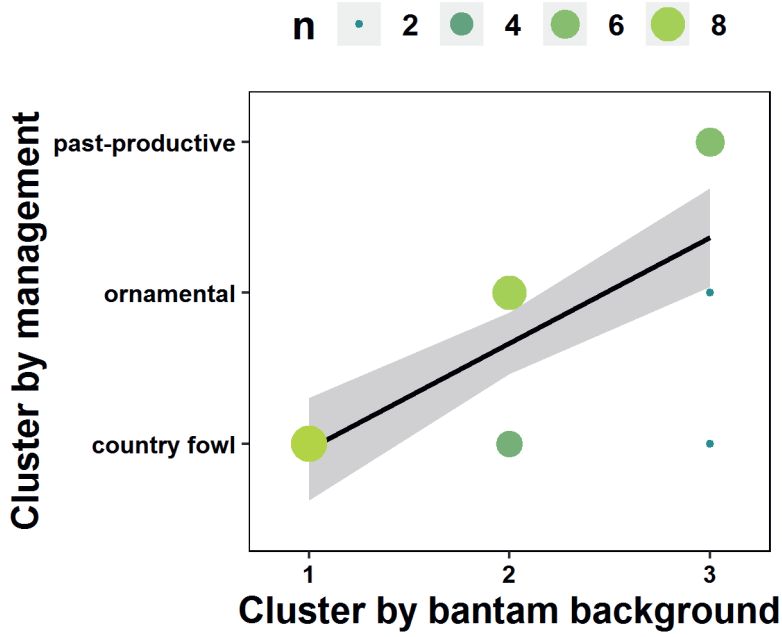

Figure 6.1 The correlation of assignments of individuals based on the two clustering approaches. The x-axis displays the three bantam clusters defined by bantam ancestries (as described in chapter 3). The y-axis shows the three clusters determined by the management standards (as described in chapter 5). The circles illustrate the assignment of breeds between two clustering approaches, with the size and color of circles demonstrating the number of breeds for the assignment.

The relationship between the factors that subdivide a population of traditional breeds are complex. Often, traditional breeds are physically separated by geographic dispersal followed by adaptation to the environment and/or human interventions (e.g., selective breeding for specific features). Subsequent adaptation or selection further enhances the (ancestral) genetic differentiation by constraining gene flow among breeds. This will eventually result in several sub-populations showing distinguishable characteristics. In genomic analysis, to detect and account for population stratification has been challenging, especially in genome-wide association studies (GWAS) (Price et al., 2010). I will more extensively discuss this aspect in section 6.4. In genomic analyses, the strategy to detect population substructure and pool related breeds into specific groups has the advantage in reducing stochastic effects compared to treating

the population as a whole. This advantage is commonly used in many genomic studies for various species (Elferink et al., 2012; Rochus et al., 2018; Liu et al., 2019). However, thanks to the complexity of the population structure, valuable biodiversity is retained in traditional breeds, which makes them excellent reservoirs of phenotypic variation (Hillel et al., 2003; Elferink et al., 2012; Bortoluzzi et al., 2020).

6.2.2 Determination of hybrid origin

In traditional breeds, it is important to understand the hybrid origin on a genomic level and to evaluate crossbreeding consequences or heterosis. Several approaches have been developed to assign origin of breeds for improving genomic prediction (Baran et al., 2012; Vandenplas et al., 2016). Likewise, determination of allelic origin of specific variants in three-way crossed pigs has been successful (Sevillano et al., 2016). However, this is different for the crossbreeding in traditional breeds. The neo-bantams usually originated from various bantam ancestries and the crossbreeding activities can date back to more than two generations ago. Moreover, repeated backcrossing was observed following the hybridization event. The introgressed genomic segments and genetic components derived from the bantam ancestries have been broken down by recombination and are largely diluted (or “flushed out”) by human-mediated backcrossing. During the backcrossing, only the bantam associated regions were positively selected for, which in turn makes these crossbred breeds interesting models to study the bantam genotype-phenotype relationship. Therefore, the genetic composition and haplotype blocks of the crossbred neo-bantams are essentially different and more diverse compared to that of commercial crossbreds.

Another challenge in determining a bantam’s origin is the elusive genetic makeup of ancestral populations (or donors). This depends on the divergence between ancestral populations and the genetic diversity of ancestries. I showed that using the genetic relatedness between breeds to determine the hybrid origin of neo-bantams may not be sufficient (chapter 3). This is probably due to the fact that the divergence time between the ancestral breeds used in bantamization is assumed to range from decades to centuries, and therefore may limit the difference between the ancestral breeds to distinguish them. Genetic diversity of ancestries is commonly seen in the recorded history of bantam introgression, I therefore demonstrated the importance of taking the ancestral genetic diversity into account. Furthermore, this diversity and variation found in the ancestral breeds are complicating the interpretation of hybrid origin through the effect such as genetic drift during bantamization; it could result in a lower estimation of haplotype sharing between the donor and recipient breeds.

Future studies to understand the hybrid origin, should take into account the genomic complexity of the traditional breeds. By incorporating multiple aspects of the complex

bantamization history, simulations like demographic modelling can be potentially improved (Silverman et al., 2018).

6.3 Evolutionary perspective on dwarf/bantam genetic studies

When studying the gene function in domesticated animals, the knowledge of evolutionary biology, particularly the information of conserved sequences, usually provides important clues about functionality. Furthermore, knowledge of evolutionary models and methodologies can be translated to study artificial selection and model demographic history of populations. In this section, I first discuss how the evolutionary conserved information can assist in predicting unknown gene function. I then address the similarity between events of naturally occurring introgression and human-mediated bantamization, and how this can be used in bantam analyses.

6.3.1 Orthologous genes and beyond

The information of conserved sequences between species has been broadly used to predict unknown gene function and to identify genomic regions that are likely to be functional, especially when there is no adequate functional annotation or phenotype associated information in the studied organism. In chapter 2, I predicted the genetic consequence of a loss-of-function mutation in a highly conserved gene, *TMEM263*, by comparing the sequences of orthologues across vertebrate species.

However, the information provided solely by orthology is insufficient in its ability to interpret the biological function, even more so for non-coding elements and sequences. Recently, a framework was developed to combine additional sources of data to supplement the prioritization of genetic variants, known as ch(icken) Combined Annotation-Dependent Depletion (chCADD) (Groß et al., 2020). I here employed the chCADD score to give prominence to the substantial amount of candidate variants identified in the bantam association studies presented in chapter 3. The distribution of the chCADD scores for the associated SNPs discovered by the meta-analysis is shown in Figure 6.2. The most significant SNP discovered by the meta-analysis is located in the first intron of the *HMGA2* gene and has a high chCADD score of 12.98. This is much higher than the chCADD score of SNPs generally found in introns (score ranging from 2.00 to 3.00) (Groß et al., 2020). In addition, there are a few variants in the candidate list that even have a higher score than this variant, but their significance P-values are all lower in the GWAS meta-analysis. This illustrates how the evolutionary conserved information combined with integrative annotations can help us in our attempt to identify likely functional variants also in the non-protein-coding

fraction of the chicken genome that subsequently can be prioritized for further functional validation.

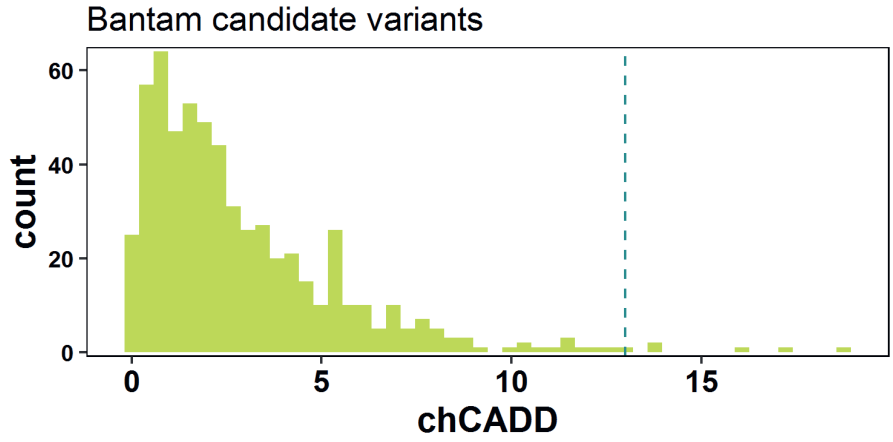

Figure 6.2 Distribution of chCADD scores for a total of 591 SNPs associated with bantam identified in the meta-GWAS. The dashed line displayed the most significant SNP in meta-analysis (NC_006088.5:g.34,326,548G>C), showing a value of 12.98.

6.3.2 Introgression model and bantamization demography

Darwin's analogy between selection under domestication and natural condition has been further developed to describe the post-domestication process leading to breed formation, i.e., selective breeding (Evans, 1984). Selective breeding with a purpose to improve the current population or to introduce desired characteristics is an implementation of modern artificial selection which was mediated in an intense and rapid manner. In chapters 2 and 5, I borrowed and translated some analyses used in evolutionary studies to assist us in understanding the bantamization history and the genetic impact. In the theory of evolution, introgression is a process of gene flow from one species to another, genetically divergent, species through hybridization, which is usually followed by the event of backcrossing and selection (Anderson and Hubricht, 1938; Harrison and Larson, 2014). The bantamization therefore resembles this process and its genetic consequences in terms of the genomic composition across the genome. Moreover, the genetic consequence of bantamization is further comparable to soft selective sweeps, since both scenarios can result in diverse haplotypes surrounding the selected loci (Novembre and Han, 2012).

These similarities support the further use of analytical approaches to study the demographic history of (neo-)bantam breeds. The backcrossing process aims to consolidate only the bantam phenotype in neo-bantams while for the remaining features neo-bantams are expected to resemble their ‘large’ fowl counterparts. When

performing phylogenetic analysis, one would expect that the neo-bantam and the normal-sized counterpart cluster together at a whole-genome level (Figure 6.3A). Whereas at the bantam related regions, as identified in the GWAS, the neo-bantams with the same bantam background should cluster together. (Figure 6.3B). In chapter 3, we used this concept of "phyloGWAS" (Pease et al., 2016; Wu et al., 2018) to study the phylogenetic topology of the bantam introgressed regions of the genome.

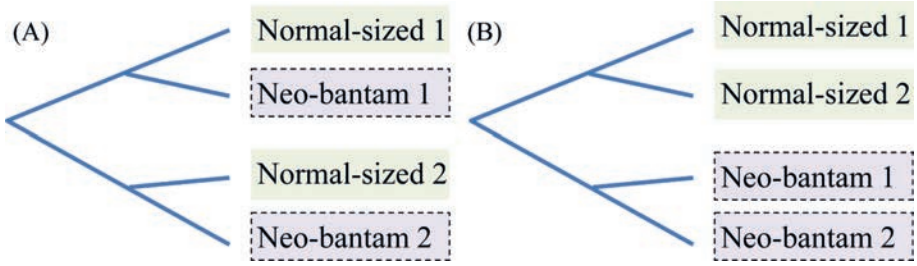

Figure 6.3 Schematic illustration of the initial concept of "phyloGWAS" in the context of bantam phenotype. Suppose there are two normal-sized breeds both with a neo-bantam counterpart, denoted by breed 1 and 2. (A) The phylogenetic tree displays the theoretical topology of breed relatedness at the whole-genome level. The normal-sized and neo-bantam breeds cluster in two groups representing the corresponding counterparts, which are similar in appearance but differ in size. (B) The phylogenetic tree displays the topology of only the bantam associated regions of the genome showing breeds that group according to the bantam phenotype.

The similarity between the natural selection and human-mediated selection enables the usage of the evolutionary theory and analytical approaches to study the breeding history and genetics of bantamization process, providing a broader perspective for understanding breed formation of (neo-)bantams. Furthermore, the bantamization process is an accessible model to reveal the influence manifested in introgression. However, in the majority of introgression studies, the focus has been on introgression events between much more divergent populations than in our study of bantams. E.g., in the study of Bosse et al. (2014), the eastern and western pig populations that were introgressed some 200 years ago, diverged approximately 1.2 Mya (Groenen et al., 2012). This is in sharp contrast to the bantamization history which is assumed to cover a range from decades to approximately a hundred years.

6.4 Genetic mapping and functional validation

The major aim of this thesis is to identify the genes and genetic variants associated with the two types of chicken dwarfisms. In this section, I discuss the optimization of the genetic mapping for a complex phenotype, with the awareness of phenotypic and genetic heterogeneity. Moreover, I address validation approaches employed to study the biological function of the effect of genetic variants post genetic mapping. There are different ways to perform a validation and here I specifically discuss a genome-

editing experiment using CRISPR-Cas9 to study the gene function of the *TMEM263* gene by producing a knock-out in zebrafish.

6.4.1 Accounting for phenotypic heterogeneity

The performance of genetic mapping approaches, such as GWAS, depends on a number of factors (Andersson and Georges, 2004; Visscher et al., 2017; Schaid et al., 2018), one of which is the underlying biology (e.g., the number of causative variants and phenotypic heterogeneity). Although the heterogeneity of complex traits within domesticated animals is expected to be lower relative to more outbred populations like human (Andersson and Georges, 2004), different subtypes of the bantam phenotype exist among Dutch breeds shown in chapter 3 and 4. Such a set of varied subtypes within a breed suggests phenotypic heterogeneity. This heterogeneity is mostly caused by heterogeneous genetic factors, derived from unidentified different ancestries, or simply by chance events like drift (Evangelou and Ioannidis, 2013; Korte and Farlow, 2013). The difficulty of disentangling this heterogeneity is usually due to a weak definition of the phenotype, which applies to, not only polygenic, but sometimes also monogenetic traits (Evangelou and Ioannidis, 2013).

Accounting for heterogeneity is especially important when studying complex traits or diseases, such as growth or susceptibility to Salmonella infection (te Pas et al., 2012; Xu et al., 2013; Johnsson et al., 2018). These polygenic phenotypes, measured by continuous indexes, harbor a multitude of loci and alleles within each locus that can cumulatively determine the phenotype (Andersson and Georges, 2004). The polygenic nature of complex traits has been significantly characterized by large-scale meta-analyses incorporating multiple studies, thereby increasing the power in identifying genuine associations (Evangelou and Ioannidis, 2013; Magosi et al., 2017). Although the biological mechanisms underlying monogenic traits are considered to be less complex, sometimes to refine the (sub)phenotypes may help to enhance the power to identify the underlying molecular cause.

6.4.2 Genetic heterogeneity in gene expression

The genotype-to-phenotype model essentially involves the expression of genes. It has been shown that failing to incorporate informative heterogeneity may influence the power and rigor of expression studies (Leek and Storey, 2007; Sasaki et al., 2018). In chapter 4, I showed two important variables that can influence gene expression analyses of bantams. First, I demonstrated that sex has a significant effect on the gene expression between individuals with contrasting body sizes. For instance, at embryonic stage E13, I showed that the expression of the *IHH* (Indian hedgehog) gene is much higher in male than in females independently of the body size. Second, genetic heterogeneity was displayed in the differentially expressed genes identified between different bantam breeds. This suggests that in gene expression studies, discovering

informative heterogeneity may reveal interesting biological mechanisms, e.g., the precise effect on phenotype (Zeggini and Ioannidis, 2009). Such mechanisms may function through complex signaling pathways (e.g., how FGF, BMP and IHH signaling pathways interactively regulate the chondrocyte proliferation contributing to musculoskeletal development).

Negating such heterogeneous associations may hamper and reduce the optimal power in genetic mapping. However, how much of the heterogeneity is truly informative and reflects the biological facts or just results from errors and biases between datasets, needs to be answered carefully (Zeggini and Ioannidis, 2009). Moreover, reducing phenotypic heterogeneity does not necessarily increase genetic homogeneity (Chaste et al., 2015).

6.4.3 Validation of causative candidate variants

A crucial step in understanding the genotype-phenotype mechanism is the post GWAS validation of associated genes and genetic variants. Because of the refined quality of the chicken genome assembly (GRCg6a) and the advance of variant effect prediction methods (e.g., VEP, SIFT, and CADD), the whole-genome sequence data now allows us to verify and predict the function of genetic variants at locations across almost the complete genome. In chapter 2 and 3, the genetic variants associated with dwarf phenotypes were predicted for its functional importance based on the annotation of the genome. As discussed in section 6.3.1, the high impact of a nonsense mutation in the gene coding for a transmembrane protein (*TMEM263*) is much easier to predict than that of non-protein coding candidates, such as the intronic or upstream variants of *HMGA2*. Validations targeting specific loci might consist of laboratory experiments (e.g., gene expression assays, western blots, or reproduce variants in animal models) or of in silico predictions (e.g., protein modelling) (Hou and Zhao, 2013). One particular powerful approach is reproducing the causative variants in animal models e.g., by gene knock-in, knock-down or knock-out experiments in mice and other model organisms using tools, such as RNA interference and genome-editing. I specifically focus on using the genome-editing tool, CRISPR-Cas (clustered regularly interspaced short palindromic repeats-CRISPR associated protein) systems (Terns and Terns, 2011; Wiedenheft et al., 2012; Cong et al., 2013; Mali et al., 2013), to generate knock-outs in a model animal. Because of its features of time-efficiency, low cost and ease of customization, the CRISPR-Cas system is used broadly to modify certain regions of the genome and cells of diverse organisms (Wang et al., 2016). Creating a customized guiding RNA, enables localizing and targeting specific genomic regions to obtain a functional understanding of the genome, theoretically, on a single base level.

6.4.3.1 Cross species validation: an attempt to knock-out TMEM263 in zebrafish

In this section, I discuss the genome-editing experiment we performed by using CRISPR-Cas9 to validate the gene function of *TMEM263* in zebrafish. This is especially useful in the case of the autosomal dwarfism (adw) demonstrated in chapter 2. Approximately twenty years ago, the adw chickens were discarded and abandoned, thereby hampering the creation of the adw trait and the direct validation of the consequence of the nonsense mutation (Trp59*) in chicken. Therefore, a gene editing experiment was attempted to create a dysfunctional TMEM263 protein in zebrafish (see **Supplementary file**). Although a mutant knock-out zebrafish was not successfully created, I nevertheless am able to present a workflow in **Supplementary file** and discuss the challenges encountered to optimize future attempts to do so (Figure 6.4).

Figure 6.4 Experimental setup of the genome editing in zebrafish. From left to right, (1) the setup of experimental animals; (2) microinjection; (3) zebrafish embryos and larvae under a microscope.

To validate the gene function potentially associated with a phenotype or disease, zebrafish has been an ideal model organism being used increasingly in experiments (Hwang et al., 2013; Varshney et al., 2013; Li et al., 2016), including CRISPR-Cas9 method. This can only be applied when the gene of interest shows a high degree of conservation or identity on DNA and protein level between zebrafish and the target organism. For the *TMEM263* genes in chicken and zebrafish, that appeared to be the case. The identity of the orthologous *TMEM263* genes between chicken and zebrafish is around 72.4% (of DNA sequences) and 74.1% (of protein sequences), which enabled us to design the assay targeting the exons of the adw candidate gene *TMEM263*. Nevertheless, the divergence between chicken and zebrafish is ~400 Mya (Zhang et al., 2018) and it is unknown whether the gene has the same function in these two species. This might hamper the success rate to produce a similar dwarf phenotype in zebrafish as in chicken.

6.4.3.2 Efficiency of CRISPR-Cas systems

In general, the efficiency of the editing depends largely on the features of the single-guide RNA (sgRNA) as well as on the property of the genomic context (Hiranniramol

et al., 2020). This may be a possible explanation for the lack of success in our genome editing experiment. I will address the following three challenges encountered in a CRISPR-Cas assay, (1) the efficiency of the target sgRNA; (2) the mosaic and unpredictable mutant sequence; (3) the potential lethal effect of an edit in the orthologous gene in another species.

First of all, one of the challenges for the effective application of CRISPR-Cas9 is to carefully design the sgRNA, which contains a complementary sequence to anchor the target region in the genome. Three sgRNAs were designed and employed in our assay, however, not all sgRNAs exhibit similar levels of efficiency at introducing on-target mutation. In short, the sequence and structural features of sgRNAs, including (position-specific) nucleotide composition and the folding of RNA, are usually considered for optimum affinity and specificity (Hiranniramol et al., 2020). Moreover, the epigenomic properties of the target genome (e.g., open chromatin structure) affecting accessibility and efficiency of the mutagenesis (Wu et al., 2014; Horlbeck et al., 2016; Chuai et al., 2018; Uusi-Mäkelä et al., 2018).

The second challenge is the identification of the mutant sequence post editing. The challenge relates to the DNA non-homologous end joining (NHEJ) repair mechanism in a gene knock-out. NHEJ has long been considered error-prone which triggers almost random sequence alterations at the breakpoint, resulting in insertions, deletions or point mutations (Bétermier et al., 2014; Guo et al., 2018). The resulting mutant sequence is not predictable in knock-out assays, thus in order to determine the set of desired mutations for subsequent analysis, it is necessary to test the sequence surrounding the target region. One additional challenge is the accurate identification of mosaic mutant sequences (i.e., ambiguous base calls spanning the target region).

Finally, the third challenge, is the potential lethality or affected viability caused by the induced mutation. The lethal effect may be caused by the sgRNA (Shin et al., 2017), the loss-of-function effect of the gene of interest (Wang et al., 2016), or even by the physical damage caused by microinjection.

To date, various in silico tools have been proposed to predict the optimized sgRNA design to maximize efficiency and minimize off-target effects avoiding excessive experimental screening. However, our understanding of accurately predicting optimal genome-editing is still incomplete. Therefore, it is desired to screen a considerable number of sgRNAs to increase the possibility of a highly efficient CRISPR-Cas design.

6.5 Utilization of dwarf traits in poultry industry

Animal breeding is currently facing changes and challenges that require commercial breeding to become more sustainable and more animal welfare friendly. Introducing

the dwarf trait into commercial poultry breeding can be a valuable option to overcome some of the problems in breeding due to its advantages regarding feed efficiency and animal well-being. For a recessive dwarf trait, incorporating one or multiple dwarf lines in a commercial four-way crossing strategy can still allow the final offspring to be unaffected in terms of both body size and viability. Figure 6.5 is showing one of the different options of introducing dwarfism in commercial broiler breeding, where the roosters of the dam line are kept dwarf. Similarly, one could even make use of (two or more) different recessive variants or traits in parallel in the core lines without affecting the size of the final offspring. Alternatively, dwarfism can be introduced into a layer breeding system even with the final layer line producing smaller sized eggs which has economic benefits and has been accepted by the market. In China, the initial development of a sex-linked dwarf brown layer line named “Nongda No.3” has been promoted to the market holding with at least a 5% market share (Zhang et al., 2005; Ning et al., 2013). The wide interest for small birds is the merit saved from feed costs which compensates the reduced income from egg production (Ning et al., 2013). The reduced feed consumption may lower the ecological footprint, therefore dwarf animals can provide a sustainable alternative under the increased global food crisis (Food Security Information Network, 2020).

However, one of the concerns to use dwarf/bantam is that breeders need to adjust the existing facilities and management for the small-size animals (e.g., in commercial settings). In addition, studies about using dwarf poultry in industry have been mainly limited to the sex-linked recessive gene (Merat, 1984). This, most likely, because it is the only known dwarf mutation(s) that reduces the size without the cost of viability or production performance (Hutt, 1959; Cole, 2000). A comprehensive understanding of the performance (i.e., the economic modelling of the margin rate) and biological characteristics (including the side-effect) of additional dwarf phenotypes is needed to better exploit, conserve, and utilize dwarf chickens.

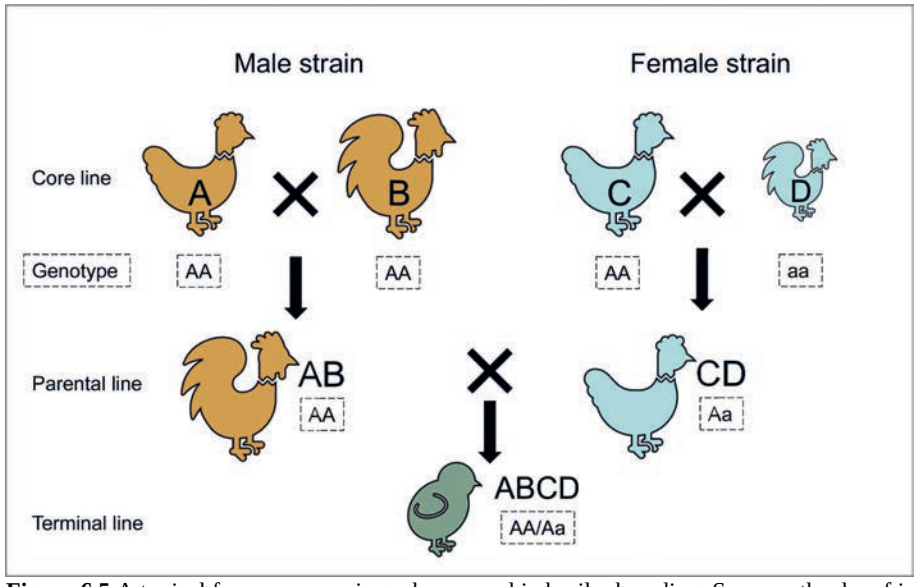

Figure 6.5 A typical four-way crossing scheme used in broiler breeding. Suppose the dwarf is of autosomal recessive inheritance, the 'A' stands for normal-sized allele, the 'a' allele stands for the dwarf allele. The terminal line is from the cross of male (AxB) and female (CxD) crossed strains.

6.5.1 Introducing a new phenotype into another population

There are multiple applications to introduce a dwarf phenotype into a population. Here I discuss the opportunities and challenges in the rather traditional interbreeding approach as well as by genome-editing. First of all, the interbreeding approach is performed through crossbreeding and the subsequent selection of desired characteristics, which has been successfully used in plants and animal breeding. In addition, the utilization of genomic information (such as genomic selection) has considerably reduced the breeding interval compared to the conventional breeding solely based on phenotypic selection (Cabrera-Ponce et al., 2018; Nadeem et al., 2018). Nevertheless, the selection efficiency regarding the time is still substantial when extensive backcrossing is required. When introducing a dwarf trait into an existing breed, it can take many generations of backcrossing to reduce other loci that may hitchhike with loci of interest. An experimental study to introduce a dominant monogenic trait, blue eggshell, from indigenous breeds to a high performing White Leghorn chickens started in 2016 (http://www.imageh2020.eu/). In this model, backcrossing and intercrossing have been performed for four generations. The still ongoing study suggests that this interbreeding approach is powerful, but is time consuming and at a considerable cost. The backcrossing process needs to be monitored every generation by genotyping or sequencing to ensure the frequency of

the introduced mutation and to decrease the genome content of the undesired donor line.

A faster way of introducing a new phenotype is by genome-editing. Precisely modifying genomic regions and introducing bantam alleles using CRISPR-Cas offers a new opportunity to accelerate the rate of breeding for dwarfisms. In the traditional intercrossing process, repeated backcrossing often results in a population bottleneck. The resulting hitchhiking and genetic drift effects can potentially introduce the risk of genomic inbreeding and increased genetic load (Bosse, 2019; Bortoluzzi et al., 2020). I show this hitchhiking effect in chapter 5 where a multitude of genomic regions in the genome of the recipients is assumed to be irrelevant to the bantam phenotype. Recent studies have focused on how genome-editing techniques like CRISPR-Cas can change traditional animal breeding. Bastiaansen et al. (2018) compared scenarios of genomic selection in combination with or without genome-editing with the aim to increase the desired allele frequency of a monogenic trait (polledness). They showed that the combination of genome-editing and genomic selection can speed up the selection for a monogenic trait in the population, thereby potentially revolutionizing the implementation of genetic improvement of livestock and other species. When comparing the two approaches, genome-editing is particularly valuable for small populations like Dutch chicken breeds. However, there is a trade-off between the benefits of shortening the time to fix a desired allele and the number of animals to be edited. Its potential role as a “game changer” in animal breeding depends on future validations on the costs and the polygenic nature of the economic trait of interest. In addition, ethical regulations and animal welfare of genome-edited livestock have not reached a global consensus, also limiting its widened application.

6.6 Concluding remarks

The small size of the chicken genome provides many opportunities for genomic studies. With this thesis, I focused on the topic of dwarfism in chickens. I investigated the genetic backgrounds of the autosomal dwarfism and the bantam phenotype. Using resources of Dutch traditional chicken breeds, I presented a genomic perspective of how human-mediated breeding activities consequently influence the population structure. These findings are valuable to comprehend the genetic basis underlying growth and body size variation in animals, which shows the opportunities for detecting and using dwarfism on a broader scale.

Reference

Anderson, E., and Hubricht, L. (1938). Hybridization in Tradescantia. III. The Evidence for Introgressive Hybridization. *Am. J. Bot.* 25, 396. doi:10.2307/2436413.

Andersson, L., and Georges, M. (2004). Domestic-animal genomics: Deciphering the genetics of complex traits. *Nat. Rev. Genet.* 5, 202–212. doi:10.1038/nrg1294.

Baran, Y., Pasaniuc, B., Sankararaman, S., Torgerson, D. G., Gignoux, C., Eng, C., et al. (2012). Fast and accurate inference of local ancestry in Latino populations. *Bioinformatics* 28, 1359–1367. doi:10.1093/bioinformatics/bts144.

Bastiaansen, J. W. M., Bovenhuis, H., Groenen, M. A. M., Megens, H. J., and Mulder, H. A. (2018). The impact of genome editing on the introduction of monogenic traits in livestock. *Genet. Sel. Evol.* 50, 18. doi:10.1186/s12711-018-0389-7.

Bétermier, M., Bertrand, P., and Lopez, B. S. (2014). Is Non-Homologous End-Joining Really an Inherently Error-Prone Process? *PLoS Genet.* 10, e1004086. doi:10.1371/journal.pgen.1004086.

Bortoluzzi, C., Bosse, M., Derks, M. F. L., Crooijmans, R. P. M. A., Groenen, M. A. M., and Megens, H. J. (2020). The type of bottleneck matters: Insights into the deleterious variation landscape of small managed populations. *Evol. Appl.* 13, 330–341. doi:10.1111/eva.12872.

Bosse, M. (2019). No "doom" in chicken domestication? *PLoS Genet.* 15, e1008089. doi:10.1371/journal.pgen.1008089.

Bosse, M., Megens, H. J., Frantz, L. A. F., Madsen, O., Larson, G., Paudel, Y., et al. (2014). Genomic analysis reveals selection for Asian genes in European pigs following human-mediated introgression. *Nat. Commun.* 5, 4392. doi:10.1038/ncomms5392.

Cabrera-Ponce, J. L., Valencia-Lozano, E., and Trejo-Saavedra, D. L. (2018). "Genetic modifications of corn," in *Corn: Chemistry and Technology, 3rd Edition*, 43–85. doi:10.1016/B978-0-12-811971-6.00003-6.

Chaste, P., Klei, L., Sanders, S. J., Hus, V., Murtha, M. T., Lowe, J. K., et al. (2015). A genome-wide association study of autism using the Simons simplex collection: Does reducing phenotypic heterogeneity in autism increase genetic homogeneity? *Biol. Psychiatry* 77, 775–784. doi:10.1016/j.biopsych.2014.09.017.

Chuai, G., Ma, H., Yan, J., Chen, M., Hong, N., Xue, D., et al. (2018). DeepCRISPR: Optimized CRISPR guide RNA design by deep learning. *Genome Biol.* 19. doi:10.1186/s13059-018-1459-4.

Cole, R. K. (2000). An autosomal dwarfism in the domestic fowl. *Poult. Sci.* 79, 1507–1516. doi:10.1093/ps/79.11.1507.

Cong, L., Ran, F. A., Cox, D., Lin, S., Barretto, R., Habib, N., et al. (2013). Multiplex genome engineering using CRISPR/Cas systems. *Science (80-.).* 339, 819–823. doi:10.1126/science.1231143.

Elferink, M. G., Megens, H. J., Vereijken, A., Hu, X., Crooijmans, R. P. M. A., and Groenen, M. A. M. (2012). Signatures of selection in the genomes of commercial and non-commercial chicken breeds. *PLoS One* 7, e32720. doi:10.1371/journal.pone.0032720.

Evangelou, E., and Ioannidis, J. P. A. (2013). Meta-analysis methods for genome-wide association studies and beyond. *Nat. Rev. Genet.* 14, 379–389. doi:10.1038/nrg3472.

Evans, L. T. (1984). Darwin's use of the analogy between artificial and natural selection. *J. Hist. Biol.* 17, 113–140. doi:10.1007/BF00397504.

Food Security Information Network (2020). Global report on food crises 2020. Available at: https://www.wfp.org/publications/2020-global-report-food-crises.

Groenen, M. A. M. M., Archibald, A. L., Uenishi, H., Tuggle, C. K., Takeuchi, Y., Rothschild, M. F., et al. (2012). Analyses of pig genomes provide insight into porcine demography and evolution. *Nature*

491, 393–398. doi:10.1038/nature11622.

Groß, C., Bortoluzzi, C., de Ridder, D., Megens, H.-J., Groenen, M. A. M., Reinders, M., et al. (2020). Prioritizing sequence variants in conserved non-coding elements in the chicken genome using chCADD. *PLOS Genet.* 16, e1009027. doi:10.1371/journal.pgen.1009027.

Guo, T., Feng, Y. L., Xiao, J. J., Liu, Q., Sun, X. N., Xiang, J. F., et al. (2018). Harnessing accurate non-homologous end joining for efficient precise deletion in CRISPR/Cas9-mediated genome editing. *Genome Biol.* 19. doi:10.1186/s13059-018-1518-x.

Harrison, R. G., and Larson, E. L. (2014). Hybridization, introgression, and the nature of species boundaries. *J. Hered.* 105, 795–809. doi:10.1093/jhered/esu033.

Hillel, J., Groenen, M. A. M., Tixier-Boichard, M., Korol, A. B., David, L., Kirzhner, V. M., et al. (2003). Biodiversity of 52 chicken populations assessed by microsatellite typing of DNA pools. 35. Available at: http://www.gsejournal.org/content/35/6/533 [Accessed April 30, 2018].

Hiranniramol, K., Chen, Y., and Wang, X. (2020). "CRISPR/Cas9 Guide RNA Design Rules for Predicting Activity," in *Methods in Molecular Biology* (Humana Press Inc.), 351–364. doi:10.1007/978-1-0716-0290-4_19.

Horlbeck, M. A., Witkowsky, L. B., Guglielmi, B., Replogle, J. M., Gilbert, L. A., Villalta, J. E., et al. (2016). Nucleosomes impede cas9 access to DNA in vivo and in vitro. *Elife* 5. doi:10.7554/eLife.12677.

Hou, L., and Zhao, H. (2013). A review of post-GWAS prioritization approaches. *Front. Genet.* 4, 280. doi:10.3389/fgene.2013.00280.

Hutt, F. B. (1959). Sex-linked dwarfism in the fowl. *J. Hered.* 50, 209–221. doi:10.1093/oxfordjournals.jhered.a106909.

Hwang, W. Y., Fu, Y., Reyon, D., Maeder, M. L., Tsai, S. Q., Sander, J. D., et al. (2013). Efficient genome editing in zebrafish using a CRISPR-Cas system. *Nat. Biotechnol.* 31, 227–9. doi:10.1038/nbt.2501.

Johnsson, M., Henriksen, R., Höglund, A., Fogelholm, J., Jensen, P., and Wright, D. (2018). Genetical genomics of growth in a chicken model. *BMC Genomics* 19, 72. doi:10.1186/s12864-018-4441-3.

Korte, A., and Farlow, A. (2013). The advantages and limitations of trait analysis with GWAS: A review. *Plant Methods* 9. doi:10.1186/1746-4811-9-29.

Leek, J. T., and Storey, J. D. (2007). Capturing heterogeneity in gene expression studies by surrogate variable analysis. *PLoS Genet.* 3, 1724–1735. doi:10.1371/journal.pgen.0030161.

Li, M., Zhao, L., Page-McCaw, P. S., and Chen, W. (2016). Zebrafish Genome Engineering Using the CRISPR–Cas9 System. *Trends Genet.* 32, 815–827. doi:10.1016/j.tig.2016.10.005.

Liu, L., Bosse, M., Megens, H. J., Frantz, L. A. F., Lee, Y. L., Irving-Pease, E. K., et al. (2019). Genomic analysis on pygmy hog reveals extensive interbreeding during wild boar expansion. *Nat. Commun.* 10. doi:10.1038/s41467-019-10017-2.

Magosi, L. E., Goel, A., Hopewell, J. C., and Farrall, M. (2017). Identifying systematic heterogeneity patterns in genetic association meta-analysis studies. *PLOS Genet.* 13, e1006755. doi:10.1371/journal.pgen.1006755.

Mali, P., Yang, L., Esvelt, K. M., Aach, J., Guell, M., DiCarlo, J. E., et al. (2013). RNA-guided human genome engineering via Cas9. *Science (80-.).* 339, 823–826. doi:10.1126/science.1232033.

Merat, P. (1984). The sex-linked dwarf gene in the broiler chicken industry. *Worlds. Poult. Sci. J.* 40, 10–18. doi:10.1079/wps19840002.

Nadeem, M. A., Nawaz, M. A., Shahid, M. Q., Doğan, Y., Comertpay, G., Yıldız, M., et al. (2018). DNA molecular markers in plant breeding: current status and recent advancements in genomic selection and genome editing. *Biotechnol. Biotechnol. Equip.* 32, 261–285. doi:10.1080/13102818.2017.1400401.

Ning, Z., Wu, C., Yang, N., and Zhang, Q. (2013). Breeding of Grain-saving Small Laying Hens--Nongda No . 3 Layer. *J. Agric. Biotechnol.* 21, 753–756. doi:10.3969/j.issn.1674-7968.2013.06.015.

Novembre, J., and Han, E. (2012). Human population structure and the adaptive response to pathogen-induced selection pressures. *Philos. Trans. R. Soc. B Biol. Sci.* 367, 878–886. doi:10.1098/rstb.2011.0305.

Pease, J. B., Haak, D. C., Hahn, M. W., and Moyle, L. C. (2016). Phylogenomics Reveals Three Sources of Adaptive Variation during a Rapid Radiation. *PLoS Biol.* 14, e1002379. doi:10.1371/journal.pbio.1002379.

Price, A. L., Zaitlen, N. A., Reich, D., and Patterson, N. (2010). New approaches to population stratification in genome-wide association studies. *Nat. Rev. Genet.* 11, 459–463. doi:10.1038/nrg2813.

Rochus, C. M., Tortereau, F., Plisson-Petit, F., Restoux, G., Moreno-Romieux, C., Tosser-Klopp, G., et al. (2018). Revealing the selection history of adaptive loci using genome-wide scans for selection: An example from domestic sheep. *BMC Genomics* 19. doi:10.1186/s12864-018-4447-x.

Sasaki, E., Frommlet, F., and Nordborg, M. (2018). GWAS with heterogeneous data: Estimating the fraction of phenotypic variation mediated by gene expression data. *G3 Genes, Genomes, Genet.* 8, 3059–3068. doi:10.1534/g3.118.200571.

Schaid, D. J., Chen, W., and Larson, N. B. (2018). From genome-wide associations to candidate causal variants by statistical fine-mapping. *Nat. Rev. Genet.* 19, 491–504. doi:10.1038/s41576-018-0016-z.

Sevillano, C. A., Vandenplas, J., Bastiaansen, J. W. M., and Calus, M. P. L. (2016). Empirical determination of breed-of-origin of alleles in three-breed cross pigs. *Genet. Sel. Evol.* 48, 1–12. doi:10.1186/s12711-016-0234-9.

Shin, H. Y., Wang, C., Lee, H. K., Yoo, K. H., Zeng, X., Kuhns, T., et al. (2017). CRISPR/Cas9 targeting events cause complex deletions and insertions at 17 sites in the mouse genome. *Nat. Commun.* 8. doi:10.1038/ncomms15464.

Silverman, E., Bijak, J., Courgeau, D., Franck, R., and Silverman, E. (2018). "Modelling in Demography: From Statistics to Simulations," in *Methodological Investigations in Agent-Based Modelling* (Springer International Publishing), 167–187. doi:10.1007/978-3-319-72408-9_9.

te Pas, M. F. W., Hulsegge, I., Schokker, D., Smits, M. A., Fife, M., Zoorob, R., et al. (2012). Meta-analysis of Chicken - Salmonella infection experiments. *BMC Genomics* 13, 146. doi:10.1186/1471-2164-13-146.

Terns, M. P., and Terns, R. M. (2011). CRISPR-based adaptive immune systems. *Curr. Opin. Microbiol.* 14, 321–327. doi:10.1016/j.mib.2011.03.005.

Uusi-Mäkelä, M. I. E., Barker, H. R., Bäuerlein, C. A., Häkkinen, T., Nykter, M., and Rämet, M. (2018). Chromatin accessibility is associated with CRISPR-Cas9 efficiency in the zebrafish (Danio rerio). *PLoS One* 13, e0196238. doi:10.1371/journal.pone.0196238.

Vandenplas, J., Calus, M. P. L., Sevillano, C. A., Windig, J. J., and Bastiaansen, J. W. M. (2016). Assigning breed origin to alleles in crossbred animals. *Genet. Sel. Evol.* 48, 61. doi:10.1186/s12711-016-0240-y.

Varshney, G. K., Lu, J., Gildea, D. E., Huang, H., Pei, W., Yang, Z., et al. (2013). A large-scale zebrafish gene knockout resource for the genome-wide study of gene function. *Genome Res.* 23, 727–735. doi:10.1101/gr.151464.112.

Visscher, P. M., Wray, N. R., Zhang, Q., Sklar, P., McCarthy, M. I., Brown, M. A., et al. (2017). 10 Years of GWAS Discovery: Biology, Function, and Translation. *Am. J. Hum. Genet.* 101, 5–22. doi:10.1016/j.ajhg.2017.06.005.

Wang, H., La Russa, M., and Qi, L. S. (2016). CRISPR/Cas9 in Genome Editing and beyond. *Annu. Rev. Biochem.* 85, 227–264. doi:10.1146/annurev-biochem-060815-014607.

Wiedenheft, B., Sternberg, S. H., and Doudna, J. A. (2012). RNA-guided genetic silencing systems in

bacteria and archaea. *Nature* 482, 331–338. doi:10.1038/nature10886.

Wu, M., Kostyun, J. L., Hahn, M. W., and Moyle, L. C. (2018). Dissecting the basis of novel trait evolution in a radiation with widespread phylogenetic discordance. *Mol. Ecol.* 27, 3301–3316. doi:10.1111/mec.14780.

Wu, X., Scott, D. A., Kriz, A. J., Chiu, A. C., Hsu, P. D., Dadon, D. B., et al. (2014). Genome-wide binding of the CRISPR endonuclease Cas9 in mammalian cells. *Nat. Biotechnol.* 32, 670–676. doi:10.1038/nbt.2889.

Xu, Z., Nie, Q., and Zhang, X. (2013). Overview of Genomic Insights into Chicken Growth Traits Based on Genome- Wide Association Study and microRNA Regulation. *Curr. Genomics* 14, 137–146. doi:10.2174/1389202911314020006.

Zeggini, E., and Ioannidis, J. P. A. A. (2009). Meta-analysis in genome-wide association studies. *Pharmacogenomics* 10, 191–201. doi:10.2217/14622416.10.2.191.

Zhang, L. C., Ning, Z. H., Xu, G. Y., Hou, Z. C., and Yang, N. (2005). Heritabilities and genetic and phenotypic correlations of egg quality traits in brown-egg dwarf layers. *Poult. Sci.* 84, 1209–1213. doi:10.1093/ps/84.8.1209.

Zhang, Q.-L., Zhang, G.-L., Yuan, M.-L., Dong, Z.-X., Li, H.-W., Guo, J., et al. (2018). A Phylogenomic Framework and Divergence History of Cephalochordata Amphioxus. *Front. Physiol.* 9, 1833. doi:10.3389/fphys.2018.01833.

Supplementary file

Gene function validation using CRISPR-Cas9 editing: an attempt to knock-out *TMEM263* in zebrafish

1. Introduction

The advent of genome-editing techniques has greatly changed the field of molecular biology and functional genomics. CRISPR-Cas (clustered regularly interspaced short palindromic repeats-CRISPR-associated protein) systems are involved in the adaptive immunity of bacteria and archaea (Terns and Terns, 2011; Wiedenheft et al., 2012), which now has been making breakthroughs as a convenient genome-editing tool (Cong et al., 2013; Mali et al., 2013). Of many applications of CRISPR-Cas, one is to study the gene function by either disrupting target sequences or introducing desired genetic variants. Creating a gene knock-out in zebrafish is a powerful platform to validate candidate genes and genetic variants identified in other less accessible organisms (Hwang et al., 2013; Varshney et al., 2013).

The aim of this report is to present our design of a genome-editing assay using CRISPR-Cas9 mediated knock-out in zebrafish. Our objective is to perform a cross-species validation in order to understand the function of a causative loss-of-function mutation that was suggested to alter body growth and to affect the development in autosomal dwarf chickens (Wu et al., 2018). We will use it as an example to show the following aspects in designing and performing a genome-editing assay in zebrafish:1) design the target guide-RNA; 2) the microinjection; 3) evaluate the phenotype; 4) analyze the sequence data.

2. Methods

2.1 Design and create the target guide-RNA

In this article, we present an experimental strategy for designing and performing genome-editing to generate a knock-out in zebrafish using the CRISPR-Cas9 system. The experimental design and setup are based on the protocol provided by Sylvia Brugman (Wageningen University& Research) modified from Den Hertog (2017). Note that our aim is to verify gene function by creating a cross-species genome editing, therefore, it is essential to first examine the conservation of the gene in terms of the DNA and protein sequence identity. In this study, the target gene encoding transmembrane 263 (*TMEM263)* is a highly conserved gene among many vertebrate species. For the purpose of validating the function of the gene, we designed three sgRNA oligos (named oligo 17, 31, and 33, respectively) targeting different exons of *TMEM263* in zebrafish. The target sequence for the three oligos is presented in Figure 1.

We determined the targeting sites of the gene using the online tool, CHOP-CHOP (https://chopchop.cbu.uib.no/). The guide target site sequence is preferably around 20 bp and located at the beginning of a gene or exon. We ordered the specific oligos that used to transcribe to guide RNA, containing the following sequences: T7 promotor sequence, the guide target oligo without the PAM site, and the oligo overlapping with the constant oligo (Figure 2). These three sequences are located adjacent to each other. In order to generate the single-guide RNA (sgRNA), annealing and extension of guide RNA with the constant oligo for the double stranded template was performed in a single step. The protocol for the extension reaction is presented in Table 1. Cleaning up of the reaction product is performed with 2 µl of ExoSAP at 37 ℃ for 15 min to remove primers and dNTP, this reaction is stopped by incubation at 80℃ for 15 min (deactivation of ExoSAP-It enzymes). Next, using the cleaned double stranded sequence as the template, we transcribed the sgRNA by using the in vitro transcription single stranded template (T7 kit from Ambion). The single stranded RNA is purified with ammonium acetate and ethanol. The final product of sgRNA oligo was stored in aliquots of 1 µl at a concentration of 600 ng/µl at -80°C. Note that for the final injection, the desired concentration of the RNA is 100 ng/µl in a volume of 6 µl, together with 4 ng Cas protein.

2.2 Microinjection

1. One day before the injection, we set up the experiment by preparing a set of one female and (usually two to three) male adult zebrafish maintained under the standard protocol by WUR. We prepared them in a single breeding tank with a nest as a divider that the males stay above the nest while the female was separated below.
2. We prepared the following solutions for the injection in low protein binding tubes: 1 µl prepared sgRNA oligo (600 ng/µl), 3.9 µl KCl, 0.8 µl Cas9 (5 ng/µl) (product: IDT Alt-R s.p. Cas9 nuclease V3), and 0.3 µl phenol red for the visualization during the injection. Solutions were mixed and incubated at 37 °C for 5 min. To avoid precipitation, we did not put the solution back on ice.
3. Embryos were obtained from natural spawning, and we collected them around 15 min post mating.
4. Load the injection solution and calibrate the approximate volume under the microscope. We carefully adjusted the position of the embryo and injected the 1 nl solution in the cell when the embryos are at the one-cell stage. It is desired to inject into the cell or in the yolk where it is extremely close to the cell. Make sure the injection is conducted when the embryos are at the one-cell developmental stage to avoid mosaicism (Figure 3).

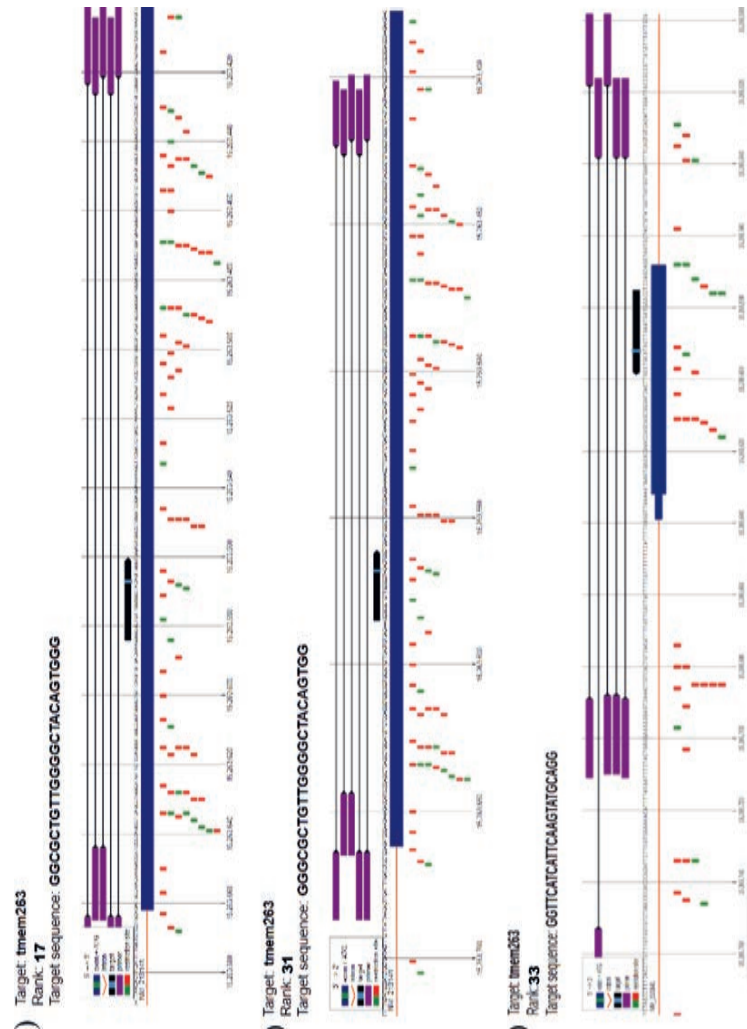

Figure 1 Screenshots from the CHOPCHOP website show three oligos used in this study and their relative coordination to the gene *TMEM263*. The large navy-blue boxes display the exons of *TMEM263* in the zebrafish genome (*Danio rerio* genome assembly: GRCz11, chr18:15.25-15.27 Mb), while the black boxes denote the sites targeted by the guide RNA whose sequences can be found at the top left, the purple arrow-like boxes show the recommended primers for PCR amplification of the target region. (A-B) The sgRNA oligo 17 and 31 were designed to target regions in exon 3. (C) The target region of sgRNA oligo 33 was in exon 2.

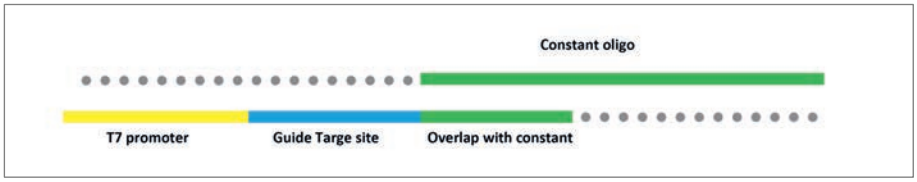

Figure 2 Schematic illustration of the annealing and extension of the target-specific oligo with the constant oligo.

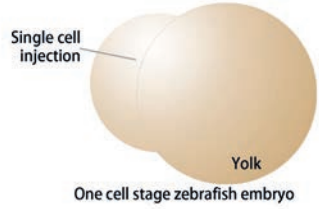

Figure 3 Schematic representation of microinjection to a one-cell stage zebrafish embryo. The grey line indicates the desired single cell injection.

Table 1 Reaction used for annealing and extension of the guide RNA with constant oligo.

Reagents (Diamond Taq kit)	Reaction (µl)
Constant oligo (10µM)	2
Gene specific oligo (10µM)	2
dNTPs (10 µM; 2.5 µM each dNTP)	2
10x Reaction Buffer	2
25µg Mg solution	1.2
RNase/DNase free water	10.3
Taq polymerase (Diamond)	0.5
TOTAL	20

2.3 Post-injection evaluation of the phenotype and malformation

After the microinjection, various phenotypes can be collected and studied. Here, we studied the phenotype of reduced growth, therefore, we measured the phenotype of the fish at 5 dpf (day post fertilization); we also daily recorded the number of dead or malformed embryos/larvae post fertilization. Morphological evaluation of the fish enabled us to record the development on a daily basis. To simplify the phenotyping, we focused on the mortality and malformation of the zebrafish. To obtain a standard rule to evaluate malformation, we considered embryos or larvae as malformed according to a morphology scoring system. The principle for determining the malformation in embryos or larvae can be referred to the standardized scoring system described in Hermsen et al. (2011) and Beekhuijzen et al. (2015). A summary note

for the scoring system is available online at https://osf.io/xbkgs/?view_only=2e2f430c1feb4117b490465fd8c5d32d.

1. At 1dpf, we checked the mortality by comparing injected versus non-injected siblings. Damaged embryos were removed.
2. At 2dpf until 5dfp, we collected the data of malformed embryos (and removed dead ones), un-hatched eggs (kept if not dead), and when hatched, the morphology of the larvae was evaluated.
3. At the end of 5dpf, we collected the larvae and measured the body size under a microscope (for an example see Figure 4).
4. The body length of the larvae was measured using the Java based program ImageJ (Schneider et al., 2012). Note that sometimes in the image, the fish were shown in lateral or dorsal view. We ensured that the length measurements were consistent and standardized.
5. Finally, the larvae were collected in lysis buffer for later DNA isolation.

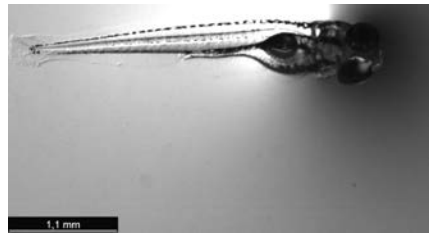

Figure 4 Dorsal view of a 5dpf zebrafish, with a scale bar representing the scale of the image at the bottom left.

2.4 Sequencing the target region

Before growing the injected larvae to maturity, it is important to test the efficiency of the sgRNA for generating mutations. There are various ways of assessing the sgRNA efficiency. For example, perform a T7EI assay to detect heteroduplexes formation of the DNA (Yin et al., 2015); clone into a vector (e.g., plasmid) and screening individual clones; alternatively, perform a PCR assay to amplify the sequence surrounding the target region of the F0 siblings. Below we present a PCR assay and the subsequent sequence analysis for mutation detection in the F0 mosaic siblings. Samples were collected from both injected embryos and un-injected controls.

DNA isolation protocol

1. Take enough tissue of one zebrafish at 5dpf
2. Add 300µl lysis solution, vortex to dissolve the tissue.
3. Add 5µl proteinase K to the lysate
4. Incubate overnight at 55℃, if necessary, add the second time proteinase K and mix in the middle of incubation, and make sure the larvae dissolved.
5. Protein precipitation

a) Cooldown the samples to room temperature
b) Add 10µl protein precipitation solution to the lysate
c) Vortex vigorously at high speed for 20 seconds to mix the solution uniformly with the lysate
d) Incubate samples on ice for 30 minutes
e) Centrifuge at 14000rpm for 5 minutes.

Note: The precipitated protein should form a tight pellet, if not repeat steps c-d-e with longer incubation on ice.

6. DNA precipitation
   a) Pour the supernatant containing the DNA into a clean tube containing 30µl 100% isopropanol
   b) Mix the sample by inverting
   c) Centrifuge at 14000rpm for 30minutes (A white DNA pellet should form)
   d) Carefully pour off supernatant
   e) Add 30µl 70% ethanol to wash the DNA pellet
   f) Centrifuge at 14000rpm for 5 minutes
   g) Pour off the ethanol
   h) Air dry pellets for 30 minutes at room temperature
7. DNA hydration
   a) Add 10 to 50µl Milli-Q water to the pellet
   b) Rehydrate DNA by incubating sample for 1 hour at 65℃ or overnight at room temperature
   c) DNA concentration is measured on the Nanodrop
   d) Use 30 to 60 ng of DNA for PCR amplification based on the primers targeting the mutant region or store the DNA at -20℃ for later usage.
8. Check the PCR products on the agarose gel and prepare samples for sequencing (here we employed the Sanger sequencing).

2.5 Analyze the heterogeneous sequence data

The mechanism of a gene knock-out is not only based on the CRISPR-Cas system to produce the DNA cleavage of a double strand break (DSB) but also on the non-homologous end joining (NHEJ) mechanisms to trigger DNA repair thus induce mutagenesis. NHEJ has long been considered error-prone and causes almost random sequence alterations at the breakpoint, which results in insertions, deletions (InDels), or sometimes site mutations (Bétermier et al., 2014; Shin et al., 2017; Guo et al., 2018). The resulting mutant sequence is not predictable, thus in order to determine the set of desired mutations for subsequent analyses, it is necessary to test the sequence surrounding the target region. One challenge for the interpretation of the sequence is the mosaic nature of the mutant sequence due to the unpredictability of the method. Because in general, zebrafish F0 embryos are mosaic for the target locus, validation using Sanger sequencing directly on the PCR products will result in a chromatogram

with "double peaks" (an indication of ambiguous base calls) at the start of the region that has been edited. Approaches using computational models like the Poly Peak Parser can be used to interpret this heterogeneous sequence and to distinguish the probable breakpoint (Hill et al., 2014). The main function of the tool is to untangle the sequence data into wild-type and mutant allele sequences (consisting of deletions or insertions) from "double peak" data. We used the R-based package "sangerseqR" (Hill et al., 2014).

3 Results

3.1 The *TMEM263* gene is highly conserved between chicken and zebrafish

In this study, we used CRISPR-Cas9 to validate a nonsense mutation found in the *TMEM263* gene that is associated with chicken autosomal dwarfism (adw). Because adw chickens were discarded over a decade ago, to recreate adw chickens and perform the validation in chicken was not feasible. Thanks to the high conservation of the *TMEM263* gene across species, it is possible to validate the function in a more accessible experimental animal by creating a mutation within this gene in zebrafish. The identity of the DNA sequence of the orthologous *TMEM263* genes between chicken and zebrafish is around 72.4%, and the identity in the protein sequence is 74.1% (Figure 5).

3.2 The three sgRNAs used in this study

We designed three sgRNA oligonucleotides (oligo 17, 31, and 33) targeting the second (oligo33) and third exon (oligo17 &31) of *TMEM263* as showen in Figure 1 A-C. For oligo 31 and 33, we collected phenotypic data of fish body length and daily mortality. In total, two batches for oligo 31 and three batches for oligo 33 were generated for the zebrafish (Table 2-3).

Table 2 Number of embryos used for sgRNA Oligo31.

Oligo31_Batch	Injected	Un-injected
1	106	31
2	29	17

Table 3 The number of embryos used for sgRNA Oligo33.

Oligo33_Batch	Injected	Un-injected
1	68	16
2	88	92
3	31	8

3.3 Phenotypic estimation showed no difference at the early stage

In order to validate the potential alteration in body growth, we recorded the mortality on a daily basis, and the body lengths of fish were measured at 5 dpf. The results of the mortality rate, including the damaged or dead eggs, un-hatched, and malformed embryos is shown in Figure 6. There is no statistical difference regarding the mortality rate, however, there is a trend showing that controls have lost fewer embryos over the course of development compared to the injected ones from the same batch. When looking at the length of the larvae at 5 dpf, we found no significant difference between controls and injected individuals for both of the sgRNAs (oligo 31 and 33).

Figure 5 Multi-species alignment of TMEM263 orthologous protein sequences. The red arrows indicate the zebrafish and chicken sequence respectively. The conserved amino acid 59, highlighted by the dashed box, is the associated mutation site in adw chicken. The asterisks (*) shown below the sequence alignment indicate positions, fully conserved in all species. The period (.) indicates conservation between groups of weakly similar properties, and the colon (:) indicates strongly similar conservative properties.

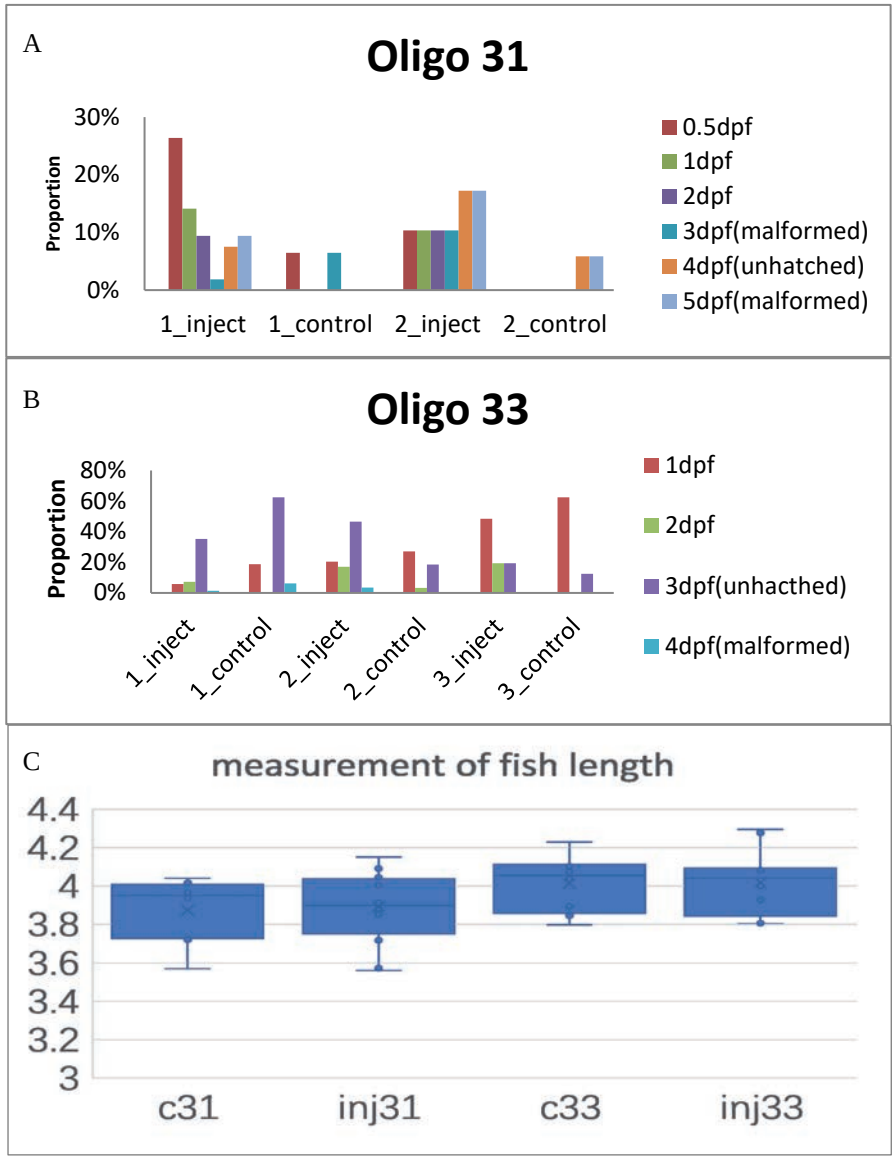

Figure 6 (A-B) The mortality rate of zebrafish embryos or larvae after the injection of the two sgRNA (31 and 33). The x-axis shows the injected embryos and un-injected controls for different batches (two for 31, three for 33). For the injection of sgRNA 31, we also recorded the damaged or dead eggs at 0.5 dpf (day-post-fertilization). At 3 and 4 dpf, we evaluated the malformed morphology or the un-hatched eggs, of which many resulted in dead embryos. (C) The measurement of body length of the fish (in mm) at 5 dpf. The first two columns show sgRNA 31, c31 displays the control individuals and inj31 shows the injected ones. The last two columns are for sgRNA 33 showing the size of injected and un-injected fish. The cross inside the box displays the mean value.

3.4 Sequence of target regions shows no mutations

We amplified the PCR products around the target region and made alignment using the sequences to detect InDels or SNP. Among the 10 sequenced individuals per sgRNA, we did not find any indication of mutations at the expected edit site. The sequence of the injected individuals did not show any variation as shown by the example in Figure 7. The expected edited site is close to the guided target sequence, typically 3 to 4 bp before the PAM sequence (-NGG). Researchers showed the median deletion size using sgRNA is 9 bp in mouse (Shin et al., 2017), while a study screening indels in zebrafish showed variants of a maximum size of 182 bp for deletion and 52 bp for insertion respectively (Varshney et al., 2015).

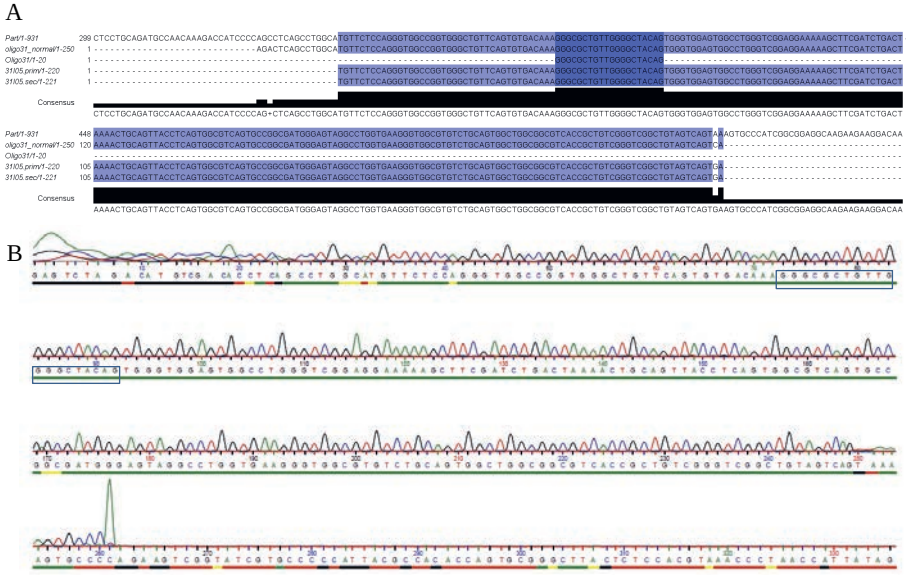

Figure 7 (A) A multi-sequence alignment to detect the sequence of an injected sample. There are 5 sequences in the alignment, from top to bottom; (1) the reference sequence of zebrafish genome; (2) the sequence of a non-injected control sample; (3) A designed target single guide RNA sequence; (4) the primary peak call and (5) the secondary peak call of an injected individual (labeled 31I05). (B) The chromatogram of the same sample confirms that there is no pattern of double peaks. The target sgRNA oligo is highlighted by blue boxes.

4 Conclusion

To summarize, here we presented a detailed workflow from designing the target single guide RNA to the microinjection, as well as the usage of the downstream analytical tools to identify mosaic sequences. Although the example we presented here shows no mutagenesis, this nevertheless highlights the importance of further understanding the undesired outcomes and the hidden factors underlying the results in this assay, e.g., the efficiency of the sgRNA, the property of the genome context, or the potential lethality caused by the induced mutation in zebrafish. These aspects will need to be

improved by future studies with optimized tools to definitely answer the question about the involvement of the identified mutation in the *TMEM263* gene for the adw phenotype in chicken.

5 Acknowledgement

I gratefully acknowledge Sylvia Brugman for providing the genome-editing protocol and the experimental arrangement leading to the results. A special thanks to Agnes de Wit for providing help with the microinjection. I would also like to thank Caroline Lute and Bert Dibbits for the support in the lab. I thank Martien Groenen and Richard Crooijmans for valuable suggestions on the analyses and for proofing reading the report.

6 Reference

Beekhuijzen, M., de Koning, C., Flores-Guillén, M. E., de Vries-Buitenweg, S., Tobor-Kaplon, M., van de Waart, B., et al. (2015). From cutting edge to guideline: A first step in harmonization of the zebrafish embryotoxicity test (ZET) by describing the most optimal test conditions and morphology scoring system. *Reprod. Toxicol.* 56, 64–76. doi:10.1016/j.reprotox.2015.06.050.

Bétermier, M., Bertrand, P., and Lopez, B. S. (2014). Is Non-Homologous End-Joining Really an Inherently Error-Prone Process? *PLoS Genet.* 10, e1004086. doi:10.1371/journal.pgen.1004086.

Cong, L., Ran, F. A., Cox, D., Lin, S., Barretto, R., Habib, N., et al. (2013). Multiplex genome engineering using CRISPR/Cas systems. *Science (80-.).* 339, 819–823. doi:10.1126/science.1231143.

Guo, T., Feng, Y. L., Xiao, J. J., Liu, Q., Sun, X. N., Xiang, J. F., et al. (2018). Harnessing accurate non-homologous end joining for efficient precise deletion in CRISPR/Cas9-mediated genome editing. *Genome Biol.* 19. doi:10.1186/s13059-018-1518-x.

Hermsen, S. A. B., van den Brandhof, E. J., van der Ven, L. T. M., and Piersma, A. H. (2011). Relative embryotoxicity of two classes of chemicals in a modified zebrafish embryotoxicity test and comparison with their in vivo potencies. *Toxicol. Vitr.* 25, 745–753. doi:10.1016/j.tiv.2011.01.005.

Hill, J. T., Demarest, B. L., Bisgrove, B. W., Su, Y. C., Smith, M., and Yost, H. J. (2014). Poly peak parser: Method and software for identification of unknown indels using sanger sequencing of polymerase chain reaction products. *Dev. Dyn.* 243, 1632–1636. doi:10.1002/dvdy.24183.

Hwang, W. Y., Fu, Y., Reyon, D., Maeder, M. L., Tsai, S. Q., Sander, J. D., et al. (2013). Efficient genome editing in zebrafish using a CRISPR-Cas system. *Nat. Biotechnol.* 31, 227–9. doi:10.1038/nbt.2501.

Mali, P., Yang, L., Esvelt, K. M., Aach, J., Guell, M., DiCarlo, J. E., et al. (2013). RNA-guided human genome engineering via Cas9. *Science (80-.).* 339, 823–826. doi:10.1126/science.1232033.

Schneider, C. A., Rasband, W. S., and Eliceiri, K. W. (2012). NIH Image to ImageJ: 25 years of image analysis. *Nat. Methods* 9, 671–675. doi:10.1038/nmeth.2089.

Shin, H. Y., Wang, C., Lee, H. K., Yoo, K. H., Zeng, X., Kuhns, T., et al. (2017). CRISPR/Cas9 targeting events cause complex deletions and insertions at 17 sites in the mouse genome. *Nat. Commun.* 8. doi:10.1038/ncomms15464.

Terns, M. P., and Terns, R. M. (2011). CRISPR-based adaptive immune systems. *Curr. Opin. Microbiol.* 14, 321–327. doi:10.1016/j.mib.2011.03.005.

Varshney, G. K., Lu, J., Gildea, D. E., Huang, H., Pei, W., Yang, Z., et al. (2013). A large-scale zebrafish gene knockout resource for the genome-wide study of gene function. *Genome Res.* 23, 727–735. doi:10.1101/gr.151464.112.

Varshney, G. K., Pei, W., Lafave, M. C., Idol, J., Xu, L., Gallardo, V., et al. (2015). High-throughput gene targeting and phenotyping in zebrafish using CRISPR/Cas9. *Genome Res.* 25, 1030–1042. doi:10.1101/gr.186379.114.

Wiedenheft, B., Sternberg, S. H., and Doudna, J. A. (2012). RNA-guided genetic silencing systems in bacteria and archaea. *Nature* 482, 331–338. doi:10.1038/nature10886.

Wu, Z., Derks, M. F. L., Dibbits, B., Megens, H. J., Groenen, M. A. M., and Crooijmans, R. P. M. A. (2018). A novel loss-of-function variant in transmembrane protein 263 (TMEM263) of autosomal dwarfism in chicken. *Front. Genet.* 9, 193. doi:10.3389/fgene.2018.00193.

Yin, L., Jao, L. E., and Chen, W. (2015). "Generation of targeted mutations in zebrafish using the CRISPR/Cas system," in *Methods in Molecular Biology*, ed. L. Fiedler, 205–217. doi:10.1007/978-1-4939-2917-7_16.

Summary

The phenotype of individuals is determined by the genome together with the environment. The diverse phenotypic variation of domesticated animals is reflected in their genome. With this thesis, I employed genomic analyses to obtain valuable insights into the underlying genetic causes of size variation in chickens. The genetic causes of two dwarf phenotypes (autosomal dwarfism and bantam) in chickens were identified, prioritized, and validated. I addressed the genetic basis of the dwarf phenotypes in terms of the underlying genetic variants, gene expression, and the human-mediated bantamization history. I provide a comprehensive understanding of the function of dwarf related genes, which can potentially be utilized in poultry breeding.

In **chapter 2**, I describe a fine-mapping experiment to identify the causal gene and genetic variant underlying autosomal dwarfism (adw) in chickens. Within the earlier detected candidate region on chromosome 1 (52–56 Mb), a novel nonsense mutation NP_001006244.1:p.(Trp59*) was identified in the transmembrane protein 263 gene (*TMEM263*). The effect of the associated nonsense mutation is expected to truncate the transmembrane protein within the membrane-spanning domain, resulting in a loss-of-function alteration. The results point towards a potentially causative role of *TMEM263* in growth reduction and provide the molecular basis of the development in autosomal dwarf chickens.

Chapter 3 focuses on a study to identify the genetic basis of the bantam phenotype in Dutch traditional chicken breeds by using Genome-Wide Association Studies and a meta-analysis. The Dutch breeds can be divided into three different clusters. Different bantam associated genomic regions were identified depending on different bantam clusters of breeds, which include the growth-related genes *HMGA2* and *PRDM16*. The bantam associated regions clearly show distinct bantam introgression signals and haplotype diversity across the bantam clusters. The observation of heterogeneity indicates that the bantam phenotype in the Dutch chicken breeds is a complex trait caused by multiple underlying genes and variants. Collectively, the genomic analyses on the bantam phenotype offer valuable insights into the human-mediated bantam crossbreeding history.

The objective of **chapter 4** is to provide a comprehensive understanding of the bantam phenotype from a gene expression perspective. RNA-seq data of embryonic samples derived from bantam and normal-sized chickens was generated to identify differentially expressed genes (DEGs) associated with size variation at two developmental stages (E5 and E13). Overall, the gene expression data shows a developmental stage-specific pattern across the samples. I was able to detect DEGs associated with growth in bantam chickens as early as E5. DEGs compared between breeds or developmental stages showed limited overlap, in agreement with the expected heterogeneity of the bantam phenotype. Many of the detected genes are

involved in growth-related signaling pathways (e.g., FGF) and biological processes (myogenesis and osteogenesis) in the expression study.

In **chapter 5**, I describe the population structure of Dutch traditional chicken breeds. Using the Dutch chicken breeds as a model, I demonstrate the complexity of the admixed subdivided population structure. This complexity was dissected and attributed to human-mediated selection and crossbreeding, of which I highlight the influence of selection based on different management purposes and for phenotypic diversification. In particular, I identified signatures of selection involved in phenotypic selection between Dutch traditional chicken breeds, such as loci associated with the bantam trait and the plumage color. In addition, I describe a case study (of Drenthe fowl bantam) providing further genomic insight into the ongoing process of bantamization and the effect of human-mediated crossbreeding.

Finally, in the general discussion (**chapter 6**), I address the challenges and opportunities for the genomic study and the utilization of dwarf phenotypes. With regard to genomic analyses, I emphasize the importance of accounting for population structure in local traditional breeds as well as the phenotypic and genetic heterogeneity in dwarfisms. Moreover, I discuss how to translate the methodological approaches and analytical strategies used to study naturally occurring introgression into studying human-mediated bantamization. In addition, I discuss an experimental attempt to knock-out the ortholog of the adw candidate gene (i.e. *TMEM263*) in zebrafish using CRISPR-Cas. I end my discussion by highlighting the potential implementation of dwarf phenotypes in poultry breeding by addressing the options to introduce a dwarf phenotype into a population, with specific emphasis on the option of using genome-editing.

Acknowledgements

During the four years of my PhD project, I had the pleasure to meet many marvelous people. I would like to take this opportunity to thank all those people who have contributed to this thesis and helped me through this journey.

First, I would like to express my gratitude to my supervisors. Martien, you have been supportive throughout my PhD project. Thank you for allowing me the opportunity to start this journey within ABG; thank you for the guidance on my research; thank you for the scientific criticism during our discussion; and most importantly, thank you for the incomparable environment you have provided. Richard, I am grateful for so many things. I appreciate your dedication to my project and your endless support both scientifically and mentally. Thank you for talking to me when I felt frustrated; thank you for telling me to "let it go" when I needed to; thank you for collecting Jumbo spaarkaart so that I can have a good pan :). You are the most supportive supervisor that I can ask for, this four-year studying in the Netherlands will be the most precious memory because of you (you are the best! :)).

I would like to further express my gratitude. Mirte, I admire your insightful thoughts and passion for science. Although you are not in my supervision team, I am very thankful for your unreserved input on my work, for always being supportive and willing to help. I enjoyed every discussion with you, especially when I had difficulty expressing my ideas, you magically helped me declutter my mind. Hendrik-jan, thanks for all the chats and meetings, your passion for science is unmatched. It is amazing how enthusiastic you were when you showed me the book of Chinese pig encyclopedia even it is completely in Chinese. Also, thank you for giving me the book, *De Kippen Encyclopedie*, that has helped me tremendously in my project. Ole, I have learnt a lot from you during meetings and discussions (it is a pity that we only had one meeting to discuss my paper), I am always impressed by your knowledge, super chill life philosophy, and your friendly smiles. Sylvia, thanks for leading me to the world of zebrafish and CRISPR-Cas. I appreciate your guidance and patience throughout the experiments and thank you for all the "fingers crossed" afterwards.

I also want to express gratitude for the support that I received. Agnes, thank you for providing the help with microinjection, it was a pleasure to work with you. Bert and Kimberley, thanks for your support in the lab and for answering my questions no matter big or small. Lisette, Fadma, and Rosilde, thanks for your endless support and kindness.

I am very grateful to all my colleagues at ABG for making this journey of PhD joyful. First of all, thanks to all the unbelievable and well-organized events. I enjoyed all the activities, whether a research-related discussion, a holiday celebration, a running dinner, day-to-day coffee breaks, or a drink after work (although it always ends up with more than just one drink :p). Thanks for organizing these amazing events that

never failed to surprise me, they have made my life living in a new country memorable and less alone. Thanks to all who participated in my GxE study on pepper plants.

I am so lucky to have met many outstanding people. Although I cannot mention every name, I am sincerely grateful for all your accompany: thank you for the biertje and taking care of me when I had a little too much to drink :); thank you for the good coffee during walks; thank you for sharing movie and anime lists with me; thank you for inviting me to dinners, tea, parties, and boardgames. Special thanks to the Monday Genomics team: Vinicius, Maulik, Chrissy (also thanks for being such a nice co-author :)), Lim, Henri, Fatma, Rayner, Jani, Gibbs, Carolina among others. I have learnt so much from you, and you have made this meeting a wonderful room where I feel free to share my thoughts and raise any kinds of questions (even stupid ones) since I know there will always be a help.

I would like to thank my paranymphs. Harmen, we knew each other on day one and we have shared the office ever since. Sitting opposite to each other allowed me for moments like, “Can I borrow your mind?”, “Time for foosball”, “Let’s practice your presentation”, and “Are you measuring the slide with a RULER?” (so classic). The time we spent together are like pieces of a big puzzle, together it is a complete picture of this four years. We stood on the stage of Aula many times, it is unlikely that I will defend at Aula, but with you being my paranymph, it would feel like a (Wageningen sweater) team. Martijn, you are not only a wonderful co-author but also a close friend. You are very sweet and loving, I admire your passion for coding and soccer, caring for animals (especially Zoef), I will definitely miss your typical dance at parties, your “hangover” face on Monday :P, and your beer brewing technique. I really enjoyed chatting and working with you.

My dear office mates. I was lucky to work in an office that turns out to be the most popular one. Captain Robert, it was my pleasure to meet you and work with you. I really admire how friendly and optimistic you are. Maria, mi amor, thanks for all the Spanish lessons (we still practice “tengo hambre” on a daily basis for clear reasons:)); thank you for being caring and “integrative”; thank you for being my hairdressing model, and thank you also for putting up with my ostrich runs and silly jokes (If you sweat in a sweater…). Chiara, you joint this office a bit late, but the friendship with you was there since the beginning. You and Miguel are very special to me, full of surprises and nerdiness (which I love!). Thanks for the “sweeeeetie” with big hugs, Friday afternoon Chinese lessons (the quiz is on the way), ‘Otaku’ chats and discussions of books (the Three Body Problem and 1Q84), and of Totoro and Stalin (who would expect they appear in the same sentence). Especially, thanks for the late-night calls as you sensed I was exploding (well, for good reasons, in my own defense). Most importantly, for knocking at my windows and going for corona-proof walks. Annabelle, Raymond, Lisanne, Lim (our hoary officemate), and others: thanks for

every “goedemorgen” and “fijne avond” with hugs. I also want to thank Kyle for setting up the Linux desktop, I benefited tremendously from the “kyle-workstation” over the last years.

感谢我的中国小伙伴。包曼，秋宇，海博，思远，喻运，小飞，文哲小天使，宏瑞，其通，彭业博，卓实，潘学，乔老师，倩倩。特别的，小包，谢谢你在我刚刚来瓦村的时候带着我玩耍（不是 buddy 胜似 buddy），一起逛吃逛吃，深夜的螺蛳粉，还有无数的约饭和冰激凌，以及在写论文时给我的鼓励。小桃，从本科第一天认识你，到一起坐着飞机抵达荷兰，超过十年的时间，我们互相依靠也见证了彼此的成长。十年的北欧之约是有点困难了，但我相信我们都有美好的未来！曹露，在最后的日子里，我们一起走过了对我而言最艰难的一段，有你一起每天计划工作、讨论进展，是我极大的动力。感谢我的朋友张雅文，感谢你和我分享博士生的科研生活，友谊天长地久。网络虽然是个好东西，还是希望我们能尽快奔现，嘻嘻。

刘琅青，你好哇，谢谢你见证我的这几年，你是我的战友，也是中华小当家。感谢你包容我的“忽明忽暗一千八百种坏毛病”，谢谢你告诉我要相信未来。也感谢你的父母对我的关怀和尊重。

感谢我的家人。妈妈，你是我生活的榜样，你总能给我温暖的慰藉也总能直击要害的说出我的困惑。这几年我离家太远，但我们之间不仅有亲情，更有深刻的互相理解。依旧希望当我到你的年纪能像你一样对生活保有好奇心和智慧。感谢爸爸对我人生的引导和尊重，感谢你告诉我要相信自己，放心去做，你是我的定心丸。你们给了我无私的爱护和无条件的支持。再一次，谢谢爸爸妈妈把我生的这么好（笑）。未来的生活才刚刚开启，你们的关爱是我路上的光，我会继续努力。

Curriculum Vitae

About the author

Zhou Wu (吴舟) was born on the 17th of October 1992 in Fujian, China. Her interest in biology has started since high school when she attended the Biology competition. In 2014, she received her bachelor's degree in Animal Science and Technology at China Agricultural University in Beijing. During her BSc, Zhou started her research journey with the 'URP' project for bachelor students. During this project, Zhou performed a study of genes related to the reproductive performance of porcine by gene set enrichment analysis. In 2016, Zhou obtained her MSc degree in Animal Genetics and Breeding from China Agricultural University. During her MSc, Zhou worked on the genetic basis of feathering traits and related research in production performance in chicken under the supervision of Prof. Changxin Wu and Junying Li. Part of her MSc thesis was published in the journal *Frontiers in Genetics* in 2020. After she received her MSc degree, Zhou continued to pursue her passion in animal genomics, more specifically, chicken genomics, she started her PhD project at Animal Breeding and Genomics group at Wageningen University and Research. She focused the PhD project on chicken dwarf phenotypes under the supervision of Prof. Martien Groenen and Dr. Richard Crooijmans, the results of this project are presented in this thesis.

Peer reviewed publications

Wu, Z.*, Bortoluzzi, C., Derks, M. F. L., Liu, L., Bosse, M., Hiemstra, S. J., et al. (2020). Heterogeneity of a dwarf phenotype in Dutch traditional chicken breeds revealed by genomic analyses. Evol. Appl., eva.13183. doi:10.1111/eva.13183.

Wu, Z., Derks, M. F. L., Dibbits, B., Megens, H. J., Groenen, M. A. M., and Crooijmans, R. P. M. A. (2018). A novel loss-of-function variant in transmembrane protein 263 (TMEM263) of autosomal dwarfism in chicken. Front. Genet. 9, 193. doi:10.3389/fgene.2018.00193.

Liu, X., **Wu, Z.**, Li, J., Bao, H., and Wu, C. (2020). Genome-Wide Association Study and Transcriptome Differential Expression Analysis of the Feather Rate in Shouguang Chickens. Front. Genet. 11, 613078. doi:10.3389/fgene.2020.613078.

Conference proceedings

Wu, Z., Bortoluzzi, C., Derks, M. F. L., Groenen, M. A. M., and Crooijmans, R. P. M. A. (2019). Genome-wide Association Studies of Dwarf Phenotypes in Dutch chicken breeds. in International Society for Animal Genetics Conference (ISAG) (Lleida, Spain).

Wu, Z., Derks, M., Dibbits, B., Groenen, M., and Crooijmans, R. (2017). Autosomal dwarfism in chicken is caused by a nonsense mutation in in TMEM263. in Animal Genetics and Disease (Hinxton, UK).

Awards and honors

2017 Best short talk winner in Animal Genetics and Disease, Hixton, UK

Training and Education

The Basic Package (3.0 ECTs)	
WIAS Introduction Day	2016
Course on philosophy of science and/or ethics	2017
Course on essential skills	2017

Disciplinary Competences (16.5 ECTs)	
Writing research proposals	2016
MSc courses: Genomics	2016
MSc courses: Advanced Bioinformatics	2017
Emerging technologies	2017
Characterization, management and exploitation of genomic diversity in animals	2018
Summer school in ChIP-seq	2019

Professional Competences (3.4 ECTs)	
Scientific writing	2017
Poster and pitching	2018
Final touch	2019
Last Stretch of the PhD Programme	2020
Writing propositions for your PhD	2020

Presentation Skills (3.0 ECTs)	
Animal genetics and disease, Hinxton, Cambridge	2017
WIAS science day,oral	2018
ISAG(International Society for Animal Genetics Conference),Spain, oral	2019

Teaching competences (maximum 6 ECTs)	
Supervising practice for WUR Genomics-2017-2018-period 5	2018
Supervising practice for WUR Genomics-2018-2019-period 2	2018
Supervising practice for WUR Genomics-2018-2019-period 5	2019
Supervising practice for WUR Genomics-2019-2020-period 2	2019
Supervising theses-MSc thesis	2019

Total Credits:	31.9

Colophon

The research described in this thesis was financially supported by Wageningen University. Sequence data used in this research was financially supported by the IMAGE project from the European Union's Horizon 2020 Research and Innovation Programme (Grant Agreement No. 677353).

Zhou Wu was sponsored by a Chinese Scholarship Council (CSC) fellowship (File No. 201606350175).

Cover design: Holifey (Sina weibo @-Holifey-) and Zhou Wu

Printed by Digiforce | ProefschriftMaken